# Engineering and characterization of a binder to inhibit *in vivo* α-synuclein aggregation

Inaugural-Dissertation

zur Erlangung des Doktorgrades
der Mathematisch-Naturwissenschaftlichen Fakultät

der Heinrich-Heine-Universität Düsseldorf

vorgelegt von

**Aziz Gauhar**

aus Afghanistan

Düsseldorf, Februar 2015

aus dem Institut für Physikalische Biologie

der Heinrich-Heine-Universität Düsseldorf

Gedruckt mit der Genehmigung der

Mathematisch-Naturwissenschaftlichen Fakultät der

Heinrich-Heine-Universität Düsseldorf

Referent: Dr. Wolfgang Hoyer

Korreferent: Prof. Dr. Dieter Willbold

Tag der mündlichen Prüfung: 24.03.2015

**Erklärung an Eides statt**

Ich versichere an Eides statt, dass die Dissertation von mir selbstständig und ohne unzulässige fremde Hilfe unter Beachtung der „Grundsätze zur Sicherung guter wissenschaftlicher Praxis an der Heinrich-Heine-Universität Düsseldorf" erstellt worden ist. Die Dissertation wurde in der vorgelegten oder in ähnlicher Form noch bei keiner anderen Institution eingereicht. Ich habe bisher keine erfolglosen Promotionsversuche unternommen.

Düsseldorf, den 16. 02. 2015

_____

Aziz Gauhar

# Acknowledgements

*To my family*

# Table of contents

# List of figures

# List of tables

# Abbreviations

| | |
|---|---|
| APP | Amyloid precursor protein |
| ATP | Adenosine triphosphate |
| Aβ | Amyloid beta |
| C. elegans | Caenorhabditis elegans |
| dAbs | Single-domain antibody |
| E. coli | Escherichia coli |
| EGCG | Epigallocatechin gallate |
| ELISA | Enzyme Linked Immuno-Sorbent Assay |
| Fab | Antigen-binding fragment |
| Fc | Fragment crystallizable |
| FRAP | Fluorescence Recovery After Photobleaching |
| GFP | Green Fluorescent Protein |
| IAPP | Insel-Amyloid-Polypeptid (Amylin) |
| IDP | Intrinsically Disordered Protein |
| LBD | Lewy Body Disease |
| MES | Mouse Embryonic Stem |
| MTT | 3-(4,5-dimethylthiazol-2-yl)-2,5-diphenyltetrazolium bromide |
| NSF | N-ethylmaleimide Sensitive Factor |
| PCR | Polymerase Chain Reaction |
| PD | Parkinson's disease |
| POU | Pit-Oct-Unc |
| PTM | Post-Translational Modification |
| S. cerevisiae | Saccharomyces cerevisiae |
| scFv | Single chain variable fragment |
| SILAC | Stable Isotope Labeling by Amino acids in Cell culture |
| SNARE | Soluble NSF Attachment Protein Receptor |
| SPA | Staphylococcal Protein A |
| SUMO | Small ubiquitin-like modifiers |
| tg | transgenic |
| ThT | Thioflavin T |

# Summary

α-Synuclein is a neuronal protein that is predominantly localized around the vesicles in the presynaptic terminals. Although its exact function is not well known, the protein is implicated in the pathogenesis of Parkinson's disease and other related disorders collectively known as synucleinopathies. Misfolding and aggregation of α-synuclein caused by aberrant events, including certain mutations and polymorphisms of the *SNCA* gene, result in the generation of toxic soluble oligomers and fibrillar deposits. Therefore inhibiting or reversing α-synuclein self-assembly could constitute a key approach for therapeutic intervention.

The β-wrapins are engineered binding proteins selected from combinatorial libraries generated via random mutagenesis from the $Z_{A\beta3}$ scaffold. The β-wrapin AS69 specifically binds α-synuclein and inhibits its aggregation by sequestering the hydrophobic β-hairpin region that forms concomitant to binding. AS69 occurs as a homodimer where the individual subunits are connected through a disulfide bridge.

This work investigates the possibility of creating a single-chain version of AS69 through head-to-tail linkage of its subunits. Findings of this work highlight the importance of suitable linker choice for preserving functional binding of AS69 to α-synuclein. Comparison of several constructs revealed the glycine-serine rich flexible linker as an appropriate choice. Incorporation of the linker sequence yields the AS69-GS3 single-chain homodimer that exhibits affinity equivalence with the solely disulfide linked AS69. The AS69-GS3 construct is characterized under oxidizing and reducing conditions to evaluate the impact of the Cys28-disulfide bond on structure, stability and α-synuclein binding. Results show that formation of the disulfide bond causes compaction of the fusion protein, increases its thermostability, and is essential for high affinity binding to occur. Moreover, the linker sequence further contributes to increased stability of the construct and promotes α-synuclein binding by affording accelerated disulfide bond formation. Considering the susceptibility of the disulfide bond to reducing conditions, AS69-GS3 represents a viable construct for *in vivo* application.

The second part of this work addresses the potential of β-wrapins in blocking or mitigating α-synuclein-induced toxicity in a cell culture model. The MTT assay is employed to evaluate viability of human SH-SY5Y neuroblastoma cell line. Results demonstrate that cell viability is thoroughly rescued at stoichiometric concentrations of AS69-GS3, while at substoichiometric concentrations viability is significantly improved. Likewise, the β-wrapin AS10 is equally effective in inhibiting aggregation and

cytotoxicity of not only α-synuclein, but also that of Amyloid-β and Insel-Amyloid-Polypeptide.

Findings of this work suggest that stabilization of monomeric α-synuclein represents a workable strategy in preventing aggregation and pathogenesis of PD and other synucleinopathies.

# Zusammenfassung

α-Synuclein ist ein neuronales Protein, das vorwiegend in der Umgebung von Vesikeln in den präsynaptischen Nervenenden lokalisiert ist. Die genaue Funktion von α-Synuclein ist zwar wenig bekannt, dennoch ist das Protein an der Pathogenese der Parkinson-Krankheit und weiterer Synucleinopathien beteiligt. Fehlfaltung und Aggregation von α-Synuclein, die der Entstehung der löslichen Oligomeren und fibrillären Ablagerungen zugrunde liegen, werden durch aberrante Ereignissen, einschließlich bestimmter Mutationen und Polymorphismens der SNCA-Gen, hervorgerufen. Deshalb könnte die Stabilisierung von α-Synuclein, die zur Verhinderung der Selbsassoziation des Proteins führen soll, als Ansatzpunkt für die Arzneimittelentwicklung dienen.

β-Wrapine sind kleine Bindepoteine, die aus kombinatorischen Proteinbibliotheken basierend auf $Z_{Aβ3}$ selektiert werden. Das β-Wrapin AS69 weist eine hohe Bindungsspezifität für α-Synuclein auf und inhibiert dessen Aggregation durch Beschlagnahmung der hydrophoben β-Haarnadel-Region, die sich bei der Bindung bildet. AS69 ist ein Homodimer, in dem die einzelnen Untereinheiten über eine Disulfidbrücke zwischen den Cys-28-Resten kovalent verknüpft sind.

Diese Arbeit befasst sich mit der Herstellung einer Einzelketten-Version von AS69, in der die Untereinheiten in einem Head-to-Tail Format durch einen Linker verknüpft sind. Die Ergebnisse zeigen dass die Wahl eines geeigneten Linkers für die Erhaltung der Bindung von AS69 an α-Synuclein unerlässlich ist. Ein Vergleich mehrerer Konstrukte zeigt Eignung eines Glycin-Serin-reichen flexiblen Linkers. Der Einbau der Linker-Sequenz ergibt das AS69-GS3 Einzelketten-Homodimer, das mit dem ausschließlich Disulfid-gebundenen AS69 funktionale Parität aufweist. AS69-GS3 wurde unter oxidierenden und reduzierenden Bedingungen charakterisiert, um die Auswirkungen der Cys28-Disulfidbindung auf die Struktur, Stabilität und Bindung an α-Synuclein zu beurteilen. Die Ergebnisse zeigen, dass die Bildung der Disulfidbindung zu einer Kompaktierung des Fusionsproteins führt, dessen Thermostabilität erhöht, und für Hochaffine Bindung unerlässlich ist. Darüber hinaus trägt die Linkersequenz zu einer erhöhten Stabilität des Konstrukts bei und fördert α-Synuclein-Bindung durch beschleunigte Ausbildung der Disulfidbrücke.

Angesichts der Anfälligkeit der Disulfidbindung gegenüber reduzierenden Bedingungen, stellt das AS69-GS3 ein geeignetes Konstrukt für die *in vivo* Anwendung dar.

Der zweite Teil dieser Arbeit beschäftigt sich mit der Untersuchung der Auswirkung der β-Wrapine auf die durch α-Synuclein induzierte Toxizität in einem Zellkulturmodell. Hier wird der MTT-Toxizitättest eingesetzt um die Viabilität humaner SH-SY5Y-Neuroblastomzellen zu bestimmen. Ergebnisse zeigen, dass bei stöchiometrischen Konzentrationen von AS69-GS3 die Zellviabilität vollständig gerettet wird, während sie bei substöchiometrischen Konzentrationen deutlich verbessert wird. Das β-Wrapin AS10 ist ebenso effektiv bei der Hemmung der Aggregation und Zytotoxizität von α-Synuclein. Darüberhinaus inhibiert AS10 auch die Aggregation und Zytotoxizität des Amyloid-β Peptids und des Insel-Amyloid-Polypeptids.

Die Ergebnisse dieser Arbeit weisen darauf hin, dass die Stabilisierung der monomeren α-Synuclein eine umsetzbare Strategie zur Verhinderung der Aggregation und Pathogenese der Parkinson-Krankheit und anderer Synucleinopathien darstellt.

# Introduction

## 1 Protein folding, misfolding and aggregation

Proteins are central to virtually every biological process. In order to function properly the majority of these molecules have to undergo a series of conformational changes and fold into their characteristic three dimensional structures that are determined by the amino acid sequence of each protein [1]. The high degree of conformational flexibility that yields an astronomical number of protein conformations is attributed to the properties of the peptide bond and amino acid side chains [2]. Generally under physiological conditions the native state of a protein represents the conformation that is thermodynamically the most stable. For globular proteins, this corresponds to the conformation with the lowest energy, while in case of intrinsically disordered proteins multiple isoenergetic conformations might exist representing their native states. Though it should be noted that the native conformation is not the only stable state available to the polypeptide chain, the alternative being the amyloid state [3, 4].

### 1.1 Protein folding

Given the molecular diversity and differing nature of proteins in terms of their size, stability, and topology, attempts to experimentally characterize protein folding have proven to be rather challenging. Consequently disparate interpretations of the available data have resulted in the emergence of numerous theories attempting to describe the folding process [5, 6]. However, there seems to be no agreement about which theory, if any, is correct and/or the most comprehensive; the energy landscape theory appears to have received considerable attention.

#### 1.1.1 The energy landscape theory and the funnel concept

The classical view conjectures protein folding to occur through a predetermined pathway involving a defined sequence of states leading from the unfolded state to the native state by step-wise addition of the folding units known as foldons, while giving rise to discrete on-pathway (partly folded) and off-pathway (misfolded) intermediates, including the molten globules [7-10]. The new theory, also known as the energy landscape theory, offers an alternative to the classical view for probing the details of

the folding process and suggests that folding proceeds through a multiplicity of pathways [11-16]. Here, the energy landscape is likened to a rugged funnel riddled with traps or deep valleys (local minima) in which the protein can transiently reside, thus slowing progress to the native state (Figure 1) [11,17,18].
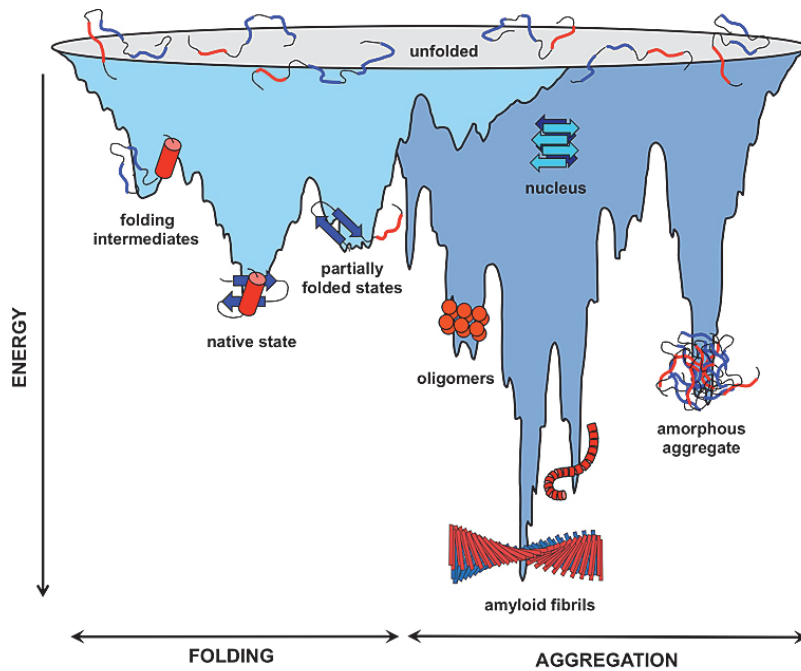


**Figure 1:** Schematic representation of an energy landscape for protein folding and aggregation. (Adopted from Jahn and Radford, 2005) [98]

The top of the funnel is populated by the protein in its denatured state possessing numerous starting conformations and high free energy. The bottom of the funnel represents the native state. Along the funnel the protein passes through an ensemble of partially folded structures while progressing to the natively folded state [1, 19]. Approaching the native state, the conformational space accessible to the polypeptide chain, the degree of disorder as well as entropy and energy decrease, whereas the number of native contacts grow. For instance, for a 60-amino acid helical protein formation of molten-globule from random coil is accompanied by a drastic reduction in the number of conformations, while a quarter of the native contacts are correctly made [20]. As the number of native contacts grow, a large ensemble of transient structures emerge leading to the formation of discrete kinetic intermediates with three-quarters of the native contacts. Should these intermediate states pose large kinetic barrier(s), they can become rate-limiting to the folding process and thereby to reaching the most stable thermodynamic state. It has been well established that the search process for the

native state is highly efficient and has a stochastic nature that requires sampling only a small number of the available conformations [17, 21, 22].

It has been proposed that the majority of proteins fold through a rugged landscape in a multi-state way that is populated by an ensemble of unfolded states, one or more intermediate states, finally navigating to the folded state. In addition, proteins that fold via a two-state transition have an energy landscape that appears relatively smooth lacking in deep valleys and high barriers and is populated only with the native and denatured states [23, 24]. However, the latter scenario seems to be rare; since the presence of partially folded states is suggested even for small proteins, evidenced by recent insights gained from new methods capable of detecting even sparsely populated transient species [11, 25].

Numerous studies suggest that folding mainly occurs via the nucleation-condensation mechanism, where a few key residues initially form the nucleus followed by condensation of the remainder of the structure [26]. The majority of the proteins fold with a single folding nucleus; however, existence of multiple folding nuclei in particular for larger proteins has also been indicated [9].

The order of events that lead to the native structure is described to involve formation of a few key contacts relatively early in the folding process with the rest of the contacts ensuing subsequently [5]. According to Dinner *et al.* conformational fluctuation enables even distant residues to come in contact with each other [15]. Moreover, native interactions are suggested to be more stable than non-native interactions, which enable finding the structure with the lowest energy [4]. However, the role played by non-native contacts in defining the folding mechanism and rate is also maintained [25].

In case of small proteins the majority of interactions involving key residues has to occur before a stable compact structure could be formed. Progression to the fully folded state follows rapidly. Folding of larger proteins is proposed to essentially take place in modules i.e. independent segments or domains of the protein. Local key interactions define the domain specific fold, while other interactions ensure the correct formation of the overall structure through appropriate interaction of the already folded regions. Once the native-like interactions within and between domains are established, a final step that entails expulsion of water molecules from the partially hydrated protein core follows, thus imparting the protein a fully native structure [27, 28]. The funnel concept is stated to have some limitations for not being suitable to describe the behavior of most polypeptide chains under physiological conditions [29], as it was developed to describe

refolding of a single polypeptide chain *in vitro* without accounting for the effects of high energy intermolecular collision, an insistent occurrence in the cell interior [30].

*In vivo*, protein folding initiates during or following its translation in the ribosome. It can wholly or partially occur in the cytoplasm or yet in more specific compartments, such as the endoplasmic reticulum [31]. Several factors are suggested to influence the folding process *in vivo*, both intrinsic and extrinsic. The intrinsic properties of the polypeptide chain such as charge, hydrophobicity, and secondary structure propensity are key not only in determining the proper and efficient folding of the polypeptide chain into a stable and functional protein, but also in avoiding formation of non-functional conformers [32, 33].

A polypeptide chain in the process of folding can be prone to non-native interactions with various molecules, while having regions exposed that are otherwise buried in the native state. This can be of particular concern if the exposed region is prone to aggregation, such as hydrophobic surfaces [34]. Furthermore, perturbations that disrupt the folding process, leading to the accumulation of unfolded and aggregated proteins, can have detrimental consequences. Such perturbations can be induced by various factors, including increased load on the folding machinery following elevated protein synthesis, and expression of mutant or misfolded proteins. To cope with such problems elaborate strategies are evolved to assist the folding process that involve a large number of auxiliary factors, including folding catalysts and molecular chaperons [35-38]. Considering the complex milieu in the cell interior crowded with an immense number of components, the role of these molecules in the efficient folding of proteins is invaluable. Molecular chaperones in particular are ubiquitous throughout the cell, and though they might carry out varied functions, their role in promoting efficient protein folding and assembly as well as preventing aggregation by binding rather non-specifically to the emerging polypeptide chain, particularly the partially folding intermediates, is considerably important. Most chaperones are suggested to work in a cooperative manner. Work by Parsall *et al.* proposes that some molecular chaperones are capable of reversing the folding trajectory of misfolded proteins; thus allowing them the opportunity to refold properly. Moreover, molecular chaperones are shown to mediate resolubilization of proteins and as a result restore their activity [39].

Although most polypeptides show a higher tendency to aggregate upon refolding under test tube conditions, less than 20% of cytoplasmic proteins are indicated to require chaperons' assistance in acquiring their native state [29]; for instance, most small

proteins (~65-80%) are able to fold rapidly following synthesis without further assistance [31]. This may indicate that folding is more efficient *in vivo* than *in vitro*, at least in case of the polypeptide chains examined in detail [40, 41].

Folding catalysts constitute another set of tools in the cellular repertoire employed to catalyze various rate-limiting steps in the folding process. For instance, disulfide isomerases enhance the rate of formation and reorganization of disulfide bonds; likewise, peptidylprolyl isomerases speed up the *cis/trans* isomerization rate of peptide bonds involving proline residues [31]. In addition to molecular chaperones and folding catalysts, the cellular machinery has evolved a stringent quality control mechanism ensuring that unfolded and misfolded proteins are properly dealt with. The importance of its role is evidenced from experimental work revealing that over half of all polypeptide chains synthesized do not meet the quality control criteria [42, 43]. The quality control mechanism is suggested to involve a series of glycosylation and deglycosylation reactions that facilitate the subsequent detection and targeting of unfolded and misfolded proteins for degradation by the autophagy and ubiquitin-proteasome system [44].

## 1.2 Misfolding and aggregation

The role of molecular chaperones and the need for a highly effective quality control mechanism in the ER has already been discussed in the context of protein folding. Aberrations in the folding process due to failure of these housekeeping mechanisms can give rise to a population of partially and or completely unfolded proteins. As pointed out, such failures might become prevalent should the chaperon response and degradatory mechanisms be overwhelmed and or rendered ineffective [45, 47].

### 1.2.1 Protein aggregation and amyloid formation

Referring to the energy landscape model of protein folding, the fully folded native state is only one of the two thermodynamically stable states available to a partially unfolded protein, the alternative being the amyloid state. First discovered in 1935 by Astbury and Dickinson as a generic protein fold, the ability to form amyloid structure is now known to be common to nearly all polypeptide chains as demonstrated by formation of these structures from proteins not associated with diseases such as myoglobin, and homopolymers such as polylysine and polythreonine [48-50]. Functional amyloids have been reported in various organisms including bacteria, fungi, insects, and human [51].

However; the propensity to form such structures may vary depending on various factors.

The reason amyloid has recently attracted so much attention is due to its implication in pathological conditions, whereby innocuous, soluble proteins, *en route* to the native state, deviate from its normal path and are converted to insoluble fibrillar protein aggregates, known as amyloid fibrils [52]. About 23 different proteins are proposed to be culpable in the development of amyloidogenic diseases, the majority of which belong to the group of intrinsically disordered proteins, the rest comprising globular proteins [53]. A crucial aspect here is the mechanism through which the precursor proteins assemble leading to the formation of amyloid fibrils. As evidenced from experiments under both physiological and denaturing conditions, aggregation can occur through partially unfolded intermediates and native-like conformations [54, 55]. Formation of amyloid fibrils from globular proteins necessitates an initial unfolding step causing the exposure of certain aggregation-prone residues of the polypeptide main chain that are largely buried in the native state. However, it is also indicated that complete unfolding may not be entirely necessary, though some level of structural flexibility is required for aggregation to occur [56]. Unfolding of the polypeptide chain can be facilitated by conditions such as low pH or certain mutations that cause local perturbations in the native state [57]. Provided that the essential arrangement of hydrogen bonds necessary to stabilize the native state are in place, some of the resulting aggregates may retain their native-like architecture even in the fibrillar state. In essence this would strictly be the case for proteins that mainly have a β-sheet structure. Conversely, helical proteins, such as insulin, would require a fundamental structural rearrangement that renders them the typical amyloid structure with β-sheets [54, 55, 58].

The amyloid state has been linked to a large number of diseases characterized by the presence of fibrillar deposits and plaques. Such deposits have been found to affect various organs including brain, liver and spleen [59]. Though its implication in neurodegenerative diseases, including Alzheimer's and Parkinson's, is of particular importance [60].

With regard to why a limited number of (globular) proteins are involved in amyloid formation and the resulting diseases, Chiti and Dobson proposes the notion that under physiological conditions the folding process takes place under the constant surveillance of molecular chaperones and other components of the quality control

mechanism, which target both unfolded and misfolded species for (re)folding or degradation. Though, minor conformational alterations generating native-like species may remain undetected, thus evading the quality control system. Moreover, given their resemblance with the native state, the energy landscape lacks barriers to limit such species being populated. Finally, the protein can proceed readily towards aggregation in particular if formation of fibrillar assemblies does not require extensive unfolding and reorganization [55, 57].

### 1.2.2 Factors contributing to amyloid formation

As already noted, proteins have an underlying propensity to aggregate unless maintained in a highly regulated environment. However, various aggregation promoting conditions have been identified that can vary the stability of the protein and further the population of intermediate states; hence, tipping the balance in favor of aggregation. Conditions such as high temperature, low pH, agitation/shear, surfaces, detergents, ions, and moderate concentrations of organic solvents are shown to promote partial unfolding of globular proteins. Furthermore, appearance of non-native conformations encountered in familial diseases is mediated through certain mutations causing to destabilize the native structure. Evidence for the correlation between conformational stability and propensity to aggregate has come from studies on proteins not associated with any diseases. Partially folded conformers of such proteins were shown to trigger aggregation even if present at a very low concentration. On the contrary, aggregation can be halted and even prevented by stabilizing the native state by employing specific affinity ligands. Furthermore, compounds such as lipids, glycosaminoglycanes, and serum amyloid P component are shown to enhance protein aggregation [61-67].

The propensity of the polypeptide chain to form aggregates can be influenced by the amino acid sequence as it may harbor regions that are characteristically aggregation-prone. These aggregation-prone regions can be inherent in the sequence, though ordinarily they remain buried in the native state, or develop following certain mutations that cause an increase in hydrophobicity or a decrease in charge. Thus, the structure and stability of protein is compromised contributing to a drift from the native to the misfolded state [68-70]. High hydrophobicity and or low net charge are indicated to induce incremental interactions with other non-native partners, thus facilitating protein aggregation. Conversely, high net charge in the sequence is shown to hinder aggregation. Moreover, it is noted that proteins have evolved such that they avoid

clusters of hydrophobic residues, thus keeping their aggregation propensity sufficiently low [71].

Another mechanism proposed for the role of mutations in amyloid formation is by increasing the likelihood of the sequence to adopt a β-sheet structure. The effect of mutations with regard to the population of various folding species has been shown on wild-type and mutant lysozyme. Under physiological conditions the mutant variant of the protein lowers the energy barrier causing to promote population of partially folded states and consequently formation of the amyloid fibers [72-73]. Mutations can increase population of partially (un)folded states by decreasing the stability or cooperativity of the native state, the latter is indicated to be a crucial factor in keeping, even marginally stable, proteins in their soluble state [74]. Mutations in the Amyloid-β peptide causing early onset Alzheimer's disease has also been studied extensively [75]. The effects of mutations on the native state of α-synuclein will be expounded on later.

Mutation in critical regions of the sequence that result in breaking β-sheet can prevent self-assembly [76]. Sequences rich in glutamine are implicated in amyloidogenesis. Mutations resulting in glutamine repeats are associated with numerous degenerative diseases, such as prions and Huntington. The number of glutamine residues occurring is correlated with the propensity of protein to aggregate as well as the severity of the disease and its onset [77-79]. Simulation studies indicate that an increase in the number of glutamine residues above a certain threshold causes more residues to become disordered [80], this is confirmed by studies performed on *C. elegans* with engineered polyglutamine peptides. A high aggregation propensity is also shown for hydrophobic residues, in particular aromatic amino acids, while proline and glycine are indicated to have a low propensity to form β–sheet structures. Furthermore, salt brides are proposed to have a stabilizing role [81-83].

Interaction of proteins with various surfaces, in particular hydrophobic or polar, is shown to influence the folding process by causing an increase in their effective local concentration and by extension in protein-protein interaction, thus leading to protein's aggregation [84]. Given the role biological surfaces may play in contributing to protein misfolding and disease generation, surfaces have been the subject of several experimental and simulation studies. These studies have been performed for various proteins, including Aβ [85], insulin [86], β2-microglobulin [87] and biological surfaces including basement membrane components i.e. collagen, fibronection, laminin, extracelluar matrix components such as proteoglycans and gycosaminoglycans.

Physiologically lipid membranes are of particular relevance and are shown to enhance protein misfolding and aggregation [96-97], they also happen to be on the receiving side of the damage caused by aggregates [88-89]. Interaction with lipid membrane, involving anionic lipids such as phosphatidylserine, is shown to bring about a conformational change, causing an increase in α-helical content as well as aggregation of α-synuclein [90-91] and hIAPP [92]; whereas single molecule studies suggest that stability of α-synuclein's helical conformation is enhanced in the presence of lipid membranes [93]. Moreover, lipid rafts containing certain gangliosides and cholesterol are implicated in misfolding and aggregation of specific amyloidogenic proteins involved in neurodegenerative disorders [94-95].

## 1.2.3 Kinetics of amyloid aggregation

The sequence of events leading to amyloid formation can be set in motion by a preceding misfolding phenomenon, for instance certain denaturing conditions brought on by factors such as ionic strength of the buffer, temperature, co-solvents, and agitation. Irrespective of the cause, the precursor proteins are thus given the ability to form endlessly propagating aggregates that consist of varying number of the forming units, ranging from dimers to particles of million Dalton or even larger.

Looking at the molecular features of fibrils originated from unrelated proteins that barely have any sequence similarity, it could be observed that they are largely comprised of cross β–sheet structures [99]. However, fibrils are shown to exhibit polymorphism i.e. depending on the induction conditions a protein can give rise to multiple forms of amyloid fibrils with differing morphologies [100-101]. The former observation implies that a common mechanism leading to amyloid formation might be in play, whilst the latter observation can be construed such that amyloidogenesis occurs via multiple pathways [102].

The two models proposed to explain the mechanism of amyloidogenesis *in vitro* are nucleation dependent fibrillation and double-concerted fibrillation, the former being more widely accepted. Fibrillation kinetics of amyloidogenic proteins can be readily traced exploiting the fibril binding properties of Thioflavin-T dye. Accordingly, the kinetic process is consisted of three distinct phases each characterized by the presence of distinct (folding) species: the lag phase, the exponential growth phase, and the stationary phase [103].

The Lag phase represents the rate-limiting step in protein aggregation that requires prolonged incubation and can occur above a certain critical protein concentration.

During the lag phase formation of the nucleus from monomers takes place, which is thermodynamically unfavorable. Once the nucleus is formed, accretion of monomers following their conformational transition becomes thermodynamically favorable, leading to the exponential growth phase where a rapid extension of the fibrillar structure occurs. Fibril growth continues until the available monomers are depleted, thus begins the stationary phase where the assembled and disassembled monomers exist in equilibrium [104]. It has been empirically shown that the lag phase can be shortened or completely abrogated by adding pre-formed fibrils (seeds) to the solution resulting in immediate aggregation. In such a scenario the seeds act as a template while propagating their morphology and structure, thus giving rise to fibrils that acquire their characteristics. The seeds are comprised of amyloidogenic conformers that enable the conversion of other conformations, leading to their attachment to the ends of the growing fibril [52, 105-106].

The exponential growth phase is suggested to involve secondary pathways such as fibril branching and fragmentation that consequently furthers the number of growth sites [107-108]. *In vivo*, secondary nucleation is considered to be a key step in dictating the propagation of deposits [109].

The nucleation-dependent model of aggregation is usually illustrated as a sigmoidal shaped time-course curve, with the three phases distinctly separated (Figure 2). The various species that emerge during the course of aggregation can be mapped on this so-called sigmoidal curve. The first species that appear early in incubation during the lag phase are described as amorphous aggregates which may then align to form protofibrils, both representing transient intermediates. The oligomeric structures are reported to appear both on-pathway and off-pathway to fibrils [52]. On-pathway oligomers undergo a concerted conformational change to form fibrils [110] (Figure 2). These fibrillar structures are suggested to be very stable, sometimes even more stable than the native state [111].

In the double-concerted fibrillation, oligomeric species are subjected to shear stress and organic solvents that leads to instantaneous fibril formation. The model consists of two steps involving an initial assembly of the monomers followed by formation of oligomeric granular species. These oligomeric granular species are suggested to serve as a growing unit for fibril formation, though necessitating some structural rearrangement that involves shifting from intra-oligomeric interactions to inter-oligomeric [106].
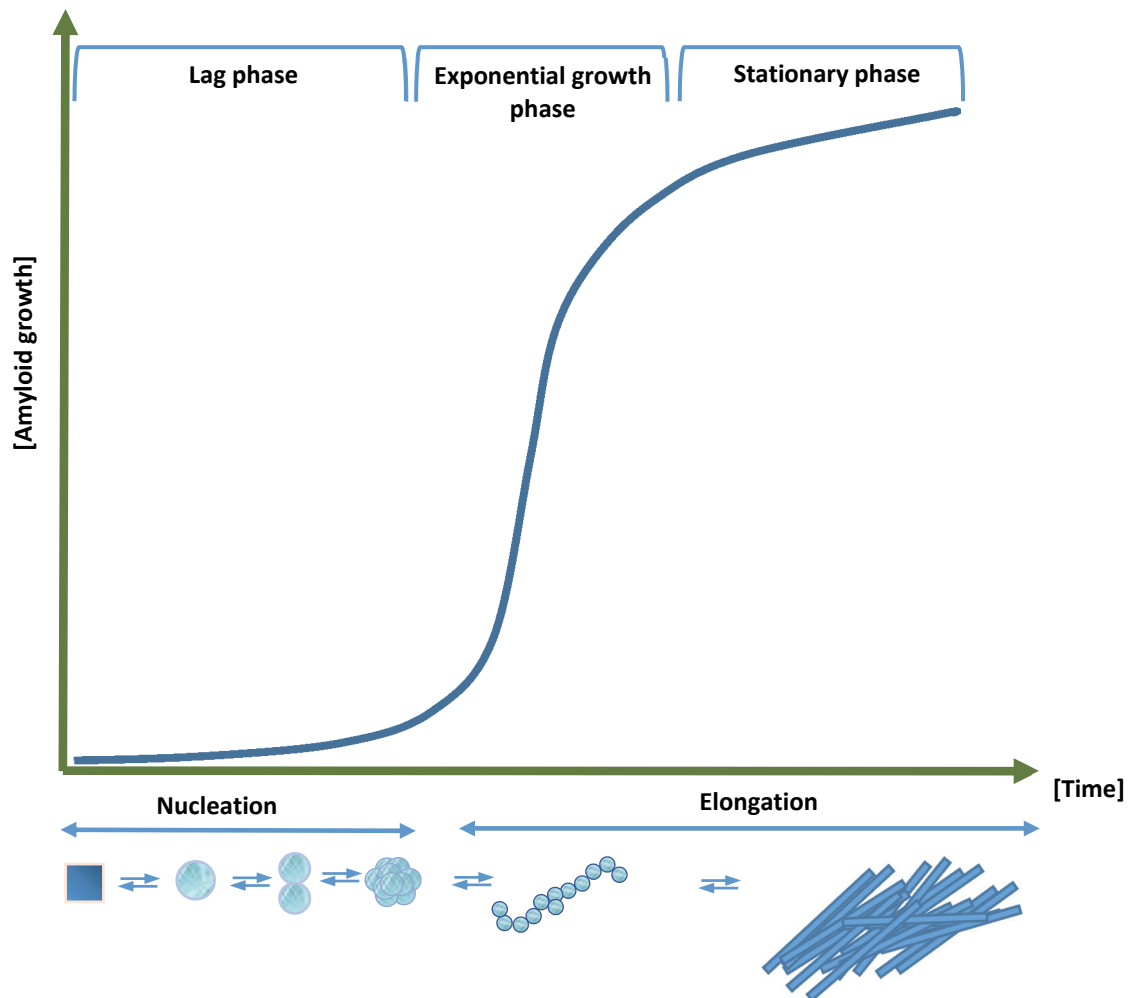
**Figure 2: Nucleation dependent model of aggregation.** Aggregation kinetics of amyloidogenic proteins consists of three distinct phases, the lag (nucleation) phase, the exponential growth (elongation) phase and the stationary phase. In the lag phase, the native form of monomeric proteins undergo conformational change converting to species capable of self-association that subsequently give rise to the oligomeric nucleus. In the growth phase monomers attach to the nucleus and thus form fibrils until saturation or depletion of the available monomers. The nucleation phase is thermodynamically unfavorable and therefore takes place over a prolonged time. Conversely, elongation is thermodynamically favorable and occurs rapidly.

### 1.2.4 Structural characteristics of amyloid

In order to be able to develop a deeper understanding about the nature of amyloidogenic diseases it is fundamental to gain insights into the structural details of the various species in play.

The degree of structural order is proposed to successively increase from oligomers to protofibrils to fibrils. The various aggregation variants may display some structural commonalities with each other as evidenced from their interaction with conformation-dependent antibodies that specifically recognize common epitopes. However, oligomers display different structural motifs that set them apart from fibrils, as evidenced by the existence of oligomer-specific antibodies. This may pertain to

differences in the organization of peptide backbone. It is posited for example that prefibrillar oligomers are composed of α–extended sheets, while fibrils are structurally β–sheets [112]. Likewise, differences in the twist, tilt, and hydrogen bonding are also hinted. Moreover, a broad range of morphologies has been reported for each species, depending on the aggregation conditions and the precursor protein [51]. Differences in the number of protofilaments giving rise to a fibril has also been observed under fixed conditions [113].

Progress in isolating and characterizing the allegedly toxic oligomeric species is largely impeded by their transient and dynamic nature. Studies with atomic force microscopy show oligomers to appear in various shapes including round, annular, and as beaded chains having diameters in the range of less than a nanometer to a few nanometers [110]. Oligomers can have a broad spectrum of molecular weights; as in the case of Amyloid-β ranging from 2 molecules to a million Dalton. Varying conditions of aggregation can cause changes in the packing of the hydrophobic groups, thus producing oligomeric species with differing toxic properties [51]. Moreover, conformation-dependent antibodies have indicated the presence of distinct types of oligomers, implying oligomeric polymorphism [114]. Recently oligomeric aggregates were shown to be detected upon binding to the dye ANS (8-Anilinonaphthalene-1-sulfonic acid) that specifically binds to exposed hydrophobic patches, indicating hydrophobic patches to be a common structural feature of soluble oligomers. Moreover, increase in ANS fluorescence intensity was correlated with increasing toxicity [115].

Unlike oligomers, the structure of amyloid fibrils has been extensively studied and is described as parallel, in-register β-sheets stabilized by intermolecular hydrogen bonds. The amyloid structure exhibits characteristic features on observation with electron microscopy (EM), X-ray fiber diffraction, and staining. Under EM fibrils appear to have long, unbranching, often twisted structure about 6-10 nm in diameter. X-ray fiber diffraction reveal a cross-β spine structure with two notable signals, a reflection at 4.7 Å along the direction of the fiber arising from the spacing between adjacent β-strands and a second reflection at 6-11 Å that occurs perpendicular to the fiber axis and corresponds to the distance between stacked β-sheets that can vary based on the composition of the side chains. Staining the fibrils with Congo Red produces an apple green color under crossed polarized light. Furthermore, staining with the dye Thioflavin-T results in an increase in fluorescence shift. The presence of high β–sheet

content can be detected both by CD and Fourier transform infrared (FTIR) spectroscopy [116-123].

Detailed structural studies show that the cross-β structure consists of β-sheets that create an interface by interdigitating the complementary side chains from the opposing sheets while excluding water molecules. This structural arrangement is referred to as a steric zipper. Depending on the orientation of the faces of the β-sheets, and the parallel or anti-parallel arrangement of strands, eight different classes of steric zippers can emerge. However, it should be noted that not all classes of steric zippers have been observed empirically. These steric zipper arrangements contribute to amyloid polymorphism by allowing amyloids to be packed in different ways [124-125]. With regard to the strand orientation, parallel structures are suggested to occur more frequently than anti-parallel, implying a more common structural motif for the majority of amyloids [126]. Another important aspect is the arrangement of the β-strands which can either occur in-register or out of register, though the former seems to prevail, probably since the latter is relatively less stable and is frequently associated with toxic oligomers [127]. There are vast differences among the fibril-forming precursor proteins, in terms of secondary structure, size, and sequence; yet the resulting fibrils, as noted above, share very high histochemical and structural similarities. This pertains to the core structure of the fibril that is composed of β-sheets and is predominantly stabilized by interactions involving hydrogen bonds of the main chain. The main chain is common to all protein molecules, explaining why fibrils derived from different proteins have similar characteristics. Nonetheless, structural organization of amyloid fibrils can be strikingly different, depending on the protein and the conditions of fibril formation, entailing the main chain to assume different arrangements. Considerable differences may exist in the number of residues from a single protein molecule packed into the core structure. Incorporation of the side chains essentially depends on the sequence. The identity of the incorporated side chains does not affect the general cross-β amyloid structure, though their interactions with each other and with the solvent significantly influence the details of the fibrillar architecture, including determining the length and orientation of the β–strands, the lengths and conformation of loops, turns, and other regions that are not part of the core structure, and lastly the number of β–sheets constituting the protofilament [128-129].

Hydrogen bonding between the side chains are shown to further contribute to the stability of the fibrillar structure [124]. The core structure is devoid of α-helical regions

and mainly consists of β-strands, and some β-loops and β-turns, these being responsible for determining the secondary structure of the fibril. The tertiary structure is defined by the alignment of strands into parallel and anti-parallel β-sheets, while the quaternary structure is molded by how the sheets are arranged with respect to one another [130].

It should be mentioned that structural studies are largely carried out using short segments of known amyloid fibril forming peptides, since fibers formed from *ex vivo* samples are too large and heterogeneous to be studied with the available techniques. High resolution structural studies of amyloid fibrils revealing subtle details has been enabled by using a combination of techniques including mutagenesis, solid-state NMR, and hydrogen deuterium (HD) exchange NMR, among others. Single point mutations, for instance, can unveil the importance of individual residues in the fibrillation process as well as in maintaining the overall structure [131-132].

## 1.2.5 Amyloid toxicity

Efforts in literature to elucidate the underlying mechanism of amyloid pathogenesis are centered on two key aspects, events corollary to the loss of proteins' physiological function and those induced by accumulation of amyloid deposits (gain of toxic function). Both aspects can be critical in determining the progress and severity of disease. Aggregation-prone proteins such as α-synuclein, Aβ, tau, and PrP$^{Sc}$ cause neurodegeneration as they form oligomers and gain a toxic function. Conversely, other proteins may lose their function due to aberrant folding, consequently affecting their substrates too. For instance mutations in parkin that lead to its misfolding can have far-reaching consequences. Parkin is a component of the E3 ubiquitin ligase complex that itself is part of the ubiquitin-proteasome system. Loss of parkin's function would therefore affect not only this immediate downstream substrate, but also other processes considering the role of ubiquitylation in various other cellular functions such as signal transduction, DNA repair, transcriptional regulation, endocytosis, and cellular trafficking [134].

A plethora of studies have established the connection between the amyloid state and various age-related diseases resulting from abnormalities in the folding process. However, the dilemma which species is primarily relevant to the disease generation remains outstanding. Substantial evidence has emerged indicating the precursor soluble oligomers as the species responsible, at least in part, for the amyloid pathogenesis [115, 135-137]. Though, all the non-native species generated can be

invariably toxic to a certain extent depending on the number and nature of exposed groups that otherwise would remain buried in the native state. These exposed groups can elicit aberrant interactions with various cellular components including membranes, proteins, and other macromolecules [136]. The role of fibrillar deposits, however, is less clear. It has been proposed that they might act either as a reservoir for a continuing supply of oligomers or as sinks of toxic oligomers; the latter follows the notion that they might be the end products of the detoxification process involving sequestration of the harmful oligomeric species; this would imply a protective role [138-140]. In case of Alzheimer's and Parkinson's diseases, it has been reported that there is no correlation between the severity of disease and the quantity of fibrillar deposits. In fact, symptoms were shown to manifest prior to the detection of such deposits, whereas in some cases patients with deposits did not show any symptoms. Levels of low molecular weight oligomeric species, on the contrary, were strongly linked with the disease severity. Mutational studies resulting in the generation of oligomers have also reinforced this toxic role. In addition, non-fibrillar oligomers were demonstrated to invoke toxicity in cell culture as well [141-144]. Systemic amyloidosis, conversely, represents a very different scenario since these are associated with large deposition of amyloid fibrils that can essentially infiltrate entire organs including heart, spleen, and liver, causing severe functional impairments in the contiguous tissues [145].

As pointed out, amyloidogenic species, both fibrils and oligomers, derived from structurally different precursor proteins, including those not associated with any disease, have a number of common structural features. Thus, with regard to the mechanism of toxicity, it is not surprising that the resulting pathological features would bear resemblance too [143].

The plasma membrane is proposed to be the primary target accessible to various oligomers arising both in the cytoplasm and in the extracellular compartments [139]. Though, oligomers are shown to subsequently disrupt intracellular membranes as well. Studies have shown that various amyloidogenic proteins including α-synuclein, Aβ, IAPP exert their toxic effects, at least partially, by forming discrete pores and single channels in the membrane; hence the channel hypothesis for explaining amyloid pathogenicity [143, 146, 147]. These channels are characterized as being irreversibly inserted into the membrane with heterogeneous and rather non-specific conductance properties. Such damages to the membrane can lead to changes in its permeability in particular with respect to ions, but also other molecules. A disturbance in ion

homeostasis such as that of $Ca^{2+}$ can have grave consequences for the cell fate, initiating a cascade of downstream events that may result in aberrant signal transduction, oxidative stress and apoptosis caused by an increase in the production of reactive oxygen species as well as release of cytochrome C; mitochondrial dysfunction, up-regulation of autophagy as well as changes in neuronal function involving synaptic plasticity, long-term potentiation and membrane potential [145, 149-152]. Dysfunction of the mitochondria might further aggravate the situation by being unable to supply the chaperone and proteasome systems with ATP, thus leading to further increase in the level of misfolded proteins [139]. Up-regulation of autophagy, triggered by the increase in amyloid aggregates, results in the accumulation of autophagic vesicles that may promote autophagy mediated programmed cell death [153]. Events leading to drastic increases in the aggregation rate would inevitably render the cellular defense mechanisms, including the chaperons and proteasome degradation systems, ineffective at preventing or containing the disease progress. As indicated disruption of the membrane is mainly instigated by oligomers, though mature fibrils are also shown to disassemble membrane lipids thus contributing to cell damage [154-156]. The lowest oligomeric species demonstrated to permeabilize the membrane were hexamers of Aβ 1-40 [157].

In addition to above-stated common mechanisms of amyloid pathogenicity, disease specific events may be attributed to the loss of function of the fibril forming protein itself and its various interacting partners. Another important consideration is the nature of the afflicted cell type. Since, cells with an effective stem cell population would be in a position to rapidly replace the affected cell with a new functional cell, making amyloid toxicity inconsequential. However, cells lacking in such potential arsenal might be particularly vulnerable, explaining why the majority of amyloid related diseases are neurodegenerative [139].


## 1.3 Protein misfolding and diseases

Protein misfolding is associated with the onset of numerous diseases (Table 1), by some estimates being accountable for close to half of all human diseases [133]. These disease are very heterogeneous in nature and their severity depends largely on the degree to which the affected protein's function is impaired. Furthermore, they have both sporadic and familial forms and can occur at various stages of life. They can have

a genetic origin or might ensue concomitant to other abnormalities at the cellular level accompanying advanced age.

Protein misfolding diseases currently represent the most common and debilitating medical conditions. For instance, Type II diabetes is estimated to affect approximately 300 million people worldwide [158].

Neurodegenerative diseases are characterized by progressive degeneration of the neurons with debilitating consequences that are largely untreatable. A key signature of these diseases is an increase in their incidence as the population ages, and with the increased life expectancy it will further continue to increase. Alzheimer's disease (AD), for instance, affects nearly 7 million people in Europe alone. Worldwide the number of sufferers stood at 26.6 million as of 2006. This figure is expected to double every 20 years, and estimated to reach 80 million during the next 40 years [161].

Regardless of the underlying mechanism of the respective protein misfolding disease, the presence of intra- and extra-cellular forms of insoluble aggregates that in the majority of cases cause the characteristic pathological lesions, is common to all [159].

**Table 1:** List of representative misfolding diseases

| Protein | Native structure | Disease | Ref. |
|---|---|---|---|
| α-synuclein | Intrinsically disordered | Parkinson's disease Dementia with Lewy bodies | [449] |
| Amyloid-β peptide (1-40/42) | Natively unfolded | Alzheimer's disease | [450] |
| Prion protein | Globular (α-helices+β-sheets) | Creutzfeldt-Jakob disease | [451] |
| Huntingtin | Largely natively unfolded | Huntingtin's disease | [455] |
| Tau | Natively unfolded | Frontotemporal dementia with Parkinsonism Alzheimer's disease | [447] |
| Islet amyloid polypeptide (Amylin) | Natively unfolded | Type II diabetes | [454] |
| Calcitonin | Natively unfolded | Medullary carcinoma of the thyroid | [448] |
| β2 microglobulin | All β | Dialysis-related amyloidosis | [452] |
| Lysozyme | Globular (α-helices+ β-sheets) | Lysozyme amyloidosis | [453] |
| Transthyretin | All β | Senile systemic amyloidosis Familial amyloid polyneuropathy Familial amyloid cardiomyopathy | [456] |

### 1.3.1 Synucleinopathies

Synucleinopathies are a group of overlapping neurodegenerative diseases characterized by the abnormal accumulation of α-synuclein aggregates in neurons, nerve fibers or glial cells in certain regions of the brain including the striato-nigral system, limbic system, frontal cortex, the insula, and subcortical nuclei [162-164].

The well-known synucleinopathies include Parkinson's disease (PD), Parkinson's disease dementia (PDD), dementia with Lewy bodies (DLB), and multiple system atrophy (MSA). In addition, various neuroaxonal dystrophies are also members of this group, though they are less-well characterized [165, 166].

Fibrillar aggregates of α-synuclein form proteinaceous intracellular clumps that are referred to as Lewy bodies and Lewy neurites in PD and DLB [167-169, 171], glial cytoplasmic inclusions in MSA and axonal spheroids in neuroaxonal dystrophies [170]. In addition to α-synuclein the clumps contain large amounts of ubiquitin.

Substantial evidence exists which implicates misfolding of α-synuclein as the underlying event leading to synucleinopathies [4].

# 2 α-Synuclein

## 2.1 Expression and localization

α-Synuclein was first identified in the synaptic terminals and the nucleus, where it derives its name from [172]. Later it was described as the non-amyloid component in plaques of amyloid-β isolated from the brains of patients with Alzheimer's disease [173]. The protein, in particular the canonical SNCA140 isoform, is abundantly expressed in various parts of the brain. High levels are particularly detected in neocortex, hippocampus, substantia nigra, thalamus, and cerebellum, though it is also present in the red blood cells. The other three alternative isoforms i.e. SNCA- 126, 112, 98 are expressed at relatively low levels [174-176]. α-Synuclein constitutes about 1% of the protein content of the neuronal cytosol, though to a lesser extent it could also be found in the glia cells. High concentrations of the protein are found in presynaptic terminals in both soluble and membrane-bound forms, with roughly 15% being membrane bound in any moment in neurons [177-178]. It is extensively localized in the nucleus as well, suggesting a function therein [174, 179]. Mitochondrial localization of the protein is

evidenced, but varies according to the brain regions, being highly expressed in olfactory bulb, hippocampus, striatum, and thalamus [180].

## 2.2 Physiological function

Despite the vast number of studies the exact function of α-synuclein still remains elusive. Though localization of the protein in various parts of the neurons might provide some clues about its role under normal as well as in disease states. Some of the proposed functions ascribed to α-synuclein include regulation of certain enzymes, transporters, and neurotransmitters, synaptic plasticity, neuronal survival, and chaperon function. Moreover, it is shown to interact with at least 30 proteins, indicating its role in cell signaling [181].

Evidence for α-synuclein's role in synaptic function, though poorly defined, has come from its localization in the presynaptic terminals where it is indicated to be involved in the regulation, storage, trafficking, and release of synaptic vesicles, and consequently in the turnover of neurotransmitters in particular dopamine. This role has been recently supported by the discovery that α-synuclein plays a critical role in controlling the degradation and affecting the assembly of SNARE complexes that are essential in releasing neurotransmitters from vesicles. More evidence for this role has emerged from studies involving α-synuclein's overexpression and knockdown models, exhibiting impairment in synaptic transmission and marked reduction in the pool size of vesicles [182-188]. In its bound state to the membranes, α-synuclein plays a key role in preventing the oxidation of membrane lipids [189]. It also contributes to neuronal survival by controlling the apoptotic response [190, 191]. Evidence for the neuroprotective function of α-synuclein has emerged from another study as well where neurons were exposed to chronic oxidative stress. It was found that neurons that expressed high levels of α-synuclein exhibited relative resistance to apoptotic changes and their viability remained unaffected as compared to a control population of cells lacking α-synuclein [192]. Instances of such protective role have been observed elsewhere too [193]. Knock-out mice for α-synuclein were shown to remain viable, implying that it may not be essential for a functioning nerve terminal; however, its neuroprotective role was proposed to become more prominent under conditions of stress or injury [194, 195].

Proponents of α-synuclein's neuroprotective role argues that degeneration in dopaminergic neurons induced by α-synuclein aggregates might be a selective case, further pointing to the lack of consistency in such results [159].

## 2.3 Structural features

### 2.3.1 Sequence organization

α-Synuclein is encoded by the SNCA gene that is mapped to chromosome 4q21.3-q22. The gene consists of seven exons, five of them being protein-coding [196]. Through alternative splicing the gene produces at least four isoforms, the full length transcript with 140 amino acids, a 126 amino acid variant lacking exon 3 (residues 41-54), a 112 amino acid version that lacks exon 5 (residue 103-130), and the 98 amino acid version that lacks both exon 3 and 5 [197, 198]. The sequence of the full-length version has three structurally distinct domains (Figure 3): The N-terminal amphipathic region comprised of residues 1-60, and contains four 11-amino acid imperfect repeats that include a conserved consensus sequence KTKEGV; the central part of the protein contains three more repeats and the highly amyloidogenic and hydrophobic NAC (non-amyloid component) region; and the C-terminal part of the protein that is made of residues 96-140 and is highly acidic and proline-rich. This part of the protein is not conserved and is believed to bear sites for interaction with other proteins, small molecules, and metals [199], while the N-terminal and central regions are suggested to modulate interactions with the membranes. Moreover, the C-terminus acts as an intramolecular chaperon whose truncation destabilizes the protein thus enhancing its aggregation [200]. Conversely, the NAC region is suggested to be indispensable for aggregation, its deletion in both *in vitro* and cell based assays was shown to result in diminished aggregation [201]. The N-terminus of the protein include the sites for the five mutations characterized so far.
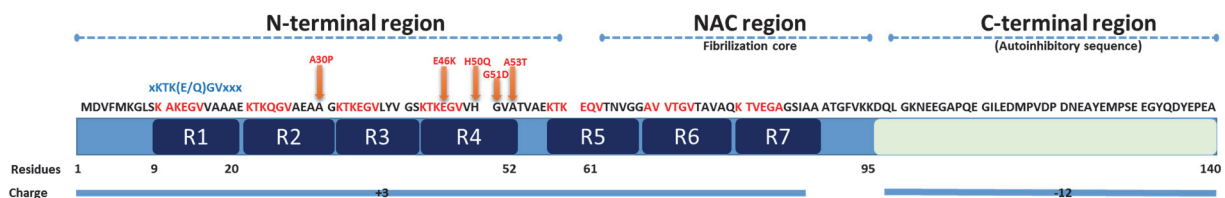


**Figure 3:** Schematic representation of human α-synuclein structural features. The N-terminus binds to cellular membranes and adopts a helical conformation. It also contains the sites of the five familial mutations A30P, E46K, H50Q, G51D and A53T. The NAC region is essential in promoting α-synuclein aggregation. The negatively C-terminal part of the protein is suggest to inhibit *in vivo* spontaneous aggregation of the protein mediated through its interaction with the other regions in a process known as functional misfolding. Net charge values determined at pH 6.

**2.3.2 α-Synuclein an IDP**

α-Synuclein belongs to the group of intrinsically disordered proteins (IDP) and displays extensive conformational flexibility [202]. The cause of its disordered state can be traced to its sequence that exhibits a profuse presence of disorder-promoting residues, in particular Gly, Glu, and Lys, whereas there is a paucity or lack of order-promoting residues such as the bulky hydrophobic amino acids (Ile and Leu) and aromatic amino acids (Trp, Tyr, Phe). Moreover, the sequence is devoid of Cys residues, which contribute to the conformational stability in proteins by forming disulfide bridges or through coordination of different prosthetic groups [203, 204].

Unlike globular proteins that have a well-defined global energy minimum in their energy landscapes, IDPs have a flat energy landscape with numerous shallower local energy minima without large energy barriers. This explains the conformational malleability of α-synuclein that allows it to sample a variety of conformations; however, depending on the prevailing conditions in its milieu and the presence of potential interaction partners, it can adopt specific structures [204]. Another aspect that sharply contrasts IDPs from globular proteins is in their predisposition to interact with unwanted partners. Globular proteins have evolved the ability to avoid such interactions by burying susceptible residues within their core structures. Given their sticky and promiscuous nature, IDPs may readily interact with non-native partners. However, it is proposed that IDPs have a protective mechanism in place, known as "functional misfolding", that avoids such unwanted interactions by involving predisposed residues in intramolecular non-native interactions, representing a sequestration process. This concept was illustrated to be valid for a number of proteins, including α-synuclein. It is noted that α-synuclein adopts varying structures in its unbound state and in complex with other proteins. The compact structure adopted in the unbound state was ascribed to intermolecular interactions between the various regions of the protein [205].

In its unbound state α-synuclein was shown to be unfolded and devoid of a tertiary structure [199]. Nevertheless the protein is not entirely without structure, as around 100 residues on the N-terminus of α-synuclein were reported to have propensity to form helical structures, while residues 1-13 and 20-34 were shown to have a nascent or transient α-helical structure [206]. Various experimental and simulation studies have revealed the presence of transient long-range interactions within the structure of α-synuclein that lead to the formation of hydrophobic clusters rendering the protein a certain degree of compactness. These interactions were indicated to be due to the

electrostatic attraction between the highly acidic and negatively charged C-terminus (residues 120-140), which carries a net charge of -8, and the somewhat positively charged central region that carries a net charge of +3. The presence of these long-range interactions were also proposed to underlie inhibition of spontaneous aggregation; therefore truncation of the C-terminus might lead to its rapid aggregation [207, 208].

### 2.3.3 Various conformers

Studies on recombinant α-synuclein expressed and purified from *E. coli*, under both native and denaturing conditions, have shown the protein to appear as an unfolded monomer. Moreover, it adopts β-sheet structure in the aggregated state and an α-helical structure upon binding to synthetic or biological membranes (Figure 4) [199, 209]. However, little is known about the available conformational state(s) present *in vivo*. The existence of the putatively monomeric state of the protein *in cellulo* has been recently challenged by studies proposing that the endogenous protein, obtained from various cell types including red blood cells and brain tissue under native conditions, occurs as folded tetramer with predominantly helical structure, which does not form toxic aggregates [210, 211]. However, these findings are still a matter of debate and have not been verified by others who still maintain that the protein retains its monomeric disordered state [212, 213]. In order to reconcile these contradictory views Gurry *et al.* generated a construct that consisted of an ensemble of α-synuclein states, predominantly populated by the monomers with some multimers (trimers and tetramers), primarily possessing helical but also some strand structures [214]. This could reflect that these dynamic structural ensembles might interconvert between the various states [215, 216].

Indeed, it is perceivable that α-synuclein might exist in equilibrium between the various conformational states. Though various events might substantially alter this equilibrium favoring one conformation or the other.

### 2.4 Aggregation

Aggregation of α-synuclein occurs in a nucleation-dependent manner yielding the typical sigmoidal curve that is comprised of the three distinct phases, the lag phase followed by the exponential growth and saturation phases [101, 217].

Aggregation of α-synuclein can give rise to both oligomeric and fibrillar species with distinct structural properties that are sensitive to variations in the aggregation
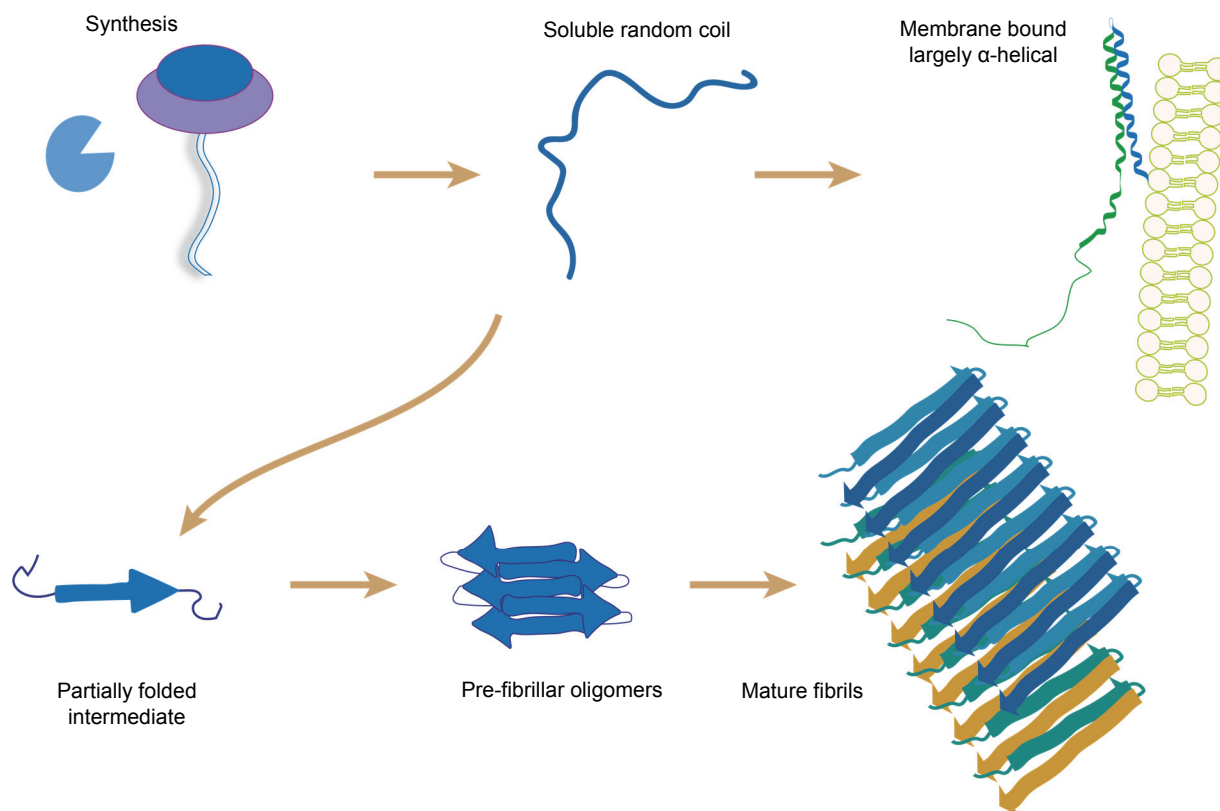
**Figure 4: Schematic representation of various α-synuclein conformers.**
Under physiological conditions α-synuclein primarily exists in a soluble random coil state. Binding to lipid membrane induces structural changes causing transition of part of the protein from random coil to α-helical conformation. Under pathological conditions, various events can trigger the conversion of the random coil state to a partially folded intermediate that is capable to self-assembly. This in turn progresses to form the toxic pre-fibrillar oligomers that finally transform to mature fibrils.

conditions [323]. The resulting fibrils are highly structured and conform to the global structural features of fibrils. They are composed of several protofilaments consisting of a cross-β structure in which the β-strands are arranged in parallel and the β-sheets in-register. Solid state NMR studies on *in vitro* grown fibrils revealed that the core of the fibrils is comprised of five β-strands involving residues 38-95 that also include the NAC segment, while the N-terminus remains rigid and the C-terminus unstructured and mobile [132, 219, 323]. Moreover, only the core region of the fibrils (residues 31–109) showed resistance to protease K digestion [218].

The population of oligomeric species are reported to be structurally diverse, some rich in β-sheets and others largely disordered, while those formed at the early stages of the aggregation being primarily α-helical [220]. Oligomers were shown to lack the canonical cross-β fibrillar fold [324], and unlike the majority of fibrils the arrangement of their β-sheets appeared to be anti-parallel [325]. Moreover, their core structure spanned

residues 4-90, as shown by Tryptophan (Trp) fluorescence and deuterium exchange studies [326-328].

Aggregation of α-synuclein is proposed to occur through a multitude of pathways and is promoted by a host of factors that give rise to conformational states that readily self-associate.

## 2.4.1 Factors influencing α-synuclein aggregation

There are numerous factors that enable conversion of α-synuclein from its unfolded form to a partially folded intermediate, which is indicated to be the precursor to fibril formation (Figure 4). These include: low pH and high temperature, agitation, polyvalent cations, di- and tri-valent metals, anions, high ionic strength, glycosaminoglycans, molecular crowding, as well as various pesticides such as rotenone, paraquat, and dieldrin [209, 225-228]. Conversely, factors capable of inhibiting α-synuclein fibrillation are also reported, such as β- and γ-synuclein and catecholamines, as well as oxidation of α-synuclein at methionine residues and its nitration. Moreover, certain factors that both inhibit and accelerate the fibril formation process depending on the conditions employed, include membranes and lipids [229, 230], simple and fluorinated alcohols [231], and osmolytes [232].

These factors are detailed in the following.


## 2.4.1.1 Effects of pH and temperature

It is proposed that the low hydrophobicity and high net charge render α-synuclein its natively unfolded structure. Changes in these two parameters, for example due to low pH or high temperature, are reported to induce partial folding of the protein that lead to the formation of the self-assembling intermediates [209].

## 2.4.1.2 Effects of factors intrinsic to the sequence

**Isoforms:** A recent study compared the aggregation properties of the full length α-synuclein with those of the other three isoforms and discovered that the alternative isoforms aggregated far less in comparison to the full-length protein. Differences were also observed in the resulting aggregates, such that the full-length protein formed straight fibrils, while the 126 and 98 amino acid isoforms formed short fibrils and annular structures, respectively [176].

**Mutations and polymorphisms:** To date five different missense mutations have been identified in the SNCA gene: A53T (Ala to Thr), A30P (Ala to Pro), E46K (Glu to Lys),

H50Q (His to Gln) and G51D (Gly to Asp). All of these are dominant mutations, implying a gain of function [233-235].

A53T was the first mutation identified that was genetically linked to early-onset Parkinsonism where the carrier exhibits cognitive decline and dementia. This mutation does not induce significant structural alterations, though a marginal increase in preference for extended conformation around the site of mutation is noted [236, 237].

A30P is involved in late-onset Parkinsonism and is found to strongly influence the structure by attenuating the helical propensity of the N-terminus of the protein [238]. E46K is associated with the early-onset DLB, and causes subtle structural changes while enhancing contacts between the N- and C-terminus of the protein [239]. All three mutations promote aggregation of α-synuclein. A53T and E46K are shown to enhance fibril formation, while A30P accelerates formation of oligomers. Furthermore, formation of specific species can be induced by introducing artificial mutations to the sequence, such as A56P and E57K that solely produce oligomers highly toxic to dopaminergic neurons [240, 241].

H50Q and G51D are two other mutations recently added to the list, the latter is associated with early-onset PD showing rapid progression [242, 243].

Overexpression of the SNCA gene resulting from quantitative mutations such as duplication and triplication are also reported to increase the risk of PD and DLB. Since these multiplications drive overexpression of the protein their effects are dose-dependent i.e. triplication results in the early development of fulminant Parkinsonism dementia, while carriers of duplication manifest later-onset PD, DLB or multiple system atrophy [244-247].

**2.4.1.3 Post-translational modifications**

Following translation in the ribosome, α-synuclein undergoes a series of post-translational modifications. They can have substantial effects in modulating the function and aggregation of α-synuclein, though the effects of such modifications are largely residue-dependent. The most important of these is phosphorylation that mainly occurs at serine residue S129. Phosphorylation at this position has been reported to enhance formation of aggregates [248, 249]. Phosphorylation at other sites such as S87, however, has been demonstrated to block its aggregation while increasing its conformational flexibility *in vitro* [250]. Ubiquitination is the second most prevalent modification resulting in attachment of ubiquitin mainly at lysine residues K6, K10, and K12, and is suggested to cause alterations in α-synuclein's function, localization and

degradation processes [251]. This modification, however, is not required for degradation of the monomeric form of α-synuclein, implying its occurrence subsequent to α-synuclein's aggregation [200]. Another important modification involves nitration of α-synuclein at various tyrosine residues, Y39, Y125, Y133 and Y136. Nitration at these positions is stated to decrease α-synuclein's binding to the lipid membrane and induce further unfolding in its structure, thus promoting aggregation. In contrast, *in vitro* experiments showed that nitration at neutral pH completely inhibits fibril formation, probably due to formation of a stable soluble oligomer [317]. Levels of phosphorylation and nitration in Lewy body diseases are noted to significantly increase [252, 253]. Oxidation of α-synuclein at methionine residues causes to disrupt its structure, leading to a highly unfolded structure that is less prone to aggregation [71]. Moreover, both N-terminal and C-terminal truncations have been reported, whereas those of the C-terminus are more common and result in very aggregation-prone fragments often associated with Lewy bodies [255]. In addition to the above state modifications α-synuclein is reported to undergo a number of other, though less frequent, modifications including SUMOylation, glycation, N-terminal acetylation, and various crosslinking reactions [197].

### 2.4.1.4 Various interaction partners

**Interaction with the lipid membrane**

Around 15% of α-synuclein is found in the presynaptic terminal in the membrane-bound form [256]. The presence of various lysine and glutamate residues in its sequence allow α-synuclein to bind to cellular membrane lipids that have a negative net charge *viz.* acidic. As a result α-synuclein is shown to undergo structural transition with a steep shift in its secondary structure from the unfolded random-coil to predominantly α-helical, with its helical content increasing from around 3% to 70% [90, 257]. *In vitro* studies show that interactions with membranes can both inhibit and promote the aggregation kinetics of α-synuclein, depending on the conditions employed in the experiment [198, 258].

**Interactions with other proteins**

α-Synuclein is known to interact with a broad array of other proteins. A SILAC based study on dopaminergic MES cells revealed 324 different proteins to be involved in formation of complexes with α-synuclein. Following differentiation of the cells with rotenone, 141 of those proteins displayed significant changes in the relative

abundance i.e. increase or decrease. Proteins identified were functionally categorized into DNA/RNA binding protein, chaperone, cytoskeleton, metabolism, protein synthesis, mitochondrial protein, ribosomal protein, protein related to signal transduction, and unknown functions [259].

In case studies, α-synuclein was to date shown to interact with around 50 ligands and proteins [191]. Some of the most prominent proteins studied individually for their interaction with α-synuclein include: Aβ [261-264], tau protein [265], PLD2 [266], parkin [267], synphilin [268], 14-3-3 protein [269], heterodimeric tubulin [270], phospholipase D [271], protein phosphatase 2A [272], DJ-1 [273], histones [274], and calmodulin [275]. Aβ, Tau, tubulin, and histones are proposed to stimulate aggregation of α-synuclein even at sub-stoichiometric concentrations in *in vitro* experiments. Given their aggregation-prone nature, these proteins are suggested to be involved in cross-seeding the aggregation of α-synuclein *in vivo*. Conversely, interaction with various chaperones was shown to suppress α-synuclein aggregation [177, 276].

It has been noted that interactions of α-synuclein with other proteins are affected by both post-translational modifications as well as point mutations associated with familial forms of diseases [200].

### Interaction with beta and gamma synuclein

β- and γ- synuclein are also members of the synuclein family, being 78% and 60% identical to α-synuclein, respectively and are abundant in brain. In spite of the structural similarities β-synuclein does not form any fibrils, while γ-synuclein forms soluble oligomers. Both β- and γ- synuclein are shown to inhibit aggregation of α-synuclein *in vitro* [277] and *in vivo* [278]. Neither β- nor γ- synuclein is found in Lewy bodies, but they are both associated with the hippocampal axon pathology in PD and DLB.

### Interaction with catecholamines

Dopamine and other catecholamines such as L-dopa are reported to inhibit α-synuclein fibrillation, and were shown to dissolve pre-formed fibrils yielding soluble oligomers. Inhibitory effect was stronger following oxidation of these compounds [279, 280]. This could be particularly important in PD pathology where the neurons substantially lose their anti-oxidant potential.

### Interactions with metals

Various metals are reported to directly cause damage to the brain. However, their role in influencing the aggregation of α-synuclein might underlie another mechanism

contributing to the increased incidence of PD in environments containing high levels of heavy metals. Some metals are indicated to directly interact with α-synuclein and induce structural changes that give rise to partially folded intermediates. Others might effect such structural changes, for instance, through oxidation [225].

Although the influence of the above-mentioned factors is well characterized *in vitro*, their relationship to aggregation *in vivo* is yet to be elucidated. Some work in this area has been carried out in cell models over-expressing α-synuclein [221, 222]. Though the recovered protein primarily appears as soluble monomers on SDS-PAGE gels [223], which makes it hard to translate its effects as well as to assess what species to hold accountable for the toxicity. A solution to this problem would be to make use of fluorescence lifetime imaging-based techniques. For instance, a recent study examined aggregation of α-synuclein in the cortex of a transgenic mouse model with moderate overexpression levels of the protein mimicking those of the multiplication mutations. The work employed multiphoton FRAP and labelled the protein with GFP. Results demonstrated that somatic α-synuclein was largely in unbound and soluble form, whereas α-synuclein in the presynaptic terminal existed in three different forms, unbound and soluble, bound to the vesicles, and as micro-aggregates [224].

## 2.5 Mechanisms underlying α-synuclein's toxicity

Levels of α-synuclein present in the CNS are governed by its synthesis, aggregation and clearance that under physiological conditions are rigorously kept in balance. However, a dysregulation in any of these processes can effectuate aberrant levels of the protein leading to the formation and/-or accumulation of toxic species while depleting the functioning protein [281-286]. Increased accumulation of the protein is suggested to activate pathways that lead to cell death [342]. As evidenced in the familial forms of Parkinsonism, synthesis of α-synuclein can be elevated due to multiplication of SNCA gene, while certain mutations are conducive to increasing its propensity to aggregate.

Clearance of α-synuclein monomers and aggregates is mediated through components of the cellular housekeeping mechanisms including direct proteolysis [287], molecular chaperones [288], the proteasome degradatory pathway [289], and the autophagy signaling cascade [290]. Disruption in any of these mechanisms can result in impaired clearance of the protein. For instance, mutant and oxidized forms of α-synuclein [291]

and overexpression of the wild-type in cell culture and *tg* mice is associated with impaired autophagy [292].

Different conformers of the protein are linked with the pathogenesis of LBD. It is suggested that the main culprits promoting toxicity and neuronal loss might be the oligomers, as indicated by data gleaned from numerous studies [143, 240, 293-295]. Though it must be noted that the extant evidence is largely circumstantial, since it mainly comes from cell culture models. Studies in animals in support of this hypothesis are relatively rare due to the limitations associated in working with *in vivo* models [329].

Conversely, the more stable and less toxic mature fibrils are suggested to be the result of a protective mechanism attempting to sequester the more toxic species. Unlike fibrils that essentially accumulate in inclusion bodies, localized in the soma, oligomers are located in the axon and presynaptic nerve terminal [222].

Oligomers are proposed to exert their toxicity by causing damage to the membrane intactness leading to alteration in its permeability to various ions, such as calcium [295]. Pore formation by α-synuclein oligomers might potentially affect several targets. For instance it might trigger the leakage of vesicles containing neurotransmitters with detrimental effects on synaptic function [296-297]. Studies in *S. cerevisiae* showed impaired vesicle trafficking from endoplasmic reticulum (ER) to Golgi [324]. Such functional disruptions of the ER, Golgi, as well as microtubules were reported elsewhere too [298-300]. Damage to the mitochondria has been observed in various cell models [299, 301, 302] and *C. elegans* [303]. Prolonged dysfunction of the mitochondria is proposed to result in ATP depletion, diminished calcium buffering, and increased oxidative stress [304].

Impairment of the protein degradation machinery *viz.* the ubiquitin-proteasome system (UPS) and lysosomal systems including autophagy has also been indicated in cell models. Though the exact mechanism is not known, disruption to the proteasome could be mediated through mitochondrial damage which results in depletion of ATP, or through direct binding of α-synuclein to the proteasome [305]. Alteration of lysosomal function is also evidenced that could either be a consequence of the proteasome inhibition or oligomer-induced leakage of the lysosome [306, 307].

In addition, toxicity may further be extended to the loss of functional α-synuclein, its mislocalization, as well as a gain of toxic function. α-Synuclein is involved in modulating enzymes responsible for dopamine synthesis [308], therefore diminished levels of functional α-synuclein can affect dopamine reserves and consequently synaptic

function. α-Synuclein is also shown to cause synaptic dysfunction by interfering with axonal transport of certain synaptic proteins such as synapsin 1 [222]. Toxicity of α-synuclein is evidenced to be more selective in dopaminergic neurons [309] probably due to the ensuing oxidative stress that promotes dopamine's oxidation, producing toxic metabolites [310, 311]. Misfolded forms of monomeric α-synuclein may also contribute to toxicity by disruption of specific cellular process as well as aberrant interaction with other proteins, small molecules, and membranes [188].

Various apoptotic markers have been detected in association with α-synuclein toxicity in cellular models, though how cell death is triggered remains unknown. It is suggested that α-synuclein dysfunction may give rise to reactive oxidative species (ROS) that in turn activates the apoptotic mechanism. Moreover, the role of mitochondria in regulating the apoptotic signal should also be noted [223, 312].

## 2.6 Cell-to-cell propagation hypothesis

α-Synuclein is an intracellular protein, though recent studies suggest that under pathological conditions both monomeric and aggregated forms are released via exocytosis from neuronal cells, without compromising the integrity of the membrane. The released species are next assimilated by contiguous neurons and glial cells via endocytosis [313]. This extracellular α-synuclein is suggested to contribute to the disease pathology by subsequently nucleating further aggregation and thus driving the dissemination of the aggregates to other parts of the brain [315,316]. Exposure of astrocytes to extracellular α-synuclein induces changes in their gene expression profile leading to inflammatory response, accompanied by activation of microglia that in turn generates ROS, nitro oxide (NO) as well as cytokines, thus further aggravating the course of neurodegeneration [317]. This observation led to the idea that extracellular α-synuclein seeds might behave in a prion-similar manner [188, 318]. Moreover, lower levels of α-synuclein have also been observed in cerebrospinal fluid (CSF) in patients suffering from AD and is proposed to originate from CNS [319-322]. Elevated levels of α-synuclein oligomers are also reported in plasma [322].

## 2.7 α-Synuclein, a therapeutic target in synucleinopathies

At present, no cure exists for synucleinopathies and the available treatment options are only palliative, i.e. they only mitigate the symptoms of the disease.

Devising disease-modifying therapeutic strategies to contain the progress of or yet better to prevent or cure the disease predicates targeting the molecular origin of the

disease, which could be enabled by furthering our understanding about the involved culprits and the underlying mechanisms of pathogenesis in play. As pointed out early, under pathological conditions the balance between α-synuclein synthesis, aggregation, and clearance is disturbed that leads to the generation and accumulation of various intracellular and extracellular conformers. While tentatively posited, it is yet to be determined whether toxicity resides in the insoluble aggregates or the soluble oligomeric precursors. Target-oriented approaches should be aimed at restoring the normal levels of α-synuclein. This can be achieved by reducing its expression level, increasing the stability of functioning protein, inhibition of self-assembly into oligomers and fibrils, and increasing the clearance rates [188, 330].

Expression level can be down-regulated for instance by silencing *SNCA* with microRNA or by repressing the gene promotor [188]. Promoting clearance would require bolstering and meshing the function of the underlying mechanisms, for instance by increasing the proteolytic breakdown and binding to chaperone like molecules such as β-synuclein and HSPs, as well as by upregulating the autophagy system. Reduction in certain PTMs such as phosphorylation and C-terminal truncations might likewise prove helpful.

The other two approaches, stabilizing the native form and reducing self-assembly have prompted a lot of research interest. Aggregation inhibitors currently in research are divided into three categories: small molecules, short peptides, and antibodies and antibody-mimetics [318].

## 2.7.1 Small molecules

Low molecular weight organic compounds including polyphenols and non-polyphenols are identified to block self-assembly of amyloid-forming proteins. This is suggested to involve engaging the hydrophobic residues of amyloidogenic protein through interaction with or binding to the polyphenolic aromatic ring and its hydroxyl group, respectively [331-332]. Likewise, the anti-oxidant property of polyphenols plays a role in alleviating the ROS mediated cytotoxicity of amyloidogenic proteins [333]. Some of these molecules are shown to inhibit the aggregation of many amyloidogenic proteins while others act more selectively.

Epigallocatechin gallate (EGCG) is one such representative molecule that is indicated to efficiently inhibit the fibrillogenesis of α-synuclein by directly binding to the natively unfolded protein and promoting the generation of off-pathway non-toxic and unstructured α-synuclein oligomers, instead of the toxic β-rich intermediates [334-335].

Curcumin is another member of this group and exhibits similar effects both *in vitro* and in SH-SY5Y cell line in inhibiting aggregation of α-synuclein [336-337].

A particular advantage presented by both EGCG and curcumin is their ability to cross the blood brain barrier (BBB) as confirmed by studies in animal models [338-339].

Baicalein, also a polyphenol, is shown in *in vitro* studies to both inhibit fibrillation of α-synuclein and disaggregate pre-formed mature fibrils [340]. The inhibitory effect was also observed in SH-SY5Y cells [341].

### 2.7.2 Short peptides

The core forming sequences of the amyloidogenic proteins are considered to be self-recognizing i.e. these regions recognize and interact with each other, and may consequently assemble into fibrils [318]. This concept has been exploited for developing synthetic peptide inhibitors based on the native sequence of amyloidogenic protein. Such inhibitors are also developed for α-synuclein consisting of the hydrophobic residues 68-72. These are next modified and flanked by two hydrophilic residues. The inhibitors are found to interact with the full-length protein and block its self-assembly into oligomers and mature fibrils [342].

### 2.7.3 Antibodies

Immunotherapy as a treatment modality for neurodegenerative diseases has been a long-standing focal point in research in particular for targeting and clearing extracellular aggregates accompanying diseases such as Alzheimer's amyloid-β. Other neurodegenerative diseases involving proteins such α-synuclein, prion protein, tau, and huntingtin are mainly characterized by the presence of intracellular aggregates, implying that they cannot be readily recognized by the immune system. Though the recent discovery that these aggregates may also accumulate on the plasma membrane and can be secreted to the extracellular environment, has provided the rationale to employ immunotherapy in these stated pathologies as well.

Essentially two categories of immune responses can be differentiated, the humoral and cell mediated. Harnessing humoral immunization involves either stimulating the immune system itself to produce antibodies directed towards the target i.e. active immunization, or directly administering target-specific antibodies to the patient i.e. passive immunization. Cell-mediate immunity involves activation of various components of the immune system including phagocytes, natural killer, cytotoxic-T cells as well as numerous cytokines [318]. The potential of all these versatile tools for application in synucleinopathies has been well explored [343-346].

Studies in transgenic mice model vaccinated with α-synuclein showed the production of antibodies with relatively high affinity that led to the reduction of the accumulated aggregates with concomitant reduction of neurodegeneration. In addition, degradation of aggregates, probably via the lysosomal pathway, was also indicated [343]. The first PD vaccine, named AFFITOPE PD01, entered into phase I clinical trials in early 2012 [347]. The vaccine was initially tested in two mouse models and was shown to ameliorate the neuronal loss caused by α-synuclein. It consists of a peptide-carrier conjugate and does not evoke an autoimmune response. However, active immunization has been known to elicit immune response when administered in patients even if this is not predicted or observed in preclinical studies [348]. Therefore, at present research is largely focused on passive immunization that targets specific epitopes on α-synuclein. The 9E4 monoclonal antibody targets the C-terminus region of α-synuclein (residues 118-126). Immunization of α-synuclein *tg* mouse model led to reduced α-synuclein accumulation and neuronal loss as well as amelioration of motor deficits [344]. This was proposed to result from clearance of extracellular α-synuclein by microglia via the Fcγ receptor located on the cell surface that facilitates its delivery to the lysosome [349]. Reduction in extracellular α-synuclein translates into curbing the disease propagation and enhanced neuroprotection, thus representing a key leverage. The 9E4 anti-α-synuclein antibody (PRX002) is currently being tested clinically.

Though antibodies might show their potential in targeting extracellular aggregates, the lack of reliable means to bring them into the cells renders them unsuitable for targeting intracellular aggregates. This problem has been addressed by developing small fragments of antibodies through genetic-engineering that are stably expressed in the cells, these are called intracellular antibodies or intrabodies and are especially applied in the scFv format [350]. Two anti- α-synuclein scFv intrabodies have been identified to effectively inhibit α-synuclein aggregation and the resulting toxicity. The D10 intrabody binds monomeric α-synuclein; its co-expression in HEK293 cells was shown to inhibit formation of high molecular weight species [351]. The second intrabody NAC32 was tested in two separate cell culture models and showed significant reduction in α-synuclein aggregation [352].

## 3 Protein engineering: A versatile tool

The orchestrated functioning of biological processes is mediated through the precise interaction of a large network of proteins. Moreover, there is an inherent relationship

between the sequence, structure, and function of proteins. Protein engineering involves exploiting this underlying relationship to effect desired changes in the structure and/or function of a given protein.

There are two strategies to engineer proteins, rational design and directed evolution. The rational design approach employs data on protein structure and function to make predictions about the outcomes of a given change in the sequence, and achieves the desired changes by using site-directed mutagenesis. Given the intricate nature of proteins and the lack of adequate structural and functional data, applying rational design may not always be an effective approach. In contrast, directed evolution utilizes random-mutagenesis and combines several mutations thus creating a diverse pool of variants. The protein with the desired function is next isolated from the pool by a selection technique. An advantage conveyed by this approach is that it does not require prior structural knowledge. Likewise it could be applied when there is ambiguity about the structure-function relationship [353, 354].

Currently protein engineering is garnering tremendous interest and its area of application is rapidly growing largely owing to the developments in combinatorial biochemistry, high-throughput screening, and recombinant DNA technology [353, 355]. Proteins can be engineered for various purposes, namely to characterize the structure-function relationship and as a result improve aspects such as stability, solubility, activity, and the like. For example introduction of a disulfide bond between the heavy and light chains of antibody was shown to increase its thermodynamic stability [456, 357]. Another example is the fusion of similar or distinct proteins via linkers at the gene level to enhance their activity [358] or solubility [392, 399].

Protein engineering can also be used to essentially generate diverse proteins with enhanced and novel functions. For example, fragments of antibodies, or antibody-mimetics.

## 3.1 Antibody-mimetics

Immunoglobulins constitute an important class of proteins that are employed by the immune system for targeting foreign entities that are suspected to pose a threat to the integrity of the host system. These molecules selectively recognize and bind to defined targets, typically proteins, but also other biomolecules, with high affinity and specificity. Their unique and inherent features have long been exploited for use in various areas, for instance in research as reagents for detection, bioseparation, and proteomic analysis, but equally importantly for application in *in vivo* diagnosis and targeted

therapies [360]. Advances in the area of recombinant technologies, the identification of bacteria and yeast as suitable host systems as well as the emergence of various selection technologies such as phage and ribosomal display, have allowed not only to efficiently select and humanize these molecules, but also to develop other antibody-based molecules as well [361].

Despite their broad spectrum of application as therapeutic, diagnostic and detective agents [362], pitfalls accompanying antibodies create certain limitations to their use, namely the risk of immunogenicity, inadequate pharmacokinetics and pharmacodynamics that involve poor tissue penetration due to their large size, need for administering high dosage, and loss of activity [362-366]. Moreover, their biophysical properties and molecular composition, consisting of a complex multi-chain architecture with disulfide bonds and glycosylation that are essential for its function, makes them difficult and costly to manufacture. The six hypervariable loops makes structural manipulations also difficult, should it be required for instance in case of generating a large synthetic library [361, 367, 368]. Likewise, smaller versions of antibodies including dAb, nanobody, scFv, and Fab fragments, can still suffer from some of the same limitations; for instance, the requisite intradomain disulfide bond that has a stabilizing role and does not form in the reducing cellular environment [368].

These caveats prompted the quest for developing new affinity ligands through the use of scaffolds with preferably small size that are organized in a single-chain, and which allow to be readily engineered for improved affinity and specificity, while lacking the antibody-associated limitations [369]. Recent advances in protein engineering combined with the colossal amount of structural data proved as immensely valuable tools in this regard. Developing novel affinity ligands in principle involves four key steps, starting with identification of a scaffold molecule with a suitable sequence. The next step is the construction of a combinatorial protein library whereby diversification in the resulting variants is achieved by introducing several mutations into the sequence of the scaffold. Once generated, the library is screened against a defined target molecule using a selection system. The selected molecules are amplified followed by their identification. In order to enrich molecules with desired binding properties the selection process, i.e. screening and amplification, is repeated several times. At this point a selected binder is isolated from the pool and subsequently further characterized [360].

These so-called antibody-mimetics offer numerous advantages over conventional antibodies including their small sizes, flexible structure, favorable biophysical and

pharmacokinetic features, and have been at the center of current research. Scaffold molecules are derived from human, butterfly (*Pieris brassicae*), and various bacterial systems. Over the past decade, more than 50 different scaffolds have been proposed as alternative structural platforms to antibodies [369, 371], of which about 10 protein classes are particularly appearing to show huge potential for application in research, diagnostics, and therapeutics. In the therapeutics field several are currently in late-stage clinical development and at least one, (Kalbitor escallantide or DX-88) based on the Kunitz domain, has made its way to the market [370]. Some representative examples are listed in Table 2. One class that has fared relatively well is the Affibody group that will be further delved into due to their relevance to this work.

**Table 2:** Antibody-mimetics. Representative non-immunoglobulin scaffolds for generation of affinity ligands

| Antibody mimetic | Scaffold | Domain features | Number of randomized aa | Selection method | Ref. |
|---|---|---|---|---|---|
| Kunitz Domains | Protease inhibitor domain of APP | α/β 6Kda (58 aa) 3 S-S | 1-2 loops | Phage display | [372] |
| DARPins | Ankyrin Repeat | α2/β2 14 KDa (67 + n×33 aa) No S-S | 7 aa on β-turn and 1 α-helix (of every repeat) | Ribosome display | [373] |
| Avimers | human A-domains | Oligomeric, ~4xloops 9-18KDa (n×~40 aa) 3 S-S | 21 aa in each domain | Phage display | [374] |
| Anticalins | Lipocalins from Human and butterfly (*P. brassicae*) | β-Barrel 20KDa (160–180 aa) 2 S-S | 4 loops (16 aa) | Phage display | [375] |
| Affibodies | B domain of protein A from *S. aureus* | α3 6.5KDa (58 aa) No S-S | 13 aa on 2 α-helices | Phage display | [376] |
| Affilins | γ-B-crystallin/ubiquitin | β 20KDa / α3 β 10KDa | 8 aa | Phage display | [377] |
| Nanofitins (formerly Affitins) | Based on Sac7d proteins | 7.6KDa (66 aa) No S-S | | Ribosome display | [378] |
| Fynomers | human Fyn SH3 domain | 7 KDa (60 aa) | 6 aa in RT and n-src-loop | Phage display | [379] |
| Adnectins (monobodies) | 10th type III domain of *human* fibronectin | β-Sandwich 10KDa (94 aa) No S-S | 2–3 loops | Phage- and mRNA-display, Yeast-two-hybrid | [380, 381] |

How successful the outcome of selection would be, largely depends on the diversity and quality of the combinatorial library. Moreover, to accommodate for the differing properties and availability of target proteins, numerous selection systems have emerged that are grouped into cell-dependent/free display and non-display systems (Table 3) [60, 368]. The most prominent and widely used of these is the phage display system.

**Table 3:** Selection systems employed in combinatorial protein engineering

| Cell-dependent systems | Cell-free systems | Non-display systems |
|---|---|---|
| Phage display [382] | Covalent DNA display [387] | Yeast-two-hybrid [393] |
| Staphylococcal surface display [383] | Ribosomal display [388] | Protein-fragment complementation assay (PCA) [394] |
| E. coli surface display [384] | mRNA display [389] | |
| APEx E. coli display [385] | CIS display [390] | |
| Yeast display [386] | DNA display [391] | |
| | Microbead display [392] | |

In addition to their use for selecting binding specificity, these systems have found other applications in proteomics research too, for instance epitope mapping, studies of protein-protein interaction, and the like.

### 3.1.1 Affibodies

Affibody molecules are small affinity proteins that are based on a 58 amino acid engineered protein domain, derived from staphylococcal protein A (SPA). SPA is a cell wall-anchored protein that is composed of five homologous domains i.e. E, D, A, B and C, each folding into a three-helix bundle with an anti-parallel arrangement (Figure 5). All domains are able to bind various mammalian proteins in particular the IgGs, where they mainly interact with the Fc region, however, in case of the human VH3 family binding to Fab is also shown. Engineering of the B domain of SPA following two point mutations, Ala1Val and Gly29Ala, yielded the Z domain analogue that despite the stated alterations retained its structural stability and affinity, though exhibiting a strong bias in binding to the Fc fragment of IgG in relation to the Fab fragment. These qualities along with its small size of ca. 6.5KDa, high solubility and the absence of disulfide bonds rendered the molecule a suitable framework for the generation of other affinity ligands [360, 395].

The first combinatorial library based on the Z domain was constructed by randomization of 13 solvent-exposed surface residues located on the first and second

helix of the molecule (Figure 5). The majority of those residues were suggested to be involved in interaction with the Fc-binding domain of SPA, hence the rationale for their randomization [396]. Follow-up work demonstrated the prospects for isolating affinity ligands from the pool using phage display selection system [376]. The library has been screened against a number of targets, among them the human amyloidogenic protein amyloid-β (Aβ) that is involved in the progress of Alzheimer's disease. One of the isolated binders, denoted $Z_{Aβ3}$, was shown to selectively bind Aβ with an affinity in the low nanomolar range (17 nM). However, this affinity was only observed when the protein was in the dimeric form, i.e. two $Z_{Aβ3}$ molecules bind one Aβ monomer. Unlike the Z-domain scaffold, $Z_{Aβ3}$ carries a cysteine residue at position 28 that enables the formation of a disulfide bridge between two adjacent $Z_{Aβ3}$ molecules. Replacing the cysteine residue with a serine resulted in diminished affinity, while construction of a head-to-tail dimer by directly linking two $Z_{Aβ3}$ molecules restored the affinity [397, 398]. Moreover, in relation to the Z domain noticeable structural changes in the $Z_{Aβ3}$ are observed, where the original three-helix bundle structure is not entirely retained i.e. the first helix becomes partially unstructured in the free form [398].

Aβ is a natively disordered protein; however, as demonstrated by liquid state NMR studies, $Z_{Aβ3}$ binds to the central/C-terminal region of Aβ (1-40) resulting in the concurrent folding of both molecules, namely Aβ adopting an antiparallel β-hairpin conformation and residues 15–18 of $Z_{Aβ3}$ forming a β-strand in the complex state [398, 399]. Moreover, formation of the complex with $Z_{Aβ3}$ was shown to stabilize the β-hairpin structure of Aβ while sequestering its aggregation-prone regions, which led to inhibition of its aggregation both *in vitro* and in a Drosophila melanogaster model of Alzheimer's disease expressing Aβ (1-42) or its more aggressive mutated E22G variant [400].

### 3.1.2 The β-wrapins

Building on the structure-stabilizing and aggregation-inhibiting characteristics of $Z_{Aβ3}$, work in our group attempted to extend the construct to other amyloidogenic proteins by generating similar affinity ligands. The $Z_{Aβ3}$ molecule was chosen as a starting point to generate a combinatorial library, therefore the gene encoding $Z_{Aβ3}$ was subjected to random mutagenesis using error-prone PCR that resulted in a pool consisting of 7 x $10^7$ variants. The library was next screened against several amyloidogenic targets using the phage display system, including α-synuclein [401, 402], tau [403], IAPP [404], and human prion protein (huPrP) (unpublished work). In order to enrich the pool of potential binders bio-panning was repeated 3-4 times. In each case a number randomly selected

clones were subjected to further screening to identify potential binders either based on their sequence or together with results of phage ELISA. The resulting binders are referred to as β-wrapins.

Binders selected against tau [403] and IAPP [404] exhibited an affinity of 260 and 220 nM, respectively. Moreover, aggregation of both proteins was inhibited in the presence of their respective binders in a concentration-dependent manner. Screening of the library against α-synuclein yielded binders carrying 1-5 mutations in relation to the scaffold molecule $Z_{Aβ3}$. Binding affinity to α-synuclein in relation to Aβ was strongly dependent on the number of mutations. For instance, AS69 and AS60 each carrying 4 and 5 mutations respectively, showed diminished or no affinity towards Aβ. AS9 and AS34 both showed relatively higher affinity towards Aβ in comparison to α-synuclein. AS10, however, appeared bound to three amyloidogenic proteins with sub-micromolar affinity, i.e. α-synuclein, Aβ, and IAPP, all forming a β-hairpin structure in complex as revealed by $^1H,^{15}N$ HSQC NMR spectroscopy studies [402]. Moreover, AS10 inhibited aggregation of the stated proteins by sequestering the monomers, since binding was shown to occur at regions critical for their aggregation, namely residues 17–36 for Aβ [399] and 37–54 for α-synuclein [401]. An aggregation inhibitory effect of AS10 was also observed for another highly amyloidogenic protein *viz.* Calcitonin (unpublished work). Conversely, no binding was observed when tested for interaction with tau (a four-repeat-domain construct) and a truncated variant of human prion protein (huPrP-23-133). Structural similarity among the former four proteins might explain the biased interaction behavior of AS10 towards the latter two [402].

Irrespective of the target protein, screening the sequences of all selected binders revealed the presence of the cysteine residue at position 28 (Cys-28) as observed in the scaffold molecule $Z_{Aβ3}$. This suggests that Cys-28 is conserved throughout the selection process against the defined targets stated.

### 3.1.2.1 The β-wrapin AS69, a bona fide partner to stabilize α-synuclein

AS69 was selected from the combinatorial library against α-synuclein, and in comparison to the scaffold $Z_{Aβ3}$ it carries four mutations, namely G13D, V17F, I31F, and L34V (Figure 5). Moreover, the presence of the conserved Cys-28 enables the formation of the homodimer that is essential to achieve the functional affinity upon interaction with the target (Figure 6).

The binding affinity of AS69 to α-synuclein was K*d* = 240 nM [389]. Liquid state NMR spectroscopy revealed AS69 binding to occur at residues 35-56 of α-synuclein. Binding

here is coupled to folding into a β-hairpin, conforming to the Aβ:ZAβ3 interaction paradigm (Figure 6).

In complex with α-synuclein AS69 shows a folding topology consisting of four α-helices and two β-strands that form a hydrophobic tunnel-like cavity burying the β-hairpin portion of α-synuclein. The β-strands are formed by residues 15-18, while the rest of the N-terminal part largely remains unstructured due to the occurrence of
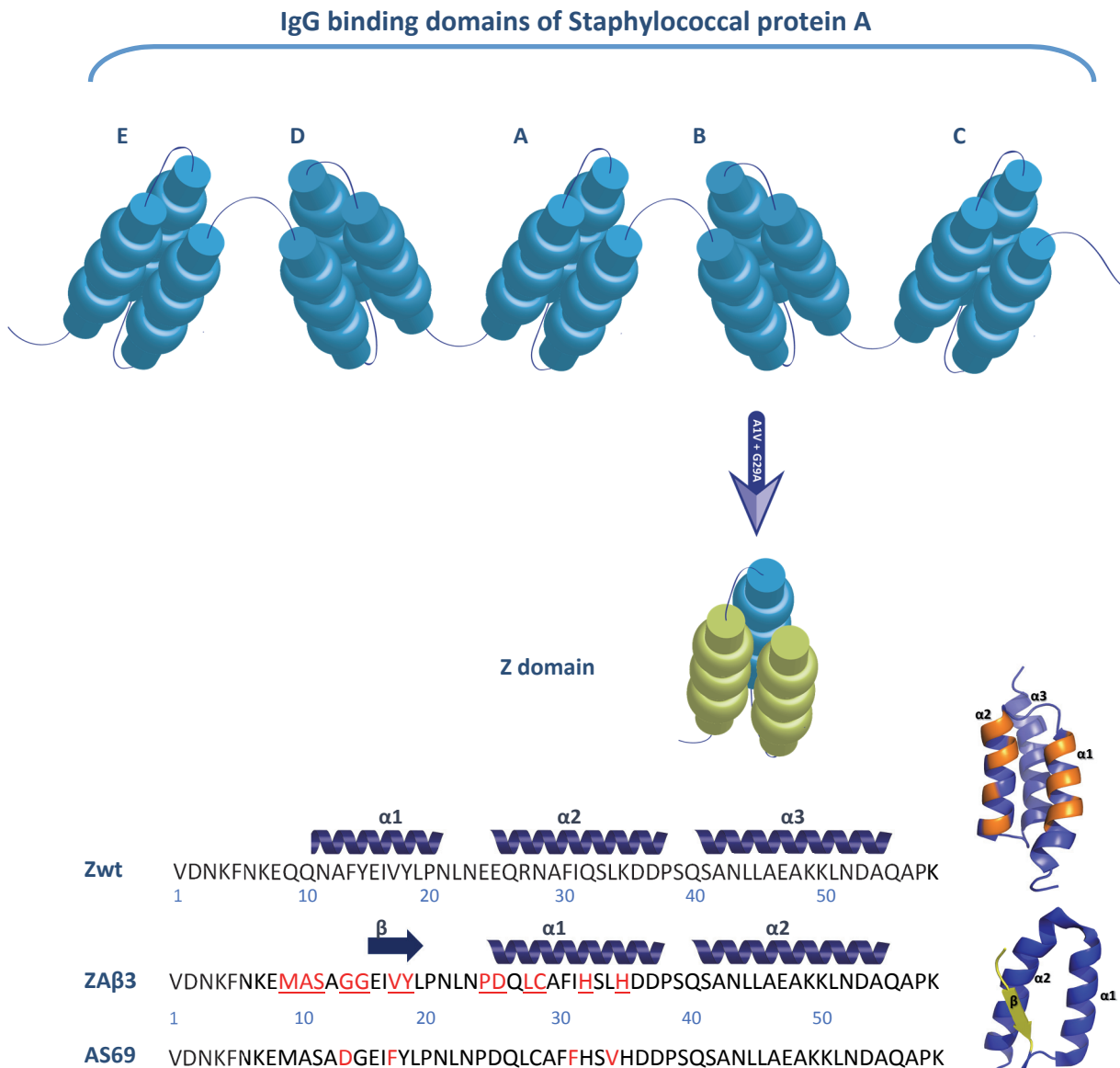


**Figure 5: Schematic representation of the sequence of events leading to the generation of β-wrapins.** Depicted are the five homologous IgG binding domains of SPA, where two point mutations, A1V and G29A, in the B domain give rise to the engineered Z domain. Randomization of 13 surface-located amino acid residues on the Z domain (the residues are colored red and underlined in the $Z_{Aβ3}$ sequence, and the positions of the residues are highlighted in orange on the first and second helix in the right upper cartoon representation; PDB: 2B89) yields the affibodies. The β-wrapins are generated by employing the affibody $Z_{Aβ3}$ as a scaffold and subjecting it to random mutagenesis. The mutated residues in the representative β-wrapin AS69 are highlighted in red. Note the transition of α-1 helix in the Z domain to β-strand in both $Z_{Aβ3}$ and β-wrapins.

helix-destabilizing residues that leads to the exposure of the hydrophobic core as in the case of the scaffold molecule $Z_{A\beta3}$ [398, 399]. Various hydrophobic AS69 residues are shown to be in direct contact with the β-hairpin, including the Phe-31 located on helices α-1. The disulfide bond is essential in bringing the helices α-1 of both subunits into contact.
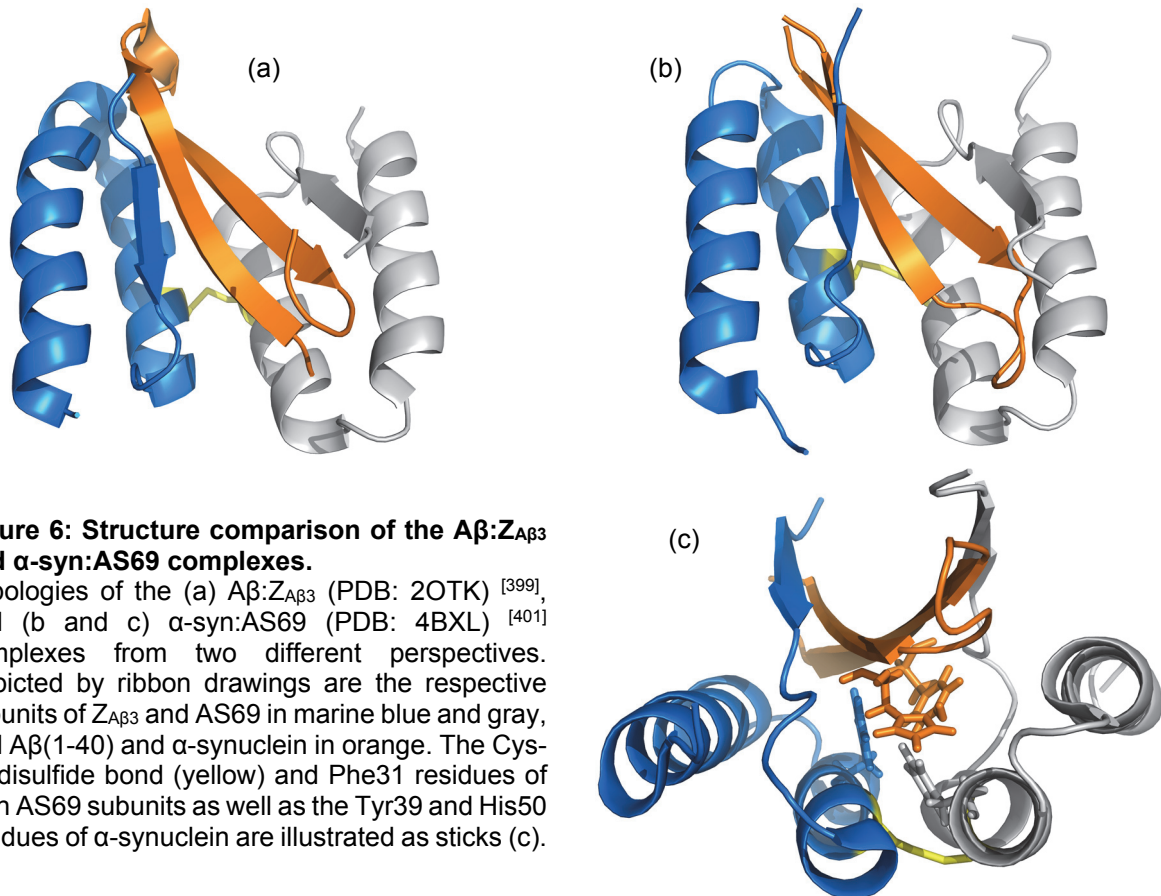


**Figure 6: Structure comparison of the Aβ:$Z_{A\beta3}$ and α-syn:AS69 complexes.**
Topologies of the (a) Aβ:$Z_{A\beta3}$ (PDB: 2OTK) [399], and (b and c) α-syn:AS69 (PDB: 4BXL) [401] complexes from two different perspectives. Depicted by ribbon drawings are the respective subunits of $Z_{A\beta3}$ and AS69 in marine blue and gray, and Aβ(1-40) and α-synuclein in orange. The Cys-28 disulfide bond (yellow) and Phe31 residues of both AS69 subunits as well as the Tyr39 and His50 residues of α-synuclein are illustrated as sticks (c).

## 3.2 Linkers

Construction of fusion proteins through covalent linkage of functionally related or distinct moieties can be potentially useful for improving their properties or functionality. Linkers or so-called spacers are short stretches of amino acid residues that connect distinct domains within a multi-domain protein. Naturally occurring linkers may carry out other functions as well, including establishing interaction between the different functional modules and maintaining biological activity [405-407]. The average length of naturally occurring linkers is calculated at 10±5.8 residues based on a database with 1280 linkers [408]. Moreover, linker length was correlated to hydrophobicity, implying the longer the linker the more hydrophilic they were. Combined results of this and another

independent study suggest the frequent occurrence of serine, glycine, aspartic acid, lysine, proline, threonine, asparagine, phenylalanine, and glutamine in natural linkers, the vast majority being either α–helical or coil. [408-409]. Presence of proline residues is suggested to reduce interaction between the linker stretch and the protein domain(s), while causing a stiffness of the linker [405]. Conversely, small amino acid residues such as glycine, serine, and threonine are suggested to provide flexibility and stability [408].

In addition to the naturally occurring linkers, numerous artificial linkers have also been developed that can be used to fuse discrete protein entities. They are classified into three groups: flexible, rigid, and cleavable [405]. Flexible linkers are generally composed of small residues such as glycine, serine, and threonine. Owing to their small size they allow a certain level of movement and flexibility. The presence of polar residues i.e. serine or threonine helps reduce interaction between the linker and the protein, thus avoiding interference with the protein function. Other polar amino acids such as lysine and glutamic acid can be added to promote their solubility [405]. The most commonly used flexible linker has the sequence motif (Gly-Gly-Gly-Gly-Ser)$_n$, where n denotes the number of repeats and can be adjusted according to the desired distance between the domains, for instance to allow proper folding or activity.

Flexible linkers may not always be useful in particular if spatial separation is critical. In this case flexible linkers may not be able to maintain effective end-to-end distance between the attached domains or avoid their interaction that might lead to altered stability and activity. In such cases, conjugation of rigid linkers might be a more appropriate alternative, such as the proline-rich linker with the sequence motif (XP)$_n$ with n being any amino acid though alanine, lysine and glutamic acid are preferred [405]. Unlike flexible and rigid linkers that form stable covalent bonds with the fusion partners, cleavable linkers can offer a distinct advantage in *in vivo* applications particularly if releasing a free functional domain is intended. For this purpose *in vivo* processes such as reducing reagents and proteases are exploited. For instance by designing a cleavable disulfide linker or by incorporating a specific protease-sensitive sequence in the linker [411].

Linker-mediated protein fusion has a broad array of applications, such as to increase protein expression or improve purification and solubility through linkage with tags or recombinant construction of chimeric proteins [412]; imaging through linkage with various dye molecules [413]; drug delivery by fusion with carrier proteins such as human serum albumin or transferrin as well as cell penetrating peptides that enable crossing

biological barriers [414-416]. Linkers are also shown to enhance folding and stability of the fusion protein.

## Aim of this work

Previous work in our group successfully constructed a combinatorial protein library employing the $Z_{A\beta3}$ affibody molecule as a scaffold. Screening the resulting library against α-synuclein yielded binders, termed β-wrapins, with favorable thermodynamics and aggregation inhibiting features. As binding thermodynamics and structural studies demonstrated, binding to the target essentially occurs in a 1:1 stoichiometry where two molecules of β-wrapins, which are covalently linked via the Cys-28 disulfide bridge, bind one molecule of the target.

The aim of the present work is to investigate the impact of the disulfide bond on the structure, stability, and α-synuclein-binding of the β-wrapin AS69. Moreover, the possibility of fusing two AS69 subunits to achieve a single-chain head-to-tail version for *in vivo* application is studied. The work also involves determining the efficacy and potency of β-wrapins AS69 and AS10 in inhibiting cytotoxicity induced by α-synuclein and other amyloidogenic proteins.

# Chapter 1

**IMPACT OF SUBUNIT LINKAGES IN AN ENGINEERED HOMODIMERIC BINDING PROTEIN TO α-SYNUCLEIN**

Aziz Gauhar, Hamed Shaykhalishahi, Lothar Gremer, Ewa A.Mirecka, and Wolfgang Hoyer

> Design and cloning of the various AS69 constructs, expression and purification of AS69 constructs, expression and purification of α-synuclein, determining binding thermodynamics with ITC, aggregation assays, determination of secondary structure and thermal stability with Far-UV circular dichroism, analytical size exclusion chromatography and reversed phase- high-performance liquid chromatography for calculating the kinetics of disulfide bond formation.

# Impact of subunit linkages in an engineered homodimeric binding protein to α-synuclein

**Aziz Gauhar[1], Hamed Shaykhalishahi[1], Lothar Gremer[1,2], Ewa A. Mirecka[1] and Wolfgang Hoyer[1,2,3]**

[1]Institute of Physical Biology, Heinrich-Heine-Universität, Universitätsstraße 1, 40225 Düsseldorf, Germany and [2]Institute of Structural Biochemistry (ICS-6), Research Centre Jülich, 52425 Jülich, Germany

[3]To whom correspondence should be addressed. E-mail: wolfgang.hoyer@uni-duesseldorf.de

**Aggregation of the protein α-synuclein (α-syn) has been implicated in Parkinson's disease and other neurodegenerative disorders, collectively referred to as synucleinopathies. The β-wrapin AS69 is a small engineered binding protein to α-syn that stabilizes a β-hairpin conformation of monomeric α-syn and inhibits α-syn aggregation at substoichiometric concentrations. AS69 is a homodimer whose subunits are linked via a disulfide bridge between their single cysteine residues, Cys-28. Here we show that expression of a functional dimer as a single polypeptide chain is achievable by head-to-tail linkage of AS69 subunits. Choice of a suitable linker is essential for construction of head-to-tail dimers that exhibit undiminished α-syn affinity compared with the solely disulfide-linked dimer. We characterize AS69-GS3, a head-to-tail dimer with a glycine-serine-rich linker, under oxidized and reduced conditions in order to evaluate the impact of the Cys28-disulfide bond on structure, stability and α-syn binding. Formation of the disulfide bond causes compaction of AS69-GS3, increases its thermostability, and is a prerequisite for high-affinity binding to α-syn. Comparison of AS69-GS3 and AS69 demonstrates that head-to-tail linkage promotes α-syn binding by affording accelerated disulfide bond formation.**

*Keywords*: alternative scaffold/amyloid/disulfide bond/α-synuclein/β-wrapin

## Introduction

Protein aggregates are a feature of several diseases, including many neurodegenerative diseases. For example, senile plaques consisting of the amyloid-β peptide (Aβ) are a neuropathological feature of Alzheimer's disease (Querfurth and LaFerla, 2010), while Lewy bodies containing α-synuclein (α-syn) as the main protein component are a characteristic of Parkinson's disease, dementia with Lewy bodies and other synucleinopathies (Lashuel et al., 2013). The development of protein aggregation inhibitors constitutes a promising therapeutic approach (Härd and Lendel, 2012). Several classes of molecules have been explored to counteract the deleterious effects of fibrils and of the particularly toxic oligomeric assemblies of α-syn. Small molecules interfering with α-syn aggregation, e.g.

various polyphenols, generally act by complex mechanisms, including direct binding to the intrinsically disordered protein, oxidation, covalent modification and stabilization of non-toxic α-syn oligomers (Li et al., 2004; Masuda et al., 2006; Ehrnhoefer et al., 2008; Meng et al., 2009; Zhou et al., 2009). The propensity to self-associate into chemical aggregates is an essential property of aggregation-inhibiting compounds (Feng et al., 2008; Lendel et al., 2009; Lamberto et al., 2011). Different hot spots for small molecule interactions were identified in the α-syn sequence, in the N-terminal region as well as in the central non-Aβ component (NAC) region and in the C-terminal region (Norris et al., 2005; Herrera et al., 2008; Lamberto et al., 2009; Lendel et al., 2009). Aggregation-inhibiting peptides with the potential to add to α-syn aggregates and to block any further aggregate growth were designed by modification of short amino acid stretches from the aggregation-prone NAC region, either by fusion of solubilizing amino acid residues or by N-methylation (El-Agnaf et al., 2004; Madine et al., 2008). Antibody-based approaches are particularly promising for the therapy of neurodegenerative diseases (Valera and Masliah, 2013). The predominantly intracellular localization of α-syn suggests the application of intrabodies, and anti-α-syn scFv antibodies indeed inhibit aggregation and toxicity upon transfection in cell culture models (Zhou et al., 2004; Lynch et al., 2008). However, recent evidence demonstrates that accumulation of α-syn oligomers in the plasma membrane and their propagation from cell-to-cell play crucial roles in the synucleinopathies (Lee et al., 2014). Therefore, extracellular targeting of α-syn is a viable approach for immunotherapy of synucleinopathies. Both active and passive immunization against α-syn proved successful in mouse models (Masliah et al., 2005, 2011). Passive immunization with the antibody 9E4 recognizing a C-terminal epitope resulted in reduced α-syn accumulation, reduced neurodegeneration, and reduced motor deficits (Masliah et al., 2011). α-Syn immunotherapy appears to be effective through a combination of mechanisms, including the binding of membrane-bound α-syn oligomers, followed by receptor-mediated endocytosis and degradation by autophagy, as well as the blocking of the propagation of misfolded α-syn (Valera and Masliah, 2013; Tran et al., 2014). One active and one passive immunization study are currently tested clinically, i.e. the vaccine AFFITOPE PD01 (Schneeberger et al., 2012) and PRX002, a humanized version of 9E4.

The Affibody molecule ZAβ$_3$ is a potent inhibitor of Aβ aggregation, obtained by phage display of a scaffold derived from staphylococcal protein A (Grönwall et al., 2007). The small size of ZAβ$_3$ (two subunits of ~60 amino acids each) has facilitated the detailed analysis of its interaction with Aβ (Hoyer et al., 2008; Hoyer and Härd, 2008). ZAβ$_3$ wraps the aggregation-prone sequence stretches of Aβ by forming a hydrophobic tunnel upon coupled folding and binding. Bound Aβ adopts a β-hairpin conformation, with those sequence regions forming an intramolecular β-sheet that otherwise build the core of the intermolecular β-sheets in amyloid fibrils (Hoyer et al., 2008). The amyloid-like conformation of ZAβ$_3$-bound Aβ prompted us to exploit ZAβ$_3$ as a scaffold for the generation

of binders to other amyloidogenic targets. We generated ZAβ3-based phage display libraries from which ligands are selected that we term β-wrapins (β-wrap proteins), referring to the observation that ZAβ3 wraps around its target which adopts a β-structure in the complex. AS69 is a β-wrapin selected to bind to α-syn, exhibiting an affinity of 240 nM (Mirecka *et al.*, 2014). In complex with AS69, α-syn forms a β-hairpin in the sequence region of amino acids 37–54, which contains most of the reported disease-related mutations (Fig. 1A) (Mirecka *et al.*, 2014). Concomitantly, α-syn aggregation is inhibited, with substantial increases in the lag time of aggregation even at low substoichiometric concentrations of AS69 (Mirecka *et al.*, 2014).

Like ZAβ3, AS69 is a homodimer covalently linked by a disulfide bridge between the subunits' single cysteine residues, Cys-28 (Fig. 1A). The disulfide bond connects the helices α1 of both subunits and is located close to the interface with the β-hairpin of α-syn. In addition to the disulfide linkage, two



**Fig. 1.** Structure and subunit linkages of β-wrapin AS69. (A) Ribbon drawing of AS69 (gray) bound to α-syn (orange), pdb entry 4BXL. The two AS69 subunits are shown in light and dark gray and are labeled AS69 and AS69′, respectively. The folded core of the complex is shown, comprising residues 13–58 of both AS69 subunits and residues 35–56 of α-syn. The disordered N-termini of the AS69 subunits are not displayed. The Cys-28 disulfide bond is shown in yellow. The amino acid sequence of AS69 is displayed and the positions of α-helical and β-sheet secondary structures in α-syn-bound AS69 are indicated by cylinders and arrow, respectively. (B) Head-to-tail fusion constructs of two AS69 subunits with alternative linker sequences. (C) Scheme of the AS69 subunit linkage configurations investigated in this study. Boxes represent AS69 subunits, yellow circles represent Cys-28 residues, and thick lines indicate head-to-tail linkage.

β-wrapin subunits can be fused on the nucleic acid level to yield head-to-tail linked dimers. Head-to-tail linkage of ZAβ3 subunits proved to be advantageous for treatment of a *Drosophila melanogaster* model of Alzheimer's disease (Luheshi *et al.*, 2010). Expression of a head-to-tail variant of ZAβ3 inhibited the toxicity of wild-type Aβ42 and of the arctic mutant Aβ42(E22G) almost completely, while expression of individual ZAβ3 subunits was only partially effective. In order to evaluate the effect of AS69 on α-syn pathology in cell culture and animal models of synucleinopathies, it would thus be desirable to likewise employ a single-chain AS69 dimer. Such a construct would also be a preferable starting point for combinatorial protein engineering for affinity maturation of AS69, since it would allow independent optimization of the subunits (Lindberg *et al.*, 2013).

Here we investigate the linker requirements for head-to-tail fusion of AS69 subunits. We generated AS69-GS3, a single-chain construct containing a glycine-serine-rich linker that exhibits the same affinity for α-syn as solely disulfide-linked AS69, and employed it to evaluate the impact of the Cys-28 disulfide bond on AS69 and its interaction with α-syn. Finally, we examined the effect of head-to-tail linkage on the kinetics of disulfide formation.

## Materials and methods

### Protein preparation

Genes encoding the head-to-tail constructs AS69-Oct1-TEV, AS69-GS2-TEV, as well as a direct head-to-tail fusion of two AS69 subunits, were obtained from Life Technologies. The gene encoding AS69-GS3 was generated from the AS69 gene by introduction of the linker sequence by PCR using specifically designed primers. Here, the first subunit was amplified employing the T7 promoter, 5′-TAA TAC GAC TCA CTA TAG GG, and the reverse primer 5′-A TAT GCC ACC CTG GCC ACT GCC ACC GCC ACC TTT CGG CGC CTG AGC, thus adding one copy of (G4S) to the first subunit. Amplification of the second subunit along with addition of two copies of (G4S) was achieved using the forward primer 5′-A TAT GGC CAG GGT GGC GGT GGC AGT GGT GGC GGT GGC AGT GTA GAT AAC AAA TTC, and T7 terminator, 5′-GCT AGT TAT TGC TCA GCG G. Genes were subjected to digestion using the appropriate restriction enzymes, i.e. EcoRI, AvrII and BglI (New England Biolabs), followed by ligation into the pET-302/NT-His expression vector and subsequent transformation into electrocompetent *Escherichia coli* JM109 cells. Sequence congruence of all constructs was verified by DNA sequencing (MWG Biotech). AS69 and the head-to-tail constructs were expressed from the pET-302/NT-His vector and purified as described previously (Mirecka *et al.*, 2014). In short, following expression and cell lysis, lysates were cleared by centrifugation and proceeded for purification on a HisTrap FF affinity column (GE Healthcare), followed by further purification on a HiLoad 16/60 Superdex 75 size exclusion chromatography column (GE Healthcare). Purity of the peak fractions was confirmed by application on 16.5% Tris-Tricine SDS–PAGE (Bio-Rad) and visualization by Coomassie Blue staining. Expression and purification of α-synuclein were performed as previously described (Mirecka *et al.*, 2014).

### Isothermal titration calorimetry

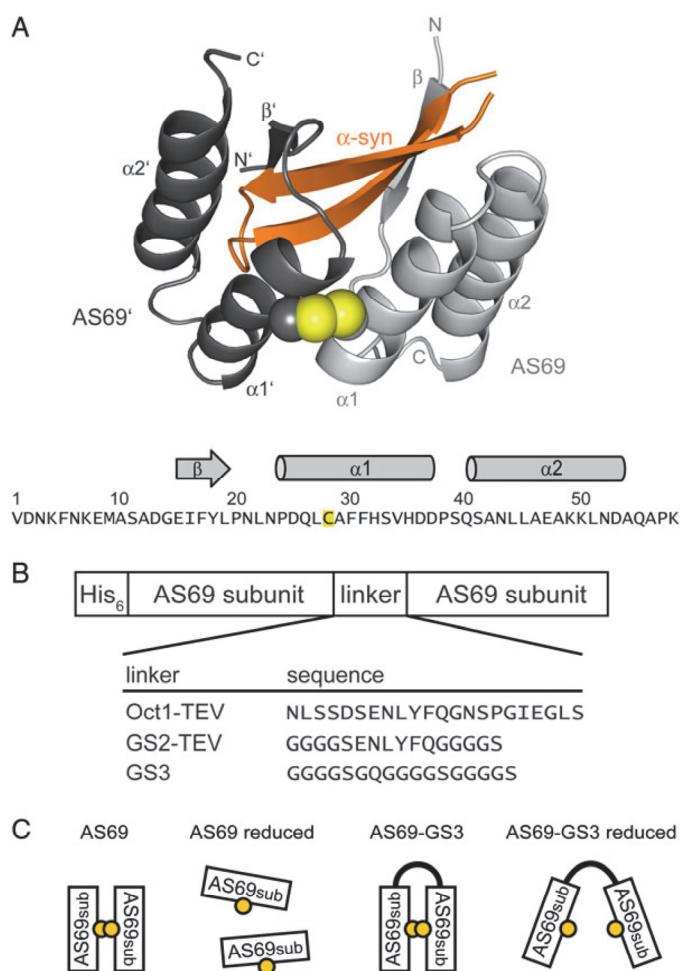Isothermal titration calorimetry (ITC) was performed on a Microcal iTC200 calorimeter (GE Healthcare) at 30°C. The

buffer was 20 mM sodium phosphate, 50 mM NaCl, pH 7.4. The titrant in the syringe was at ~10-fold higher concentration as the titrant in the cell, which was applied at a concentration in the range of 35–180 μM. For the experiment investigating the α-syn affinity of AS69-GS3 under reducing conditions, 5 mM DTT was added to the protein samples. The heat of post-saturation injections was averaged and subtracted from each injection to correct for heats of dilution and mixing. Data were processed using MicroCal Origin software provided with the calorimeter. Apparent dissociation constants $K_d^{app}$ were obtained from a nonlinear least-squares fit to a 1 : 1 binding model. AS69 and its head-to-tail variants show partial thermal unfolding (see Fig. 6) at the temperature of the ITC experiment. For those constructs with experimentally determined thermal denaturation profiles, the $K_d^{app}$ values were therefore corrected for the contribution from the coupled folding equilibrium (Dincbas-Renqvist *et al.*, 2004), yielding the $K_d$ values given in Table I.

## Aggregation assay

Aggregation of α-syn was monitored by thioflavin T (ThT) fluorescence (LeVine, 1999). Aggregation reactions contained 50 μM of α-syn and 40 μM ThT in 20 mM sodium phosphate, 50 mM NaCl, pH 6.0, 0.04% Na-azide, in a final volume of 150 μl. Aggregation was performed at 37°C with continuous orbital shaking (300 rpm) in a round-bottom 96-well black plate (Nunc) containing a 2 mm glass bead in each well. ThT fluorescence was excited at 440 nm and measured at 480 nm on an Infinite M1000 plate reader (Tecan). The signal of a buffer sample containing ThT was subtracted for background correction.

## Circular dichroism spectroscopy

Far-UV circular dichroism (CD) spectra were measured on a JASCO J-815 spectropolarimeter in a 0.5 mm Quartz cuvette (Hellma) using protein samples at a concentration of 17.5 μM. The buffer was 20 mM sodium phosphate, 50 mM NaCl, pH 7.4. For measurements under reducing conditions, Tris-(2-carboxyethyl)-phosphine (TCEP) (Thermo Scientific) was added at a concentration of 10 mM. Melting curves were recorded at 222 nm with a heating rate of 1°C min⁻¹. Melting temperatures were derived from fits of the melting curves to a two-state unfolding model (Pace *et al.*, 1998).

## Analytical size exclusion chromatography

Analytical size exclusion chromatography (SEC) was performed on a Superdex 75 10/300 GL column (GE Healthcare) connected to an ÄKTA Purifier system (GE Healthcare) at a temperature of 20°C and a flow rate of 0.5 ml min⁻¹. Proteins were detected by absorbance at 280 nm. Samples of 0.1 ml at a concentration of 180 μM (AS69) or 160 μM (AS69-GS3) were injected and eluted with 20 mM sodium phosphate, 50 mM NaCl, pH 7.4. For SEC experiments under reducing conditions, the protein samples were reduced by incubation with 10 mM TCEP for 1 h at 20°C, and 5 mM dithiothreitol (DTT) was added to the elution buffer. Molecular weight calibration was achieved with conalbumin, ovalbumin, carbonic anhydrase, ribonuclease A and aprotinin as globular protein standards.

## Analytical RP-HPLC

Separation and quantification of the oxidized and reduced fractions of AS69 and AS69-GS3 were achieved by injecting 20 μl of protein solutions at a concentration of 115 μM (subunit concentration 230 μM) onto an analytical Zorbax 300SB-C8 RP-HPLC column (5 μm, 4.8 × 250 mm, Agilent) connected to an Agilent 1260 Infinity system at a column temperature of 80°C and a flow rate of 1 ml/min. The analysis was performed using a gradient of 30–36% (vol/vol) acetonitrile, 0.1% (vol/vol) TFA, in water within 20 min, followed by an isocratic step at 36% (vol/vol) acetonitrile, 0.1% (vol/vol) TFA, in water for 3 min. Ultra-violet absorption at 214 nm was used for protein detection and relative quantification of the oxidized and reduced fractions of AS69 and AS69-GS3. Reversed phase-high performance liquid chromatography (RP-HPLC) of AS69 and AS69-GS3 in the absence and presence of 10 mM TCEP was performed to determine the elution volumes of the oxidized and reduced proteins. To follow the kinetics of disulfide bond formation, AS69 and AS69-GS3 were reduced by incubation with 10 mM TCEP for 30 min at 25°C. TCEP was removed by size exclusion chromatography on Sephadex G-25 (two HiTrap Desalting 5 ml columns (GE Healthcare) connected in series to an ÄKTA Purifier system) using 20 mM sodium phosphate, 50 mM NaCl, pH 7.4, as buffer system at a flow rate of 1.5 ml min⁻¹. Protein containing fractions were combined and immediately used for analysis of reoxidation kinetics ($t = 0$ min). The reoxidation reaction was performed by incubation at 25°C in closed reaction tubes without agitation. Aliquots were withdrawn at different time points and analyzed for the amount of oxidized and reduced states by RP-HPLC as described above.

## Kinetics of disulfide bond formation

The kinetic data of reoxidation of AS69-GS3 were fitted as a single exponential in compliance with an intramolecular reaction, yielding the first-order rate constant $k_{AS69-GS3}$. AS69 reoxidation involves dimerization and was fitted to the dimerization rate law, providing the second-order rate constant $k_{AS69}$:

$$\frac{1}{[AS69_{red}]_t} = k_{AS69}t + \frac{1}{[AS69_{red}]_{t=0}}$$

The effective concentration of subunits in the disulfide formation reaction of AS69-GS3 was calculated from the above rate constants as $2k_{AS69-GS3}/k_{AS69}$ according to Robinson and Sauer (1996).

## Results

### Linker sequence is critical to retain α-syn affinity in head-to-tail AS69 dimers

In the case of ZAβ₃, direct fusion of two subunits without introduction of an extra linker sequence was feasible for retaining a functional dimer (Hoyer and Härd, 2008; Luheshi *et al.*, 2010; Lindberg *et al.*, 2013). The N-terminal ~13 residues of ZAβ₃ remain disordered in the complex with Aβ and can therefore serve as a linker. Likewise, the N-terminus of α-syn-bound AS69 is disordered (Mirecka *et al.*, 2014). Direct head-to-tail linkage of AS69 subunits, however, resulted in a complete loss of α-syn binding according to ITC (Fig. 2A, Table I). Therefore, we introduced different linker sequences (Fig. 1B) and tested their ability

to restore the affinity for α-syn. Introduction of a 15-amino acid variant of the disordered, flexible linker of the Oct-1 POU domain (van Leeuwen *et al.*, 1997) with an additional TEV protease cleavage site resulted in the head-to-tail construct AS69-Oct1-TEV. Titration of AS69-Oct1-TEV with α-syn gave very weak, slowly decaying binding heat indicative of very slow association kinetics, demonstrating that the head-to-tail linkage interferes with binding (data not shown). Glycine-serine-rich sequences such as (Gly$_4$-Ser)$_3$ are frequently used as flexible linkers, particularly to link antibody domains in a single-chain Fv format (Huston *et al.*, 1988). We tested two glycine-serine-rich linkers, with and without an additional TEV protease cleavage site. In both constructs, AS69-GS2-TEV and AS69-GS3, the α-syn affinity of the solely disulfide-linked AS69 was recovered (Fig. 2B, Table I).

To test whether the head-to-tail linkage of AS69 interferes with its aggregation-inhibitory action, α-syn aggregation was followed in the presence and absence of AS69-GS3 (Fig. 3). The increased fluorescence of the dye ThT upon binding to the amyloid cross-β structure was used as an indicator of α-syn aggregation (LeVine, 1999). Stoichiometric amounts of AS69-GS3 completely inhibited α-syn aggregation, while sub-stoichiometric amounts led to significant increases in the aggregation lag-time (Fig. 3), matching the data previously obtained for AS69 (Mirecka *et al.*, 2014).

### The Cys-28 disulfide causes compaction and increased thermostability of AS69-GS3 and is essential for α-syn binding

We studied the properties of AS69 and AS69-GS3 before and after reduction of the disulfide bond, in order to evaluate the impact of the head-to-tail and disulfide linkages on structure, stability and α-syn binding of AS69. The investigated AS69 configurations are schematically depicted in Fig. 1C. High-affinity binding of α-syn required the presence of the Cys-28 disulfide linkage, which is evidenced by an ∼1000-fold lower affinity of AS69-GS3 as a consequence of disulfide bond cleavage upon reduction (Table I).

The secondary structure contents of AS69 and AS69-GS3 in their oxidized and reduced states were analyzed by CD spectroscopy (Fig. 4). The CD spectra of AS69 and AS69-GS3 show minima at 208 and 222 nm, in agreement with largely α-helical conformation. Upon disulfide bond reduction, a slight decrease in the 222:208 nm ellipticity ratio is observed for both, AS69 and AS69-GS3, in line with partial unfolding. SEC was performed for comparison of the hydrodynamic
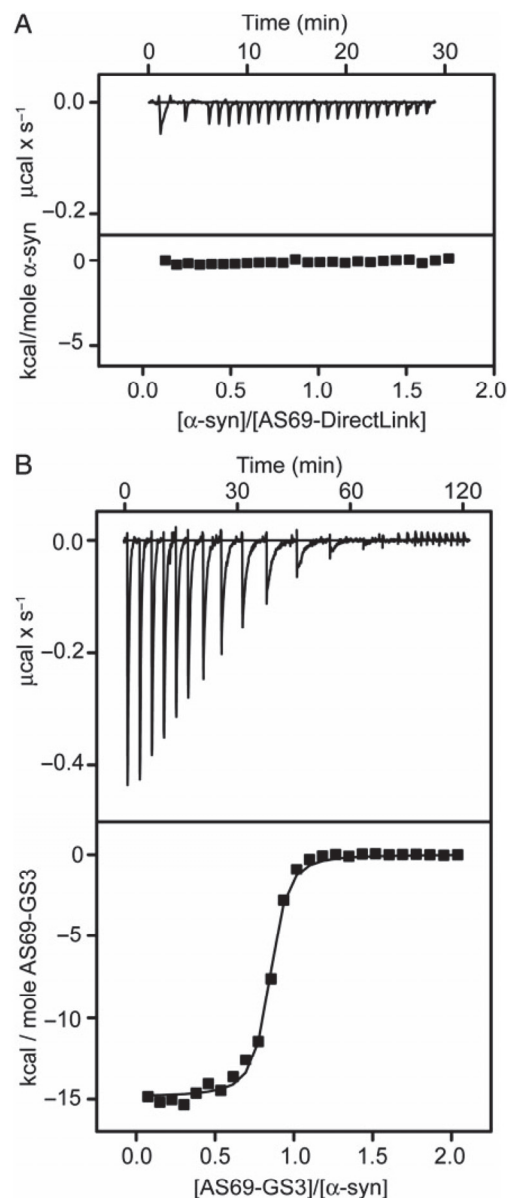


**Fig. 2.** Impact of the linker on the α-syn affinity of head-to-tail AS69 constructs determined by ITC. (A) No heat of binding were detected when 465 μM α-syn was titrated into a 54 μM solution of a head-to-tail construct in which two AS69 subunits are directly fused without an extra linker. (B) Titration of 716 μM AS69-GS3 into 75 μM α-syn, yielding an apparent affinity of $K_d^{app} = 250$ nM.

**Table I.** Affinity for α-syn of AS69 variants with different dimer linkages determined by ITC at 30°C

| Head-to-tail linkage | Cys-28 disulfide | $K_d^{app}$ (μM) | $K_d$ (μM)[a] |
|---|---|---|---|
| None | Oxidized | 0.24 | 0.18 |
| Direct head-to-tail linkage | Oxidized | n.d.[b] | |
| Oct1-TEV | Oxidized | n.d.[c] | |
| GS2-TEV | Oxidized | 0.14 | |
| GS3 | Oxidized | 0.25 | 0.21 |
| GS3 | Reduced | 280 | 200 |

[a]Corrected for coupled AS69 folding equilibrium.
[b]n.d., not detected.
[c]n.d., not determined, weak heat signal with a time profile indicative of very slow association kinetics.
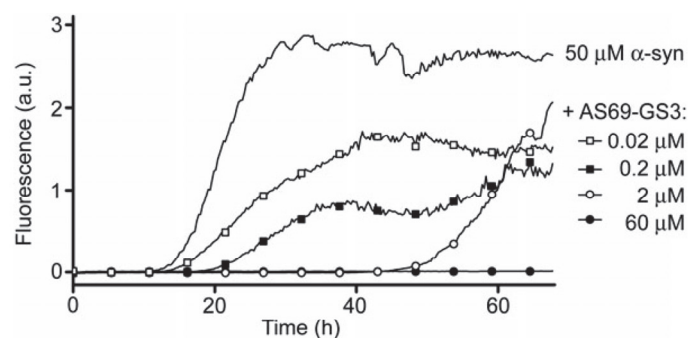
**Fig. 3.** Inhibition of α-syn aggregation by AS69-GS3. Kinetics of α-syn aggregation in the absence and presence of the indicated concentrations of AS69-GS3 monitored by ThT fluorescence.

volumes of the different β-wrapin configurations (Fig. 5). According to calibration with globular standard proteins, AS69 and AS69-GS3 eluted as proteins with apparent masses of 24 or 27 kDa, respectively, although their real molecular weight (MW) is ~15 kDa. The high apparent MW reflects the presence of disorder in the N-termini, as previously observed for ZAβ3 (Hoyer and Härd, 2008). Upon disulfide bond reduction, elution of AS69 is strongly retarded, demonstrating the separation of the homodimer into its subunits. In contrast, AS69-GS3 elutes earlier from SEC after disulfide bond reduction, at an apparent MW of 32 kDa. The increased hydrodynamic volume of reduced AS69-GS3 suggests that the interface between the subunits' α1-helices is not fully established if the disulfide bond is not formed.

Thermal melting profiles were obtained by CD at 222 nm for AS69 and AS69-GS3 in their free and α-syn-bound states and were analyzed by a two-state unfolding model (Fig. 6). Disulfide bond reduction led to a decrease in the melting temperatures of AS69 and AS69-GS3 by 11 and 8K, respectively, revealing a strong impact of the Cys-28 disulfide linkage on thermostability. Comparison of melting profiles of AS69-GS3 and AS69 showed that the head-to-tail linkage also enhanced thermostability, with an increase in melting temperatures of ~5K (Fig. 6). An additional increase in the melting temperature of 13K is observed upon complex formation with α-syn (Fig. 6), which was dependent on formation of the Cys-28 disulfide bond, in agreement with the ITC data (Fig. 2, Table I).

### Head-to-tail linkage affords accelerated disulfide bond formation

The kinetics of formation of the Cys-28 disulfide bond was monitored starting from reduced AS69 or reduced AS69-GS3, both at a subunit concentration of 230 μM (Fig. 7). The fractions of oxidized and reduced molecules were separated by HPLC and quantified by their absorbance (Fig. 7A). Disulfide bond formation in AS69-GS3 was significantly accelerated compared with AS69, even at the high protein concentrations used in this experiment, which foster the intermolecular dimerization reaction of AS69 (Fig. 7B). The first-order rate constant obtained for intramolecular disulfide bond formation in AS69-GS3 was $k_{AS69-GS3} = 1.56$ ($\pm 0.07$) $10^{-4}$ s$^{-1}$. The second-order rate constant determined for intermolecular disulfide bond formation in AS69 was $k_{AS69} = 7.7$ ($\pm 0.5$) $10^{-2}$ M$^{-1}$ s$^{-1}$. The effective concentration of subunits in the disulfide formation reaction of AS69-GS3 can be calculated from the above rate constants (Robinson and Sauer, 1996) and is $4.1 \pm 0.5$ mM.

## Discussion

In the present study, we investigated the requirements for subunit linkages of the β-wrapin AS69, an engineered binding protein to α-syn. While the head-to-tail linkage of AS69 subunits can generate functional single-chain binders to α-syn, the

**Fig. 4.** Far-UV CD spectra of AS69 and AS69-GS3 at 20°C before and after reduction of the Cys-28 disulfide bond.
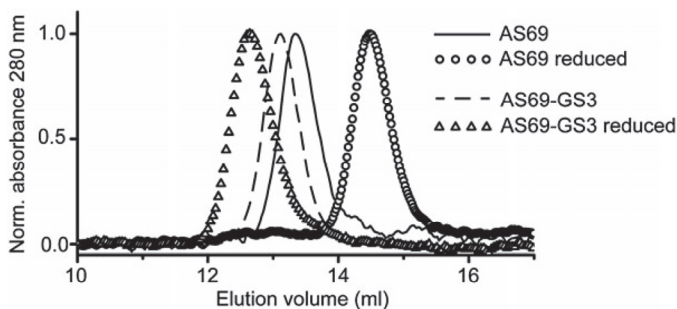
**Fig. 5.** SEC of AS69 and AS69-GS3 at 20°C before and after reduction of the Cys-28 disulfide bond.

**Fig. 6.** Thermal stability of free and α-syn-bound AS69 and AS69-GS3 before and after reduction of the Cys-28 disulfide bond. (A) Thermal denaturation monitored by CD at 222 nm using a concentration of 17.5 μM of all proteins. Lines represent fits to a two-state transition model. (B) Melting temperatures for the different proteins and conditions obtained from the fits to the two-state transition model.
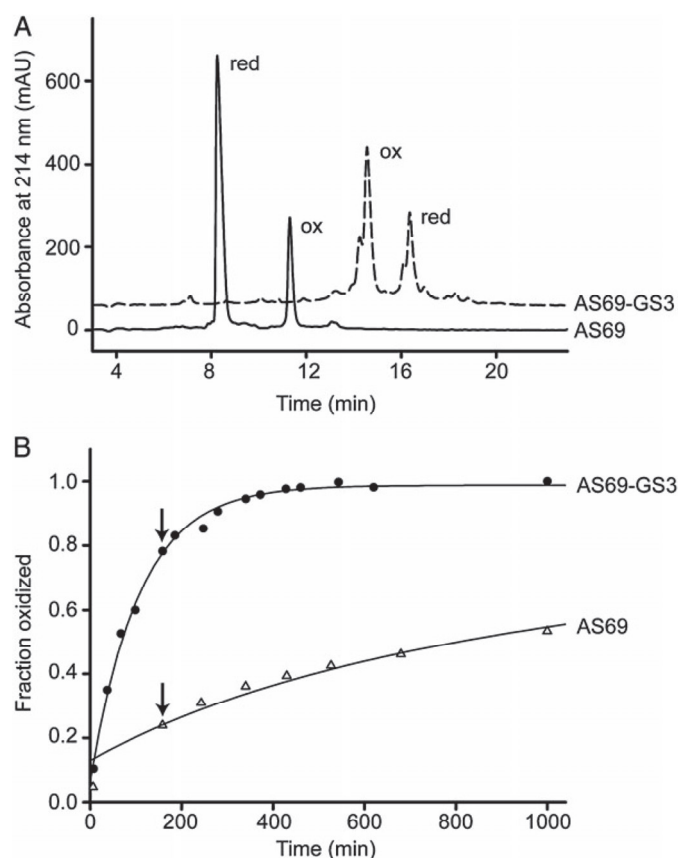
**Fig. 7.** Head-to-tail linkage leads to accelerated formation of the Cys-28 disulfide bond. The kinetics of disulfide bond formation was monitored starting from reduced AS69 and AS69-GS3, respectively. (A) The oxidized and reduced fractions were separated and quantified by HPLC, exemplified for the time point of 158 min, indicated by arrows in (B). (B) Time traces of disulfide bond formation. The lines represent fits to first-order reaction kinetics in the case of AS69-GS3 (intramolecular disulfide bond formation) and to second-order dimerization kinetics in the case of AS69 (intermolecular disulfide bond formation).

affinity is sensitive to the identity of the linker sequence. In contrast to ZAβ₃ (Hoyer and Härd, 2008; Luheshi et al., 2010; Lindberg et al., 2013), direct fusio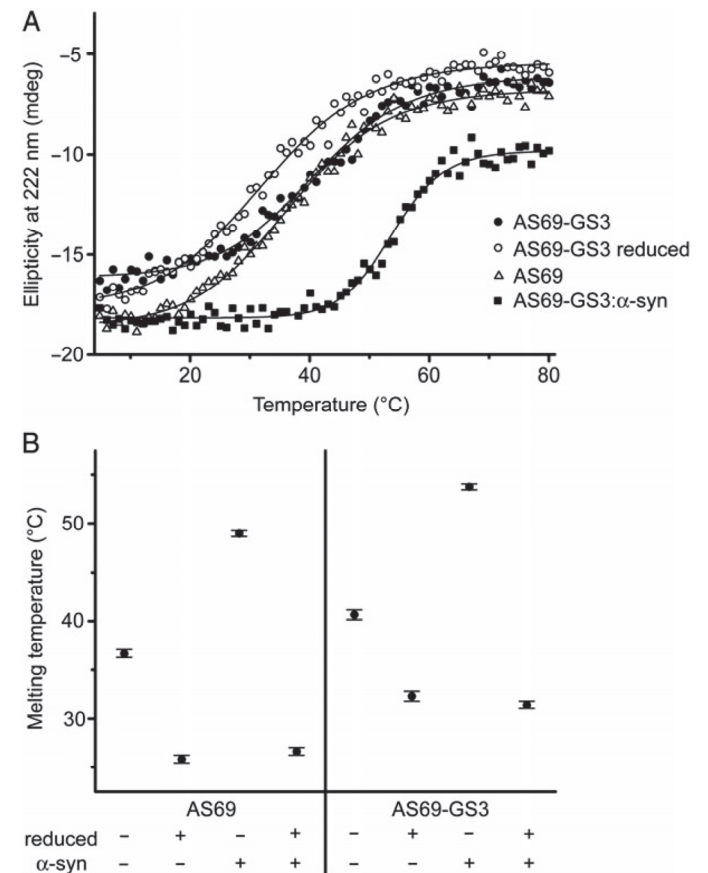n of two AS69 results in the loss of affinity for the target. On the other hand, head-to-tail constructs with glycine-serine linkers, commonly employed in the construction of single-chain antibody fragments (Huston et al., 1988), recover the α-syn affinity of solely disulfide-linked AS69.

The presence of the Cys-28 disulfide bond is a prerequisite for high-affinity binding to α-syn. This can be explained by its potential to fix the contact between the subunits' α1-helices, which in turn establishes the interaction surface for α-syn binding (Fig. 1A). In line with this, Cys-28 disulfide bond formation causes compaction and increased stability of AS69 as demonstrated by SEC and thermal melting experiments. The critical importance of the Cys-28 disulfide bond also for the ZAβ₃ : Aβ interaction is highlighted by the conserved occurrence of Cys-28 in combinatorial engineering of Affibody molecules to Aβ (Grönwall et al., 2007; Lindberg et al., 2013).

Head-to-tail linkage via a glycine-serine linker in the construct AS69-GS3 leads to increased protein stability, similar to the observations reported before for a single-chain variant of the Arc repressor dimer of phage P22 (Robinson and Sauer, 1996, 1998). In addition, head-to-tail linkage promotes α-syn

binding by entailing accelerated disulfide formation, providing an effective subunit concentration of 4.1 ± 0.5 mM for the disulfide formation reaction. This value is in good agreement with the effective subunit concentration in a single-chain variant of the Arc repressor dimer of phage P22, containing a 15-residue, glycine-rich linker (4.5 ± 1.8 mM, calculated from the bimolecular and unimolecular refolding reactions) (Robinson and Sauer, 1996).

AS69 exhibits a unique mode of interaction with α-syn (Mirecka et al., 2014). It sequesters a sequence region that is critical for α-syn dysfunction, judging from the clustering of disease-related mutations. Monomeric α-syn is stabilized at low substoichiometric concentrations of AS69, indicating that AS69 interferes with the nucleation of aggregation. The β-wrapin thus offers a distinct therapeutic approach to the synucleinopathies. The small size of the β-wrapin might support its uptake into the brain and limits the costs of production. AS69-GS3 is an advantageous construct to evaluate the therapeutic potential of β-wrapin interference with α-syn assembly in cell culture and animal models of synucleinopathies. AS69-GS3 can moreover be employed for affinity maturation of β-wrapins to α-syn as it is compatible with the independent adaption of its subunits to the target.

## Acknowledgements

## References

Dincbas-Renqvist,V., Lendel,C., Dogan,J., Wahlberg,E. and Härd,T. (2004) J. Am. Chem. Soc., **126**, 11220–11230.

Ehrnhoefer,D.E., Bieschke,J., Boeddrich,A., Herbst,M., Masino,L., Lurz,R., Engemann,S., Pastore,A. and Wanker,E.E. (2008) Nat. Struct. Mol. Biol., **15**, 558–566.

El-Agnaf,O.M., Paleologou,K.E., Greer,B., et al. (2004) FASEB J., **18**, 1315–1317.

Feng,B.Y., Toyama,B.H., Wille,H., Colby,D.W., Collins,S.R., May,B.C., Prusiner,S.B., Weissman,J. and Shoichet,B.K. (2008) Nat. Chem. Biol., **4**, 197–199.

Grönwall,C., Jonsson,A., Lindström,S., Gunneriusson,E., Ståhl,S. and Herne,N. (2007) J. Biotechnol., **128**, 162–183.

Härd,T. and Lendel,C. (2012) J. Mol. Biol., **421**, 441–465.

Herrera,F.E., Chesi,A., Paleologou,K.E., Schmid,A., Munoz,A., Vendruscolo,M., Gustincich,S., Lashuel,H.A. and Carloni,P. (2008) PLoS One, **3**, e3394.

Hoyer,W. and Härd,T. (2008) J. Mol. Biol., **378**, 398–411.

Hoyer,W., Grönwall,C., Jonsson,A., Ståhl,S. and Härd,T. (2008) Proc. Natl Acad. Sci. USA, **105**, 5099–5104.

Huston,J.S., Levinson,D., Mudgett-Hunter,M., et al. (1988) Proc. Natl Acad. Sci. USA, **85**, 5879–5883.

Lamberto,G.R., Binolfi,A., Orcellet,M.L., Bertoncini,C.W., Zweckstetter,M., Griesinger,C. and Fernandez,C.O. (2009) Proc. Natl Acad. Sci. USA, **106**, 21057–21062.

Lamberto,G.R., Torres-Monserrat,V., Bertoncini,C.W., Salvatella,X., Zweckstetter,M., Griesinger,C. and Fernandez,C.O. (2011) J. Biol. Chem., **286**, 32036–32044.

Lashuel,H.A., Overk,C.R., Oueslati,A. and Masliah,E. (2013) Nat. Rev. Neurosci., **14**, 38–48.

Lee,II.J., Bae,E.J. and Lee,S.J. (2014) Nat. Rev. Neurol., **10**, 92–98.

Lendel,C., Bertoncini,C.W., Cremades,N., Waudby,C.A., Vendruscolo,M., Dobson,C.M., Schenk,D., Christodoulou,J. and Toth,G. (2009) Biochemistry, **48**, 8322–8334.

LeVine,H., III (1999) Methods Enzymol., **309**, 274–284.

Li,J., Zhu,M., Rajamani,S., Uversky,V.N. and Fink,A.L. (2004) Chem. Biol., **11**, 1513–1521.

Lindberg,H., Johansson,A., Härd,T., Ståhl,S. and Löfblom,J. (2013) Biotechnol. J., **8**, 139–145.

Luheshi,L.M., Hoyer,W., de Barros,T.P., et al. (2010) PLoS Biol., **8**, e1000334.

Lynch,S.M., Zhou,C. and Messer,A. (2008) *J. Mol. Biol.*, **377**, 136–147.

Madine,J., Doig,A.J. and Middleton,D.A. (2008) *J. Am. Chem. Soc.*, **130**, 7873–7881.

Masliah,E., Rockenstein,E., Adame,A., *et al.* (2005) *Neuron*, **46**, 857–868.

Masliah,E., Rockenstein,E., Mante,M., *et al.* (2011) *PLoS One*, **6**, e19338.

Masuda,M., Suzuki,N., Taniguchi,S., Oikawa,T., Nonaka,T., Iwatsubo,T., Hisanaga,S., Goedert,M. and Hasegawa,M. (2006) *Biochemistry*, **45**, 6085–6094.

Meng,X., Munishkina,L.A., Fink,A.L. and Uversky,V.N. (2009) *Biochemistry*, **48**, 8206–8224.

Mirecka,E.A., Shaykhalishahi,H., Gauhar,A., Akgül,S., Lecher,J., Willbold,D., Stoldt,M. and Hoyer,W. (2014) *Angew. Chem. Int. Ed.*, **53**, 4227–4230.

Norris,E.H., Giasson,B.I., Hodara,R., Xu,S., Trojanowski,J.Q., Ischiropoulos,H. and Lee,V.M. (2005) *J. Biol. Chem.*, **280**, 21212–21219.

Pace,C.N., Hebert,E.J., Shaw,K.L., *et al.* (1998) *J. Mol. Biol.*, **279**, 271–286.

Querfurth,H.W. and LaFerla,F.M. (2010) *N. Engl. J. Med.*, **362**, 329–344.

Robinson,C.R. and Sauer,R.T. (1996) *Biochemistry*, **35**, 13878–13884.

Robinson,C.R. and Sauer,R.T. (1998) *Proc. Natl Acad. Sci. USA*, **95**, 5929–5934.

Schneeberger,A., Mandler,M., Mattner,F. and Schmidt,W. (2012) *Parkinsonism Relat. Disord.*, **18**, S11–S13.

Tran,H.T., Chung,C.H., Iba,M., Zhang,B., Trojanowski,J.Q., Luk,K.C. and Lee,V.M. (2014) *Cell Rep.*, **7**, 2054–2065.

Valera,E. and Masliah,E. (2013) *Pharmacol. Ther.*, **138**, 311–322.

van Leeuwen,H.C., Strating,M.J., Rensen,M., de Laat,W. and van der Vliet,P.C. (1997) *EMBO J.*, **16**, 2043–2053.

Zhou,C., Emadi,S., Sierks,M.R. and Messer,A. (2004) *Mol. Ther.*, **10**, 1023–1031.

Zhou,W., Gallagher,A., Hong,D.P., Long,C., Fink,A.L. and Uversky,V.N. (2009) *J. Mol. Biol.*, **388**, 597–610.

# Chapter 2

**SEQUESTRATION OF A β-HAIRPIN FOR CONTROL OF α-SYNUCLEIN AGGREGATION**

Ewa A. Mirecka, Hamed Shaykhalishahi, Aziz Gauhar, Şerife Akgül, Justin Lecher,

Dieter Willbold, Matthias Stoldt, and Wolfgang Hoyer

Proportion of contribution to this work: 30%

Design, cloning, expression, and purification of AS69-GS3, expression and purification of α-synuclein, determination of binding affinity and secondary structure, aggregation assays, cell toxicity assays

**Protein Aggregation**

# Sequestration of a β-Hairpin for Control of α-Synuclein Aggregation**

*Ewa A. Mirecka, Hamed Shaykhalishahi, Aziz Gauhar, Şerife Akgül, Justin Lecher, Dieter Willbold, Matthias Stoldt, and Wolfgang Hoyer*

*Abstract: The misfolding and aggregation of the protein α-synuclein (α-syn), which results in the formation of amyloid fibrils, is involved in the pathogenesis of Parkinson's disease and other synucleinopathies. The emergence of amyloid toxicity is associated with the formation of partially folded aggregation intermediates. Here, we engineered a class of binding proteins termed β-wrapins (β-wrap proteins) with affinity for α-synuclein (α-syn). The NMR structure of an α-syn:β-wrapin complex reveals a β-hairpin of α-syn comprising the sequence region α-syn(37–54). The β-wrapin inhibits α-syn aggregation and toxicity at substoichiometric concentrations, demonstrating that it interferes with the nucleation of aggregation.*

$T$he conversion of specific peptides and proteins into amyloid fibrils has been identified as a causative mechanism underlying several neurodegenerative conditions. Monomeric and oligomeric misfolding intermediates are key species on the aggregation pathway;[1] thus, the stabilization of partially folded states of amyloid proteins has been suggested as an approach for drug development.[1d]

The protein α-synuclein (α-syn) is the major protein component of the intracellular neuronal deposits observed in Parkinson's disease and related synucleinopathies.[2] A role of α-syn aggregation in the pathogenesis is supported by various genetic studies showing the enhanced propensity of α-syn to aggregate as a result of disease-related mutation or multiplication of the α-syn gene. Structurally, α-syn is characterized by high conformational flexibility. Free monomeric α-syn is intrinsically disordered; however, some regions of the protein show intramolecular long-range interactions.[3] When bound to synthetic or biological membranes, α-syn can readily adopt

α-helical conformation.[4] In the fibrillar form, the central region of α-syn forms several β-strands which assemble into in-register parallel β-sheets in the fibril core, whereas the N-terminal part of the protein is less ordered and the C-terminus remains unfolded.[5] In contrast to the parallel arrangement of α-syn in fibrils,[5b, 6] α-syn oligomers have been shown to adopt an antiparallel β-sheet structure.[7]

To stabilize partially structured α-syn, we generated binding ligands to α-syn using ZAβ$_3$, a binding protein to the amyloid-β peptide (Aβ), as a scaffold. ZAβ$_3$ is a disulfide-linked homodimer derived from the Z domain of protein A.[8] According to isothermal titration calorimetry (ITC), ZAβ$_3$ binds Aβ with a dissociation constant of 20 nM but shows no affinity to α-syn (Figure S1). To generate binding affinity to α-syn, we created a new phage display library through random mutagenesis of the gene encoding ZAβ$_3$. The binding ligands selected from this library are referred to as β-wrapins (β-wrap proteins). The β-wrapin clone AS69 harboring four amino acid substitutions in each subunit, that is, G13D, V17F, I31F, and L34V, was found to bind α-syn with a $K_d$ value of 240 nM (Figure S1). In comparison to the original ZAβ$_3$, the affinity of AS69 towards Aβ was 400-fold reduced. ITC indicated that the AS69:α-syn interaction follows a 1:1 stoichiometry. The binding of AS69 to α-syn was confirmed by ($^1$H-$^{15}$N) HSQC NMR spectroscopy. The spectra of free [U-$^{15}$N]-α-syn obtained at 30 °C showed only a few resonance signals stemming from the C-terminus, whereas cross-peaks from the N-terminal and central regions were not detected due to intermediate exchange.[9] However, upon addition of [NA]-AS69 to [U-$^{15}$N]-α-syn, several well-dispersed resonance signals appeared, indicating partial folding of α-syn (Figure 1a). The new resonances were assigned to the region α-syn(35–56).

To identify the conformation of α-syn(35–56), we determined the structure of full-length α-syn in complex with β-wrapin AS69 by high-resolution liquid-state NMR spectroscopy (Figure 1b,d, Tables S1 and S2). α-syn(35–56) folds into a β-hairpin comprising residues $^{37}$VLYVGSK$^{43}$ (β1) and $^{48}$VVHGVAT$^{54}$ (β2), connected by a β-turn formed by amino acids $^{44}$TKEG$^{47}$ (Figure 1b). The aromatic amino acids Tyr-39 and His-50 are located at the center of one β-hairpin face with their side chains hydrogen-bonded by the hydroxy proton of Tyr-39 and the N$^\delta$-nitrogen of His-50 (Figure 1b). The H$^\eta$ of Tyr-39 and H$^{ε2}$ of His-50 are protected from exchange with solvent as inferred from their detectability in the NMR spectra.

The sequence positions of the β-strands are in good agreement with those of the β1 and β2 strands (designated according to Vilar et al.)[5d] of fibrillar α-syn (Figure 1c). Long-range interactions between the side chains Tyr-39 in β1 and His-50 in β2 have also been detected in α-syn amyloid

[*] Dr. E. A. Mirecka,[+] H. Shaykhalishahi,[+] A. Gauhar, Ş. Akgül, Dr. J. Lecher, Prof. Dr. D. Willbold, Dr. M. Stoldt, Dr. W. Hoyer
Institut für Physikalische Biologie
Heinrich-Heine-Universität Düsseldorf
40204 Düsseldorf (Germany)
E-mail: Wolfgang.Hoyer@uni-duesseldorf.de

Dr. J. Lecher, Prof. Dr. D. Willbold, Dr. M. Stoldt, Dr. W. Hoyer
Strukturbiochemie (ICS-6), Forschungszentrum Jülich
52425 Jülich (Germany)

[+] These authors contributed equally to this work.
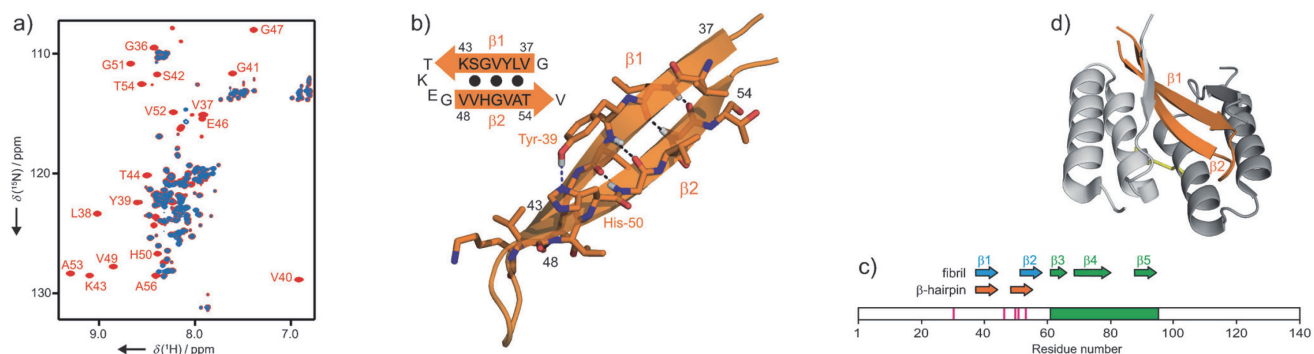
**Figure 1.** β-hairpin structure of α-syn in complex with β-wrapin AS69. a) ($^{1}$H-$^{15}$N) HSQC NMR spectra of [U-$^{15}$N]-α-syn recorded at 30 °C in the absence (blue) and presence (red) of an excess of [NA]-AS69. Assignments of peaks appearing upon complex formation are indicated. b) Ribbon drawing illustrating the β-hairpin of α-syn (orange). Amino acids forming the β1 and β2 strands are shown as sticks. The hydrogen bond between the hydroxy proton of Tyr-39 and the N$^{\delta}$-nitrogen of His-50 is indicated as a dashed blue line. Backbone hydrogen bonds are marked as dashed black lines. The corresponding amino acid sequence is shown and backbone hydrogen bonding across the strands is indicated with black dots. c) Features of the α-syn primary structure. The central NAC region is shown in green. The positions of disease-related mutations are given in magenta. The location of β-strands in α-syn within fibrils as identified by EPR and solid-state NMR analysis[5] is approximated by blue and green arrows. The location of the β-strands within the β-hairpin of α-syn is given by orange arrows. d) The α-syn:AS69 complex illustrated by ribbon drawing. Residues 13–58 of the two AS69 subunits are shown in light and dark gray, respectively. The disulfide bond is shown in yellow. The β-hairpin of α-syn is shown in orange.

fibrils.[5d] The NAC region comprising β-strands β3 to β5, including the aggregation-prone sequence stretches with the highest hydrophobicity and β-sheet propensity,[10] is unaffected by AS69 binding (Figure S2). This demonstrates the specificity of the interaction of AS69 with the β1–β2 region.

Contacts between β1 and β2 are among the most prevalent transient tertiary interactions in monomeric α-syn according to paramagnetic relaxation enhancement data.[3c] Moreover, nascent β-structure was detected in the β1–β2 region of α-syn monomers.[1c] These findings suggest that structural features of the AS69-bound β-hairpin are present within a subset of the conformational ensemble sampled by free α-syn. This is in line with the observation that the binding mechanism of intrinsically disordered proteins is not solely of the induced-fit type, but also involves conformational selection.[11]

A comparison of the structures of the α-syn:AS69 and Aβ:ZAβ₃ complexes confirmed that the introduced mutations did not affect the overall structure of the β-wrapin protein scaffold in the bound state. The AS69 molecule is a dimer of two identical subunits covalently linked by a disulfide bond involving the Cys-28 residues of both subunits. The folding topology of AS69 comprises two β-strands and four α-helices forming a large hydrophobic tunnel-like cavity in which the β-hairpin of α-syn is buried (Figure 1 d). Most of the exchanged amino acids are in direct contact with the β-hairpin (Figure S3). For example, the Phe-31 residues of both AS69 subunits are involved in aromatic–aromatic interactions with Tyr-39 and His-50 of α-syn.

The potency of AS69 to inhibit α-syn aggregation was evaluated by a Thioflavin T fluorescence assay. In the absence of AS69, a 35 μM solution of α-syn aggregated after a lag phase of roughly 10 h. However, the aggregation of α-syn was completely inhibited in the presence of an equivalent concentration of AS69 within an 8 day experiment (Figure 2 a). Addition of an equimolar amount of AS69 to α-syn

aggregation reactions at different time points prevented further fibrillation of α-syn (Figure 2 b). These observations indicate that sequestration of the β-hairpin renders α-syn monomers incompetent to aggregate. In addition, AS69 inhibited fibrillation of α-syn at substoichiometric concentrations. For AS69:α-syn molar ratios of 1:10, 1:100, and 1:1000, AS69 prolonged the lag time of α-syn fibrillation 9-fold, 6-fold, and 2-fold, respectively (Figure 2 d and Figure S4). Size-exclusion chromatography confirmed that the binding of β-wrapin AS69 to α-syn delayed fibrillation at substoichiometric ratios and furthermore revealed that during the lag time of the aggregation experiment stable oligomeric species were not formed (Figure 2 c). The substoichiometric inhibition cannot be explained by monomer sequestration. Thus, a second inhibitory mechanism must be operative which interferes with the nucleation of aggregation. This mechanism might involve the binding of AS69 to the β1–β2 region of α-syn within early aggregates. However, other α-syn epitopes may also be crucial for the substoichiometric inhibition. In this context, it is of note that α-syn oligomers exhibit antiparallel β-structure.[7] With the present data the mechanism of substoichiometric inhibition cannot be elucidated. Possible mechanisms include: 1) a small fraction of AS69-bound α-syn molecules within oligomers precludes the concerted conformational conversion to ordered amyloid fibrils; 2) AS69 binds with high affinity to fibril ends, thereby blocking fibril growth.

To evaluate the effect of AS69 on α-syn toxicity, the viability of human SH-SY5Y neuroblastoma cells was analyzed upon addition of α-syn samples aged in the absence and presence of β-wrapin AS69. For fibrillar α-syn samples, we observed a concentration-dependent decrease in the cellular viability as assessed by an MTT assay (Figure 2 e). The viability of SH-SY5Y cells was rescued when α-syn samples were incubated in the presence of AS69. The viability rescue was dependent on the concentration of AS69, with complete

↖↖ **These are not the final page numbers!**
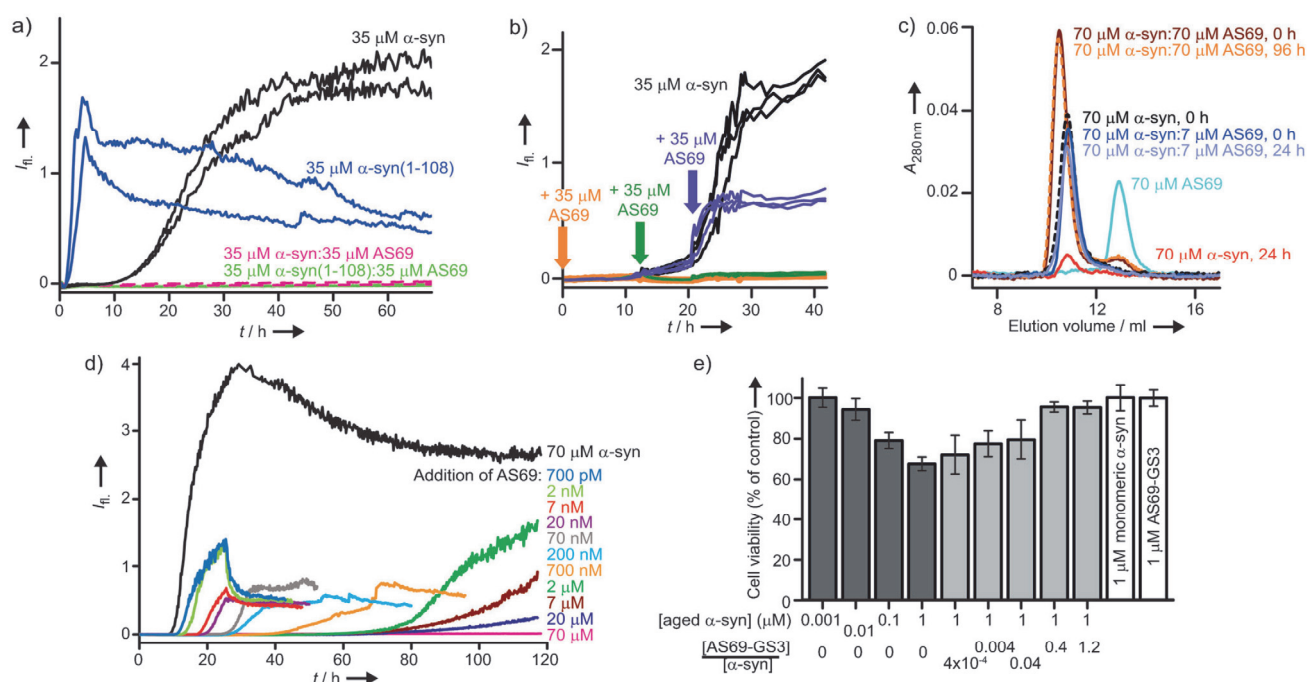
**Figure 2.** Inhibition of α-syn aggregation and toxicity by β-hairpin sequestration. a) Thioflavin T (ThT) time course of fibrillation of full-length α-syn and of the highly aggregation-prone, C-terminally truncated α-syn(1–108) in the absence and presence of AS69 in stoichiometric amounts (duplicate experiments). The extension of this experiment to 8 days did not lead to an increase in ThT fluorescence intensity for the samples containing AS69. b) Addition of stoichiometric amounts of AS69 at different time points, indicated by arrows, to fibrillation reactions of 35 μM α-syn monitored by ThT fluorescence (triplicate experiments). c) Size-exclusion chromatography analysis of α-syn aggregation in absence and presence of AS69. Protein samples at indicated concentrations were subjected to an aggregation assay for the indicated times and loaded on a Superdex 75 10/300 GL column (void volume ca. 8 mL). In the absence of AS69, the elution peak of α-syn was greatly reduced after 24 h incubation due to the formation of amyloid fibrils which do not enter the column bed. d) Fibrillation kinetics monitored by ThT versus the concentration of AS69. One example time trace for each AS69 concentration is displayed. The mean lag time determined from three experiments is shown in Figure S4. e) MTT assay to evaluate the toxicity of α-syn solutions aged in the absence (dark gray bars) and presence (light gray bars) of AS69-GS3 on SH-SY5Y cells. The data are the mean and standard deviation of 12 measurements performed in four wells for each of three independent experimental repeats.

rescue at equimolar ratio of AS69:α-syn and partial rescue at substoichiometric amounts.

This study shows that sequestration of a β-hairpin in the region α-syn(37–54) interferes with aggregation and toxicity. The importance of this region for the pathogenesis of Parkinson's disease is underscored by the fact that it contains most of the reported disease-related point mutations (Figure 1c). The H50Q, G51D, and A53T mutations are located within the β2 strand, whereas the E46K mutation resides in the turn connecting the β-strands. The A53T and E46K mutations promote oligomerization and fibril formation.[2a] Out of a set of charge-changing mutations, in particular those mutations immediately preceding (E35K) and succeeding (E57K) the β-hairpin region have been shown to accelerate oligomer formation.[1f] These results support a link between the β-hairpin region, oligomerization, and disease pathogenesis.

The data presented here provide detailed insight into the interaction of α-syn with the aggregation inhibitor β-wrapin AS69. The study shows that α-syn aggregation and toxicity can be controlled by sequestering a β-hairpin, offering

perspectives for early interference with the pathogenesis of synucleinopathies.

[1] a) C. Haass, D. J. Selkoe, *Nat. Rev. Mol. Cell Biol.* **2007**, *8*, 101–112; b) R. Kayed, E. Head, J. L. Thompson, T. M. McIntire, S. C. Milton, C. W. Cotman, C. G. Glabe, *Science* **2003**, *300*, 486–489; c) H. Y. Kim, H. Heise, C. O. Fernandez, M. Baldus, M. Zweckstetter, *ChemBioChem* **2007**, *8*, 1671–1674; d) C. E. Munte, M. B. Erlach, W. Kremer, J. Koehler, H. R. Kalbitzer, *Angew. Chem.* **2013**, *125*, 9111–9116; *Angew. Chem. Int. Ed.* **2013**, *52*, 8943–8947; e) F. Sziegat, J. Wirmer-Bartoschek, H. Schwalbe, *Angew. Chem.* **2011**, *123*, 5628–5632; *Angew. Chem. Int. Ed.* **2011**, *50*, 5514–5518; f) B. Winner, R. Jappelli, S. K. Maji, P. A. Desplats, L. Boyer, S. Aigner, C. Hetzer, T. Loher, M. Vilar, S. Campioni, C. Tzitzilonis, A. Soragni, S. Jessberger, H.

Mira, A. Consiglio, E. Pham, E. Masliah, F. H. Gage, R. Riek, *Proc. Natl. Acad. Sci. USA* **2011**, *108*, 4194–4199; g) N. Zijlstra, C. Blum, I. M. Segers-Nolten, M. M. Claessens, V. Subramaniam, *Angew. Chem.* **2012**, *124*, 8951–8954; *Angew. Chem. Int. Ed.* **2012**, *51*, 8821–8824.

[2] a) H. A. Lashuel, C. R. Overk, A. Oueslati, E. Masliah, *Nat. Rev. Neurosci.* **2013**, *14*, 38–48; b) L. Breydo, J. W. Wu, V. N. Uversky, *Biochim. Biophys. Acta Mol. Basis Dis.* **2012**, *1822*, 261–285.

[3] a) C. W. Bertoncini, Y. S. Jung, C. O. Fernandez, W. Hoyer, C. Griesinger, T. M. Jovin, M. Zweckstetter, *Proc. Natl. Acad. Sci. USA* **2005**, *102*, 1430–1435; b) M. M. Dedmon, K. Lindorff-Larsen, J. Christodoulou, M. Vendruscolo, C. M. Dobson, *J. Am. Chem. Soc.* **2005**, *127*, 476–477; c) S. Esteban-Martín, J. Silvestre-Ryan, C. W. Bertoncini, X. Salvatella, *Biophys. J.* **2013**, *105*, 1192–1198.

[4] D. Eliezer, E. Kutluay, R. Bussell, Jr., G. Browne, *J. Mol. Biol.* **2001**, *307*, 1061–1073.

[5] a) H. Heise, W. Hoyer, S. Becker, O. C. Andronesi, D. Riedel, M. Baldus, *Proc. Natl. Acad. Sci. USA* **2005**, *102*, 15871–15876; b) M. Chen, M. Margittai, J. Chen, R. Langen, *J. Biol. Chem.* **2007**, *282*, 24970–24979; c) G. Comellas, L. R. Lemkau, A. J. Nieuwkoop, K. D. Kloepper, D. T. Ladror, R. Ebisu, W. S. Woods, A. S. Lipton, J. M. George, C. M. Rienstra, *J. Mol. Biol.* **2011**, *411*, 881–895; d) M. Vilar, H. T. Chou, T. Luhrs, S. K. Maji, D. Riek-Loher, R. Verel, G. Manning, H. Stahlberg, R. Riek, *Proc. Natl. Acad. Sci. USA* **2008**, *105*, 8637–8642.

[6] A. Loquet, K. Giller, S. Becker, A. Lange, *J. Am. Chem. Soc.* **2010**, *132*, 15164–15166.

[7] M. S. Celej, R. Sarroukh, E. Goormaghtigh, G. D. Fidelio, J. M. Ruysschaert, V. Raussens, *Biochem. J.* **2012**, *443*, 719–726.

[8] C. Grönwall, A. Jonsson, S. Lindstrom, E. Gunneriusson, S. Stahl, N. Herne, *J. Biotechnol.* **2007**, *128*, 162–183; b) W. Hoyer, C. Grönwall, A. Jonsson, S. Ståhl, T. Härd, *Proc. Natl. Acad. Sci. USA* **2008**, *105*, 5099–5104.

[9] B. C. McNulty, A. Tripathy, G. B. Young, L. M. Charlton, J. Orans, G. J. Pielak, *Protein Sci.* **2006**, *15*, 602–608.

[10] a) B. I. Giasson, I. V. Murray, J. Q. Trojanowski, V. M. Lee, *J. Biol. Chem.* **2001**, *276*, 2380–2386; b) S. Zibaee, G. Fraser, R. Jakes, D. Owen, L. C. Serpell, R. A. Crowther, M. Goedert, *J. Biol. Chem.* **2010**, *285*, 38555–38567.

[11] a) P. Csermely, R. Palotai, R. Nussinov, *Trends Biochem. Sci.* **2010**, *35*, 539–546; b) M. Fuxreiter, I. Simon, P. Friedrich, P. Tompa, *J. Mol. Biol.* **2004**, *338*, 1015–1026.

↖↖ These are not the final page numbers!

# Communications

**Protein Aggregation**

E. A. Mirecka, H. Shaykhalishahi,
A. Gauhar, Ş. Akgül, J. Lecher, D. Willbold,
M. Stoldt, W. Hoyer* ———— ▮▮▮▮–▮▮▮▮

Sequestration of a β-Hairpin for Control
of α-Synuclein Aggregation
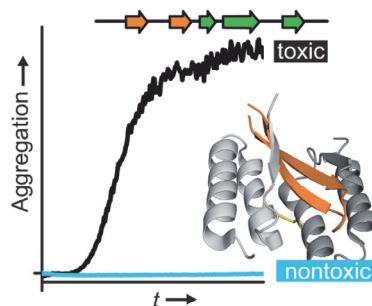
**Wrapping the hairpin**: NMR spectroscopy identifies a β-hairpin conformation of α-synuclein in complex with an engineered β-wrapin. The β-wrapin inhibits α-synuclein aggregation and toxicity at substoichiometric concentration. Sequestration of a β-hairpin is a novel approach to interfere with the initial steps of the aggregation reaction.

## Sequestration of a β-Hairpin for Control of α-Synuclein Aggregation**

Ewa A. Mirecka, Hamed Shaykhalishahi, Aziz Gauhar, Şerife Akg l, Justin Lecher,
Dieter Willbold, Matthias Stoldt, and Wolfgang Hoyer*

anie_201309001_sm_miscellaneous_information.pdf

**Table of contents**

**Supporting Experimental Section**

**Library construction and phage display selection.** A second generation β-wrapin library based on the ZAβ$_3$ scaffold [1] was generated by error-prone PCR. The library construct in a pComb3HSS vector backbone (provided by C. F. Barbas, The Scripps Research Institute, La Jolla, USA) contained OmpA leader, AQHDEA peptide derived from the region E of protein A followed by the gene encoding β-wrapin clones, c-myc-tag, albumin-binding domain from streptococcal protein G and protein III(230-406) of M13 filamentous phage. Error-prone PCR was performed with the GeneMorph II Random Mutagenesis Kit (Stratagene) in a reaction containing 200 fg of the vector template containing the gene encoding for ZAβ$_3$ monomer and vector-specific primers flanking the ZAβ$_3$ gene: 5′GCCGAGCTCGCGCAACACGATGAAGCC and 5′CGCTGATCAGTTTTTGTTCCTCGAG (MWG Biotech). The DNA was amplified for 40 cycles (95 °C 30 s, 54 °C 30 s, 72 °C 1 min) and used as a template in the second PCR with DreamTaq DNA Polymerase (Thermo Scientific) and the same set of primers. The mutated ZAβ$_3$ gene was gel purified and digested with SacI and XhoI (New England Biolabs) followed by ligation into the corresponding sites of a modified pComb3HSS vector. The library was transformed into electrocompetent *E. coli* XL1-Blue cells (Stratagene) resulting in 7 x 10$^7$ transformants. The phage library was produced by superinfection of bacteria harboring the library with M13KO7 phage (New England Biolabs) and precipitation by PEG/NaCl. In order to remove streptavidin-binding phage, a negative selection in which the phage preparation was incubated with streptavidin magnetic beads at room temperature for 1 h preceded each selection round. The library (10$^{11}$–10$^{13}$ colony-forming units) was then subjected to successive rounds of panning with biotinylated α-syn(1-108). During each round, the phage library was incubated with α-syn(1-108) at a concentration of 500, 300, 50 and 10 nM in rounds 1-4, respectively. In the first panning round, the incubation was carried out overnight at 4 °C whereas the subsequent selection rounds were done for 1 h at room temperature. The phage-target complexes were captured on streptavidin magnetic beads and following washing (1-, 5-, 8- and 20-times in rounds 1-4, respectively) with PBST-BSA (PBS, 0.1% (w/v) Tween 20, 3% (v/v) BSA) and once with PBS, bound phages were eluted by lowering the pH to 2.0. Following neutralization with 1 M Tris-HCl, pH 8.0, the eluted phages were amplified in *E. coli* XL1-Blue cells and subjected to the following panning round. After the fourth selection round, the DNA pool was subcloned into pET302/NT-His vector (Invitrogen) and DNA from 90 single colonies was sequenced (MWG Biotech).

**Protein preparation.** Full-length α-syn and α-syn(1-108) were expressed from pT7-7 vector and purified essentially as described.[2] Briefly, cell lysates were obtained from *E. coli* BL21(DE3) cells cultivated in M9 minimal medium supplemented with NH$_4$Cl (1 g/l) and glucose (2 g/l), followed by IPTG (isopropyl-β-D-1-thiogalactopyranoside) induction. Both proteins were purified using anion exchange chromatography on a HiTrap Q FF column (GE Healthcare). Full-length α-syn was eluted with a salt gradient at approximately 300 mM NaCl, whereas α-syn(1-108) was collected in the flow-through. Further purification was achieved by size-exclusion chromatography on a HiLoad 16/60 Superdex 75 column (GE Healthcare) in 20 mM sodium phosphate, 50 mM NaCl, pH 7.4. Biotinylation was performed with Sulfo-NHS-LC-Biotin (Thermo Scientific) in a reaction containing ~200 μM of α-syn(1-108) in 20 mM sodium phosphate, pH 6.5 and a 5-fold molar excess of biotinylation reagent. After incubation at 4 °C for 3 h, the protein sample was passed through a Zeba Spin desalting column (Thermo Scientific) followed by affinity purification on monomeric avidin agarose

(Thermo Scientific). The level of biotinylation was quantified by HABA assay (Thermo Scientific), yielding an average value of 2 biotin molecules incorporated per α-syn(1-108) monomer.

Aβ(1-40) was produced with an N-terminal methionine by recombinant coexpression with ZAβ$_3$.[3]

AS69 and ZAβ$_3$ containing an N-terminal His6-tag were expressed from pET302/NT-His vector in *E. coli* BL21(DE3) cells. Head-to-tail linked AS69 dimer (termed AS69-GS3) used for cell culture experiments was expressed from the same vector. Expression cultures were grown in LB medium. Protein expression was induced with 1 mM IPTG at OD 0.6-0.8 for 4 h at 37 °C. Following centrifugation at 4,000 x g, the cell pellet was resuspended in 20 mM sodium phosphate, pH 8.3, 500 mM NaCl, containing EDTA-free protease inhibitor (Roche Applied Sciences) and lysed by a cell disrupter (Constant Systems). Insoluble material was removed by centrifugation at 28,000 x g and the supernatant was loaded on a HisTrap FF column (GE Healthcare). The dimeric fractions of AS69 or ZAβ$_3$ as well as AS69-GS3 were collected from a HiLoad 16/60 Superdex 75 size- exclusion chromatography column (GE Healthcare) in 20 mM sodium phosphate, 50 mM NaCl, pH 7.4.

For NMR experiments, proteins were expressed in M9 minimal medium supplemented with $^{15}$N-NH$_4$Cl (1 g/l) and $^{13}$C$_6$-glucose (2 g/l) and purified as described for the non-isotopically enriched proteins.

**Isothermal titration calorimetry (ITC).** ITC was performed on a Microcal iTC200 calorimeter (GE Healthcare) at 30 °C. The buffer was 20 mM sodium phosphate, 50 mM NaCl, pH 7.4. For determination of affinities to α-syn, AS69 or ZAβ$_3$ were used as titrant in the cell at a concentration of ~60 μM, and α-syn at approximately 10-fold higher concentration as titrant in the syringe. For determination of affinities to Aβ, Aβ was used as titrant in the cell at a concentration of 10 μM, and AS69 or ZAβ$_3$ at 100 μM as titrant in the syringe. The heat of post-saturation injections was averaged and subtracted from each injection to correct for heats of dilution and mixing. Data were processed using MicroCal Origin software provided with the calorimeter. Dissociation constants were obtained from a nonlinear least-squares fit to a 1:1 binding model.

**Aggregation assay.** Fibrillation of α-syn was followed by thioflavin T fluorescence. The reaction contained 35 or 70 μM of α-syn and 40 μM thioflavin T in 20 mM sodium phosphate, 50 mM NaCl, pH 6.0, 0.04% Na-azide, in a final volume of 150 μl. Aggregation was performed at 37° C with continuous orbital shaking (300 rpm) in a round-bottom 96-well black plate (Nunc) containing a 2 mm glass bead in each well. Thioflavin T emission was recorded at 480 nm (excitation 440 nm) on an Infinite M1000 plate reader (Tecan). For background correction, the signal of a buffer sample containing thioflavin T was subtracted. The lag-time was defined as the incubation time at which the fluorescence intensity for the first time reaches 5% of the final steady state fluorescence of α-syn in the absence of AS69. Protein samples were analyzed before and after the aggregation assay by size-exclusion chromatography on a Superdex 75 10/300 GL column (GE Healthcare) in 20 mM sodium phosphate, 50 mM NaCl, pH 7.4.

**MTT cell viability assay.** The viability of SH-SY5Y neuroblastoma cells in the presence of α-syn was tested with an MTT assay (Cell Proliferation Kit I, Roche Diagnostic). SH-SY5Y cells (purchased from DSMZ) were seeded in 96-well tissue culture plate at a density of 20,000 cells/well in 100 μL of media (DMEM-F12, 10% fetal calf serum) and incubated for 24 h. Following application of the protein samples at the indicated concentrations, cells were further incubated for 24 h. Untreated cells and cells either exposed to monomeric α- syn or AS69 were considered as controls. To assess the effects of test samples on the cells, MTT was added to the cells at a final concentration of 0.5 mg/mL in PBS followed by incubation for an additional 4 h at 37 °C. Next, 100 μL of the solubilization solution (10% SDS and 0.01 M HCl) was added and incubation was continued overnight at 37 °C followed by measuring the absorbance at 565 nm in an Infinite M1000 plate reader (Tecan). The data was normalized to the value of untreated control cells. All cell cultures were maintained in a 5% CO$_2$ humidified atmosphere at 37 °C.

**NMR and structure determination.** NMR experiments were performed at 10 or 30 °C on Varian VNMRS instruments at proton frequencies of 800 and 900 MHz, each equipped with a cryogenically cooled Z-axis pulse-field-gradient (PFG) triple resonance probe. NMR samples contained [U-$^{13}$C,$^{15}$N]-α-syn or [U-$^{13}$C,$^{15}$N]-AS69 at a concentration of 0.7 mM and a 20% molar excess of the respective non-isotopically enriched binding partner in 20 mM sodium phosphate, 50 mM NaCl, pH 7.4. NMR data were processed using NMRPipe[4] and analyzed with CcpNmr.[5] Mean weighted chemical shift displacements were calculated as $[(\Delta\delta^1H)^2 + (\Delta\delta^{15}N)^2/25]^{1/2}$. Backbone assignments were obtained using BEST-TROSY experiments [6] and side-chain assignments were

obtained using standard triple resonance heteronuclear NMR techniques. Histidine side chain protonation states were determined using a long-range ($^1$H-$^{15}$N)-HMQC experiment.[7] Nuclear Overhauser enhancement (NOE) based distance restraints for structure calculation were derived from 3D ($^1$H-$^1$H-$^{15}$N)-NOESY-HSQC (120 ms mixing time), ($^1$H-$^{13}$Cali-$^1$H)-HSQC-NOESY (100 ms mixing time) and ($^1$H-$^{13}$Caro-$^1$H)-HSQC-NOESY (100 ms mixing time) experiments and 2D NOESY for protons H$^\eta$ of Tyr-39 and H$^{\varepsilon 2}$ of His-50 of α-syn. Backbone dihedral angle constraints were derived from chemical shifts, using TALOS+.[8] Structure calculations based on NOE distance restraints and dihedral angle restraints were accomplished with a modified version of CNS v. 1.2.1[9] using an optimized version of the PARALLHDG force field. The MD protocol contained 30 ps high-temperature torsion angle dynamics (10,000 K) and 20,000 steps during two cooling phases (2,000 K and 50 K). Ten lowest energy structures (overall CNS energy) out of 100 calculated were selected and validated using Molprobity.[10] Molecular graphics figures were created using PyMOL.[11]
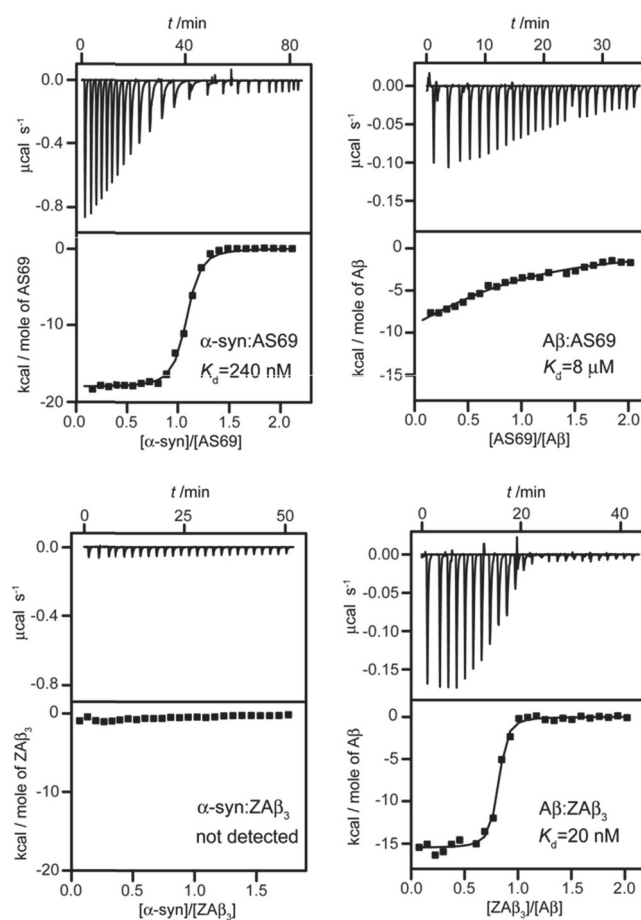
***Figure S1.*** Generation of binding specificity for α-syn. The affinity of AS69 to α-syn was analyzed by ITC. AS69 was used as titrant in the cell at a concentration of 65 μM and α-syn at 680 μM as titrant in the syringe. For comparison, the affinity of AS69 to Aβ was determined, using Aβ as titrant in the cell at a concentration of 10 μM, and AS69 at 100 μM as titrant in the syringe. The affinities of ZAβ3 to α-syn and Aβ were analyzed under similar experimental conditions. ITC experiments were performed at 30 °C.
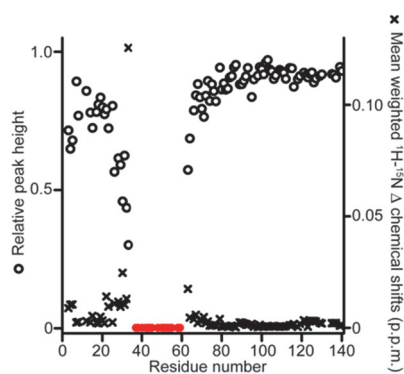
***Figure S2.*** Effect of AS69 binding on different α-syn sequence regions. ($^1$H–$^{15}$N)-HSQC NMR spectra were recorded at 10 °C. At this temperature, resonances from nearly all residues in free α-syn are visible.[12] Upon addition of [NA]-AS69 to [U-$^{15}$N]-α-syn, the resonance signals of residues in the β-hairpin region of α-syn disappeared, indicative of intermediate exchange in the complex at this temperature (red circles). According to changes in the peak height (open circles) and in the chemical shifts (crosses), AS69 binding had some effect on the conformation of the N-terminal part of α-syn, especially on the very N-terminal residues up to Met-5 and the region α-syn(22-35) preceding the β-hairpin. The changes in chemical shifts were small, however, indicating that these regions remain disordered in the bound state. The central as well as the C-terminal region of α-syn were essentially unaffected.
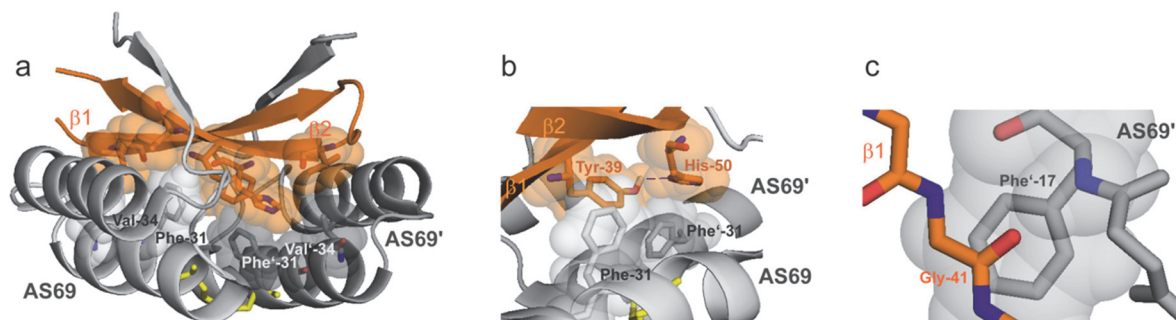
***Figure S3.*** Effect of the mutations of the scaffold present in AS69. AS69 carries four amino acid substitutions in each homodimer subunit, i.e. G13D, V17F, I31F and L34V. a) The amino acids Phe-31 and Val-34 in both subunits are in contact with the interior face of the β-hairpin contributed by residues Val-37, Tyr-39, Val-48, His-50 and Val-52. Nonpolar side chains of α-syn with <60% solvent accessibility and Phe-31 and Val-34 of both AS69 subunits are displayed as sticks and spheres. The two AS69 subunits are shown in light and dark gray and are labeled AS69 or AS69´, respectively. The disulfide bond is shown in yellow. The β-hairpin of α-syn is shown in orange. b) The Phe-31 residues of both AS69 subunits are involved in aromatic-aromatic interactions with Tyr-39 and His-50 of α-syn. c) The V17F mutation in AS69 stabilizes the β-hairpin of α-syn by aromatic rescue of a glycine, i.e. Gly-41, in the β1 strand of α-syn. The side chain of Phe-17 in one AS69 subunit adopts the gauche$^+$ $\chi_1$ rotamer and lays over the cross-strand Gly-41. For the G13D mutation located at the N-terminal end of the folded region of AS69 no specific interactions of the acidic side chain were discernible in the complex structure. However, this residue might be involved in electrostatic steering of binding,[13] e.g. by interacting with Lys-43, Lys-45, or Lys-58 of α-syn.
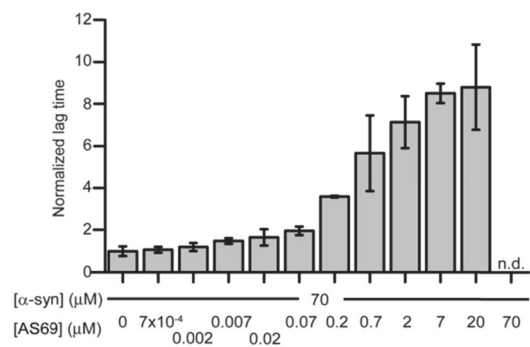
***Figure S4.*** Inhibition of α-syn aggregation by substoichiometric concentrations of AS69. The lag-time of fibrillation kinetics monitored by thioflavin T in dependence of the concentration of AS69. The mean lag time determined from three experiments is given. Error bars represent the s.d. (n.d. = no fibrillation detectable).

**Table S1. Constraint statistics of the α-syn:AS69 complex**

| Constraint type | Number |
| --- | --- |
| Distance constraints | |
|   Unambiguous NOE constraints | 3015 |
|   Intra-residue | 930 |
|   Inter-residue | 2085 |
|    Sequential ($|i - j| = 1$) | 598 |
|    Medium-range ($|i - j| \leq 5$) | 595 |
|    Long-range ($|i - j| > 5$) | 410 |
|    Intermolecular | 482 |
|   Hydrogen bonds | 1 |
|   Ambiguous NOE constraints | 319 |
| Total dihedral angle restraints | 196 |
|   $\phi/\psi$ | 98 |

**Table S2. Structure statistics of the α-syn:AS69 complex**

| Statistics | Value |
| --- | --- |
| Violations (mean and s.d.) | |
|   Distance constraints (Å) | $0.025 \pm 0.0007$ |
|   Dihedral angle constraints (º) | $1.5 \pm 0.08$ |
|   Max. dihedral angle violation (º) | 11 |
|   Max. distance constraint violation (Å) | 0.35 |
| Deviations from idealized geometry | |
|   Bond lengths (Å) | $0.0065 \pm 0.0001$ |
|   Bond angles (º) | $0.75 \pm 0.01$ |
|   Impropers (º) | $1.84 \pm 0.04$ |
| Average pairwise r.m.s. deviation* (Å) | |
|   Heavy | $0.72 \pm 0.08$ |
|   Backbone | $0.36 \pm 0.05$ |
| Ramachandran statistics | |
|   Core regions (%) | $92.7 \pm 0.6$ |
|   Allowed regions (%) | $6.3 \pm 0.6$ |
|   Generous regions (%) | $1.1 \pm 0$ |
|   Disallowed regions (%) | $0 \pm 0$ |

*Pairwise r.m.s. deviation was calculated among 10 refined structures

## Supporting References

[1]     C. Grönwall, A. Jonsson, S. Lindstrom, E. Gunneriusson, S. Stahl, N. Herne, *J. Biotechnol.* **2007**, *128*, 162-183.

[2]     W. Hoyer, D. Cherny, V. Subramaniam, T. M. Jovin, *Biochemistry* **2004**, *43*, 16233-16242.

[3]     B. Macao, W. Hoyer, A. Sandberg, A. C. Brorsson, C. M. Dobson, T. Härd, *BMC Biotechnol.* **2008**, *8*, 82. [4]
        F. Delaglio, S. Grzesiek, G. W. Vuister, G. Zhu, J. Pfeifer, A. Bax, *J. Biomol. NMR* **1995**, *6*, 277-293.

[5]     W. F. Vranken, W. Boucher, T. J. Stevens, R. H. Fogh, A. Pajon, M. Llinas, E. L. Ulrich, J. L. Markley, J. Ionides,
        E. D. Laue, *Proteins* **2005**, *59*, 687-696.

[6]     Z. Solyom, M. Schwarten, L. Geist, R. Konrat, D. Willbold, B. Brutscher, *J. Biomol. NMR* **2013**, *55*, 311-321.

[7]     J. G. Pelton, D. A. Torchia, N. D. Meadow, S. Roseman, *Protein Sci.* **1993**, *2*, 543-558.

[8]     Y. Shen, F. Delaglio, G. Cornilescu, A. Bax, *J. Biomol. NMR* **2009**, *44*, 213-223.

[9]     a) A. T. Brunger, *Nat. Protoc.* **2007**, *2*, 2728-2733; b) W. Rieping, M. Habeck, B. Bardiaux, A. Bernard, T.
        E. Malliavin, M. Nilges, *Bioinformatics* **2007**, *23*, 381-382.

[10]    V. B. Chen, W. B. Arendall, 3rd, J. J. Headd, D. A. Keedy, R. M. Immormino, G. J. Kapral, L. W. Murray, J.
        S. Richardson, D. C. Richardson, *Acta Crystallogr. Sect. D. Biol. Crystallogr.* **2010**, *66*, 12-21. [11]      The
        PyMOL Molecular Graphics System, 1.2; Schrödinger, LLC.

[12]    D. Eliezer, E. Kutluay, R. Bussell, Jr., G. Browne, *J. Mol. Biol.* **2001**, *307*, 1061-1073.

[13]    D. Ganguly, S. Otieno, B. Waddell, L. Iconaru, R. W. Kriwacki, J. Chen, *J. Mol. Biol.* **2012**, *422*, 674-684.

## Full Reference from Main Article

[1f]    B. Winner, R. Jappelli, S. K. Maji, P. A. Desplats, L. Boyer, S. Aigner, C. Hetzer, T. Loher, M. Vilar, S. Campioni,
        C. Tzitzilonis, A. Soragni, S. Jessberger, H. Mira, A. Consiglio, E. Pham, E. Masliah, F. H. Gage, R. Riek, *Proc.
        Natl. Acad. Sci. USA* **2011**, *108*, 4194-4199.

# Chapter 3

**A β-HAIRPIN-BINDING PROTEIN FOR THREE DIFFERENT DISEASE RELATED AMYLOIDOGENIC PROTEINS**

Hamed Shaykhalishahi, Ewa A. Mirecka, Aziz Gauhar, Clara S. R. Grüning, Dieter Willbold, Torleif Härd, Matthias Stoldt, and Wolfgang Hoyer

Proportion of contribution to this work: 20%

Design, cloning, expression, and purification of AS10-GS3, expression and purification of α-synuclein and human prion protein (huPrP-(23-144)), preparation of samples for NMR studies, determination of binding affinity, aggregation assays, cell toxicity assays

# A β-Hairpin-Binding Protein for Three Different Disease-Related Amyloidogenic Proteins

Hamed Shaykhalishahi,[a] Ewa A. Mirecka,[a] Aziz Gauhar,[a] Clara S. R. Grüning,[a] Dieter Willbold,[a, c] Torleif Härd,[b] Matthias Stoldt,[a, c] and Wolfgang Hoyer*[a, c]

Amyloidogenic proteins share a propensity to convert to the β-structure-rich amyloid state that is associated with the progression of several protein-misfolding disorders. Here we show that a single engineered β-hairpin-binding protein, the β-wrapin AS10, binds monomers of three different amyloidogenic proteins, that is, amyloid-β peptide, α-synuclein, and islet amyloid polypeptide, with sub-micromolar affinity. AS10 binding inhibits the aggregation and toxicity of all three proteins. The results demonstrate common conformational preferences and related binding sites in a subset of the amyloidogenic proteins. These commonalities enable the generation of multispecific monomer-binding agents.

The oligomerization and aggregation of proteins, ultimately resulting in fibrillar amyloid deposits, are pathological features of various diseases.[1] For example, senile plaques containing the amyloid-β peptide (Aβ), Lewy bodies consisting of α-synuclein (α-syn), and pancreatic islet amyloid composed of islet amyloid polypeptide (IAPP) are pathological features of Alzheimer's disease (AD), Parkinson's disease (PD), and type 2 diabetes, respectively.[2] The cross-β spine, built of stacked β-strands that are oriented perpendicular to the fibril axis, is the common core structure of the amyloid states of amyloidogenic proteins.[3] The individual polypeptide chains typically adopt β-strand–turn–β-strand motifs that align to form parallel, in-register β-sheets in β-sandwich, β-serpentine, or β-helical arrangements.[3] Structural similarities among different amyloidogenic proteins have also been recognized at the level of their oligomeric and protofibrillar states, evident for example, from the shared affinity for conformation-specific antibodies.[4]

In this work, we investigated whether the structural similarity of different amyloidogenic proteins extends to the coupled folding and binding reactions of the monomeric proteins.

[a] H. Shaykhalishahi, Dr. E. A. Mirecka, A. Gauhar, Dr. C. S. R. Grüning, Prof. Dr. D. Willbold, Dr. M. Stoldt, Dr. W. Hoyer
Institute of Physical Biology, Heinrich-Heine-Universität Düsseldorf
40204 Düsseldorf (Germany)
E-mail: wolfgang.hoyer@uni-duesseldorf.de

[b] Prof. Dr. T. Härd
Department of Chemistry and Biotechnology
Swedish University of Agricultural Sciences (SLU)
Box 7015, 750 07 Uppsala (Sweden)

[c] Prof. Dr. D. Willbold, Dr. M. Stoldt, Dr. W. Hoyer
Institute of Structural Biochemistry (ICS-6), Research Centre Jülich
52425 Jülich (Germany)

Supporting information for this article is available on the WWW under
http://dx.doi.org/10.1002/cbic.201402552.

Common molecular-recognition motifs might be involved in the dysfunction of amyloidogenic proteins. Furthermore, they would allow for the generation of multispecific binding agents that could serve in diagnostic and therapeutic applications.

β-Wrapins are engineered binding proteins obtained from phage-display libraries based on the Aβ-binding affibody protein ZAβ3. ZAβ3 is a homodimer with a disulfide bond between the Cys28 residues of the subunits (Figure 1A and C).[5] Monomeric Aβ adopts a β-hairpin conformation in complex with ZAβ3 (Figure 1A) that is reminiscent of the β-strand–turn–β-strand conformation found in Aβ amyloid fibrils.[6]

We have recently reported the selection of a binder to α-syn from a β-wrapin phage-display library obtained by random



**Figure 1.** Amino acid positions in β-wrapins critical for interaction with amyloidogenic targets. Topologies of the A) Aβ:ZAβ3 (PDB ID: 2OTK)[5b] and B) α-syn:AS69 (PDB ID: 4BXL)[7] complexes with homodimer subunits in light and dark gray. Residues 31 and 34, the two most frequently exchanged amino acids, are located at the interface between the homodimer subunits and the β-hairpins. C) Amino acid sequences of five representative β-wrapin variants selected against α-syn aligned to ZAβ3. Residues 31 and 34 are highlighted in green, Cys28 in yellow. The positions of helical and β-sheet secondary structure in Aβ-bound ZAβ3 are indicated by cylinders and arrow, respectively. D) Most frequent amino acid exchanges in ZAβ3 occurring in 90 clones selected to bind α-synuclein. Residues 31 and 34 are highlighted.

mutagenesis of ZAβ₃.[7] The phage-display library contained 7× $10^7$ transformants with an average of approximately two exchanges per ZAβ₃ subunit. To avoid selecting binders to the highly charged C-terminal domain, the C-terminally truncated construct α-syn(1–108) was used as a target.[7] After four selection rounds, the sequences of 90 individual β-wrapin clones were determined. We have previously studied the interaction of one of the clones, AS69, with α-syn.[7] Like ZAβ₃, AS69 stabilizes a β-hairpin conformer of its target and consequently inhibits its α-syn aggregation and toxicity.

Here we chose four additional clones from the selection against α-syn(1–108), that is, AS9, AS10, AS34, and AS60, which have between one and four of the most frequent amino acid exchanges (Figure 1C and D) for affinity determination towards α-syn and Aβ (Figure 2A and B, and Table 1). Isothermal titra-

**Table 1.** Affinities of β-wrapins and ZAβ₃ for α-synuclein and Aβ determined by ITC.

| β-Wrapin | Exchange in ZAβ₃ at position | | | | | $K_d$ [nM] | |
| | 7 | 13 | 17 | 31 | 34 | α-syn | Aβ |
|---|---|---|---|---|---|---|---|
| ZAβ₃[a] | – | – | – | – | – | n.d.[b] | 20 |
| AS9 | – | – | – | F | – | 2500 | 500 |
| AS10 | – | – | – | F | V | 380 | 150 |
| AS34 | – | – | – | F | I | 1200 | 190 |
| AS60 | T | D | F | F | I | 200 | n.d.[b] |
| AS69[a] | – | D | F | F | V | 240 | 5000 |

[a] Affinities for ZAβ₃ and AS69 reported in Mirecka et al.[7] [b] n.d. = not detected.

tion calorimetry (ITC) demonstrated that one of these β-wrapins, AS10, exhibited nanomolar affinity for both α-syn and Aβ (Aβ(1–40) with an N-terminal methionine[8] was used in this study). Size-exclusion chromatography confirmed that AS10 bound monomers of α-syn and Aβ (Figure S1). In order to test if AS10 also exhibits affinity for further amyloidogenic proteins, a potential interaction with IAPP was investigated. To avoid problems caused by precipitation of the highly aggregation-prone IAPP during the ITC experiment, the affinity was determined by surface plasmon resonance (SPR) in this case. Monomeric, N-terminally biotinylated IAPP was immobilized on a streptavidin SA chip. The association of AS10 was monitored for 90 s, followed by 600 s dissociation time (Figure 2C). The SPR data could be fit to a two-state conformational change model to yield a $K_d$ value of 910 nM.

We performed ¹H,¹⁵N HSQC NMR spectroscopy on ¹⁵N-labeled AS10 ([U-¹⁵N]-AS10) to investigate its binding to Aβ, α-syn, and IAPP. In the presence of the amyloidogenic target proteins, the resonance dispersion greatly increased as a consequence of coupled folding and binding, and four amide proton resonances appeared in the glycine region (stemming from Gly13 and Gly14 in the two AS10 subunits) as well as amide proton resonances in the downfield region of the spectrum with shift values typical for β-sheet conformation (Figures 2D and S2). This has been observed before for the interaction of ZAβ₃ with Aβ[5b] (Figure 2D) and for the interaction of
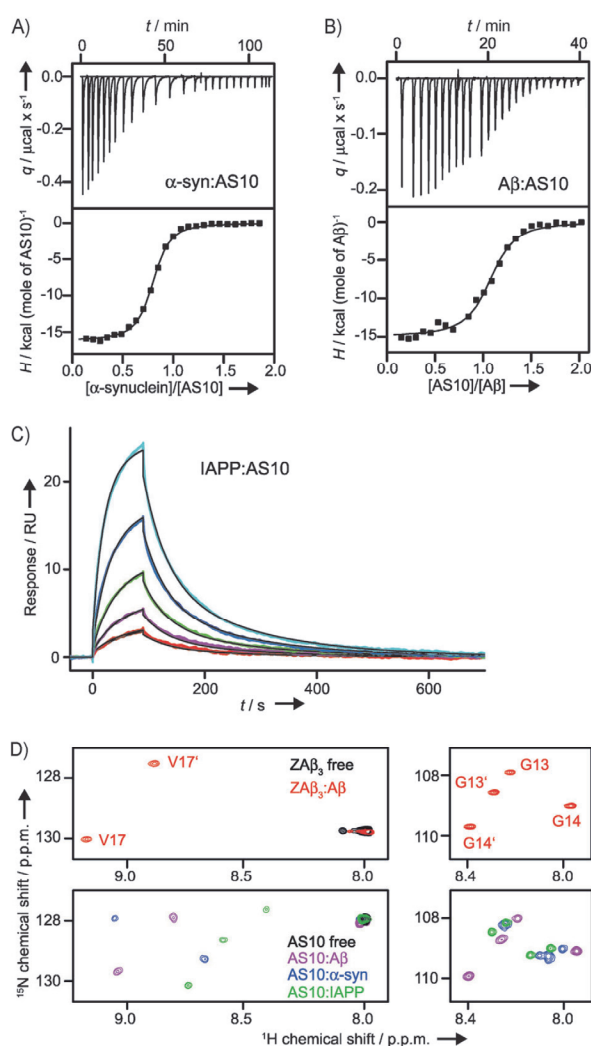


**Figure 2.** Sub-micromolar binding of AS10 to three different amyloidogenic targets. The $K_d$ values of AS10 for A) α-syn and B) Aβ were 380 and 150 nM, respectively, as determined by ITC. C) SPR analysis of binding of 2 μM (——), 1 μM (——), 500 nM (——), 250 nM (——), and 125 nM (——) AS10 to IAPP according to a two-state conformational change model gave a $K_d$ of 910 nM, with association and dissociation rate constants of $k_{a1} = 1.44 \times 10^4$ M⁻¹ s⁻¹, $k_{d1} = 1.94 \times 10^{-2}$ s⁻¹, $k_{a2} = 3.38 \times 10^{-3}$ s⁻¹, and $k_{d2} = 7.00 \times 10^{-3}$ s⁻¹. D) Downfield (left) and glycine (right) regions of the (¹H,¹⁵N) HSQC NMR spectra of [U-¹⁵N]-AS10 in the absence or presence of [NA]-Aβ, [NA]-α-syn, or [NA]-IAPP (bottom), compared to the corresponding spectra of [U-¹⁵N]-ZAβ₃ in the absence or presence of [NA]-Aβ[5b] (top). Assignment to the two ZAβ₃ subunits is indicated by presence or absence of prime symbols.

β-wrapin AS69 with α-syn.[7] These findings indicate that all three amyloidogenic targets adopt a β-hairpin conformation in complex with AS10, analogous to the interactions of Aβ and α-syn with ZAβ₃ and AS69, respectively.

AS10 has two amino acid substitutions compared to ZAβ₃, namely Ile31Phe and Leu34Val (Figure 1C). These were the two most frequent amino acid exchanges in the selected binders to α-syn, occurring in 100 or 30%, respectively, of the 90 sequenced clones (Figure 1D), thus indicating a critical role for these exchanges for the β-wrapin–α-syn interaction. According to high-resolution structures of ZAβ₃ bound to Aβ[5b] and of

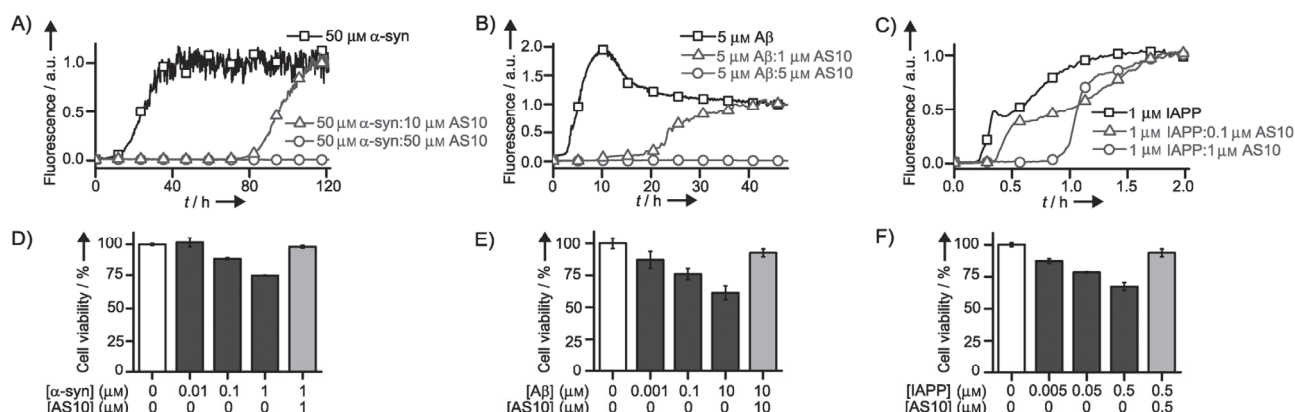↖↖ **These are not the final page numbers!**

**Figure 3.** AS10 inhibits amyloid formation and toxicity of α-syn (left), Aβ (center), and IAPP (right). Top: Amyloid formation was followed by thioflavin T fluorescence. Bottom: Toxicity to SH-SY5Y cells was assessed by an MTT assay, applying protein solutions aged in the absence (dark gray bars) and presence (light gray bars) of AS10; white bars: control.

AS69 bound to α-syn,[7] these residues are located at the interface between the homodimer subunits and the β-hairpins, which is evidently a critical region for the stability of the complexes (Figure 1 A and B).

The effect of AS10 on amyloid formation was studied by thioflavin T fluorescence (Figure 3 A–C). AS10 inhibited the aggregation of Aβ, α-syn, and IAPP. Substoichiometric concentrations of the β-wrapin were sufficient to achieve a significant delay in amyloid formation. The effect of AS10 on the toxicity of the three amyloidogenic proteins was investigated in SH-SY5Y neuroblastoma cells (Figure 3 D–F). Fibrillar samples of aged Aβ, α-syn, or IAPP caused concentration-dependent decreases in cell viability. Addition of AS10 at the beginning of the ageing reactions rescued the cell viability.

We tested for potential interactions of AS10 with further amyloidogenic proteins by $^1$H,$^{15}$N HSQC NMR spectroscopy, employing the four-repeat-domain tau protein construct K18K280/AA[9] and the Y145Stop variant of human prion protein (huPrP(23–144)).[10] Addition of AS10 to K18K280/AA or to huPrP(23-144) did not affect the NMR spectra, thus demonstrating the absence of binding (Figure S3).

This study establishes that the monomers of a subset of the disease-related amyloidogenic proteins can be bound with sub-micromolar affinity by a single engineered binding protein. Upon binding, the amyloidogenic proteins form β-hairpin motifs. In the case of Aβ and α-syn, the β-hairpins were shown to contain sequence regions that are critical for amyloid formation, namely Aβ(17–36)[5b] and α-syn(37–54).[7] These regions are enriched in hydrophobic amino acids with β-sheet propensity and, furthermore, they contain aromatic amino acids, these are features that might prime them for β-hairpin formation and for interaction with the β-wrapin scaffold. Several computer simulations revealed a propensity of amyloidogenic proteins to transiently populate β-hairpin conformations and implicated the β-hairpins in the formation of intermolecular contacts.[11] The data presented here provide experimental evidence for the preference for formation of β-hairpin motifs within at least a subset of amyloidogenic proteins.

Our results emphasize the adaptability of small, engineered binding proteins to intrinsically disordered, amyloidogenic target proteins. Binding is coupled to local folding of the targets. Coupled folding and binding is associated with an entropic cost for the disorder-to-order transition that frequently results in complexes of high specificity and relatively low affinity.[12] It is thus interesting to note that the β-wrapin AS10 binds three different amyloidogenic proteins with sub-micromolar affinity. This indicates that Aβ, α-syn, and IAPP share important properties that are not only reflected in the shared ability to form amyloid fibrils, but also in the common adoption of a β-hairpin conformation in complex with β-wrapins. This supports the view that by exploiting such commonalities general anti-amyloid therapeutic approaches could be contrived.

## Experimental Section

Experimental details are given in the Supporting Information.

## *Acknowledgements*

[1] T. P. Knowles, M. Vendruscolo, C. M. Dobson, *Nat. Rev. Mol. Cell Biol.* **2014**, *15*, 384–396.

[2] a) Y. Huang, L. Mucke, *Cell* **2012**, *148*, 1204–1222; b) H. A. Lashuel, C. R. Overk, A. Oueslati, E. Masliah, *Nat. Rev. Neurosci.* **2013**, *14*, 38–48; c) P. Westermark, A. Andersson, G. T. Westermark, *Physiol. Rev.* **2011**, *91*, 795–826.

[3] D. Eisenberg, M. Jucker, *Cell* **2012**, *148*, 1188–1203.

[4] R. Kayed, E. Head, J. L. Thompson, T. M. McIntire, S. C. Milton, C. W. Cotman, C. G. Glabe, *Science* **2003**, *300*, 486–489.

[5] a) C. Grönwall, A. Jonsson, S. Lindström, E. Gunneriusson, S. Ståhl, N. Herne, *J. Biotechnol.* **2007**, *128*, 162–183; b) W. Hoyer, C. Grönwall, A.

**These are not the final page numbers!** ↗↗

Jonsson, S. Ståhl, T. Härd, *Proc. Natl. Acad. Sci. USA* **2008**, *105*, 5099–5104.

[6] a) T. Lührs, C. Ritter, M. Adrian, D. Riek-Loher, B. Bohrmann, H. Dobeli, D. Schubert, R. Riek, *Proc. Natl. Acad. Sci. USA* **2005**, *102*, 17342–17347; b) A. T. Petkova, W. M. Yau, R. Tycko, *Biochemistry* **2006**, *45*, 498–512.

[7] E. A. Mirecka, H. Shaykhalishahi, A. Gauhar, S. Akgül, J. Lecher, D. Willbold, M. Stoldt, W. Hoyer, *Angew. Chem. Int. Ed.* **2014**, *53*, 4227–4230; *Angew. Chem.* **2014**, *126*, 4311–4314.

[8] B. Macao, W. Hoyer, A. Sandberg, A. C. Brorsson, C. M. Dobson, T. Härd, *BMC Biotechnol.* **2008**, *8*, 82.

[9] C. S. Grüning, E. A. Mirecka, A. N. Klein, E. Mandelkow, D. Willbold, S. F. Marino, M. Stoldt, W. Hoyer, *J. Biol. Chem.* **2014**, *289*, 23209–23218.

[10] T. Kitamoto, R. Iizuka, J. Tateishi, *Biochem. Biophys. Res. Commun.* **1993**, *192*, 525–531.

[11] a) I. Daidone, F. Simona, D. Roccatano, R. A. Broglia, G. Tiana, G. Colombo, A. Di Nola, *Proteins Struct. Funct. Bioinf.* **2004**, *57*, 198–204; b) N. F. Dupuis, C. Wu, J. E. Shea, M. T. Bowers, *J. Am. Chem. Soc.* **2009**, *131*, 18283–18292; c) A. C. Gill, *PLoS One* **2014**, *9*, e87354; d) M. Grabenauer, C. Wu, P. Soto, J. E. Shea, M. T. Bowers, *J. Am. Chem. Soc.* **2010**, *132*, 532–539; e) S. Mitternacht, I. Staneva, T. Härd, A. Irbäck, *J. Mol. Biol.* **2011**, *410*, 357–367; f) A. S. Reddy, L. Wang, S. Singh, Y. L. Ling, L. Buchanan, M. T. Zanni, J. L. Skinner, J. J. de Pablo, *Biophys. J.* **2010**, *99*, 2208–2216; g) D. J. Rosenman, C. R. Connors, W. Chen, C. Wang, A. E. Garcia, *J. Mol. Biol.* **2013**, *425*, 3338–3359.

[12] H. J. Dyson, P. E. Wright, *Nat. Rev. Mol. Cell Biol.* **2005**, *6*, 197–208.

**↖↖ These are not the final page numbers!**

# COMMUNICATIONS
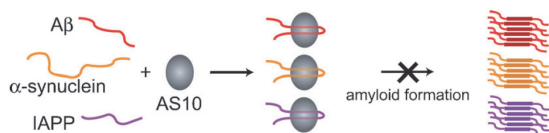


**One to three:** The binding protein β-wrapin AS10, obtained by protein engineering, sequesters monomers of the aggregation-prone proteins involved in Alzheimer's disease, Parkinson's disease, and type 2 diabetes. The common molecular-recognition motifs of amyloid-forming proteins can be exploited to develop aggregation- and toxicity-inhibiting compounds that target the monomeric state.

*H. Shaykhalishahi, E. A. Mirecka,
A. Gauhar, C. S. R. Grüning, D. Willbold,
T. Härd, M. Stoldt, W. Hoyer*

■■ – ■■

**A β-Hairpin-Binding Protein for Three Different Disease-Related Amyloidogenic Proteins**

# CHEMBIOCHEM

## Supporting Information

# A β-Hairpin-Binding Protein for Three Different Disease-Related Amyloidogenic Proteins

Hamed Shaykhalishahi,[a] Ewa A. Mirecka,[a] Aziz Gauhar,[a] Clara S. R. Grüning,[a] Dieter Willbold,[a, c] Torleif Härd,[b] Matthias Stoldt,[a, c] and Wolfgang Hoyer*[a, c]

cbic_201402552_sm_miscellaneous_information.pdf

# Supporting Information

**Table of contents**

**Supporting Experimental Section**

**Phage Display.** Library generation and selections were performed as described.[1] Briefly, a β-wrapin library based on a pComb3HSS vector backbone (provided by C. F. Barbas, The Scripps Research Institute, La Jolla, USA) containing the ZAβ$_3$ gene was generated by error-prone PCR. The library consisted of 7 x 10$^7$ transformants. After four selection rounds against biotinylated α-syn(1-108), DNA from 90 single colonies was sequenced.

**Protein Preparation.** β-Wrapins,[1] ZAβ$_3$,[1] α-syn,[1] Aβ(1-40) with an N-terminal methionine,[2] and tau K18ΔK280/AA[3] were prepared as previously described. Synthetic IAPP amidated at the C-terminus (Merck Millipore) was dissolved in 6 M guanidine hydrochloride (GdnHCl), 50 mM NaCl, 20 mM sodium phosphate, pH 6.0, and eluted at a flow rate of 0.5 ml/min from a Superdex 75 10/300 GL column (GE Healthcare) equilibrated in 20 mM sodium phosphate, pH 6.0.

huPrP(23-144) with an N-terminal 6xHis tag and a TEV-protease recognition site (ENLYFQG) was expressed from a pET-302 vector in *E. coli* BL21 DE3 and purified adopting previously published methods.[4] Briefly, following cell lysis, the pellet containing inclusion bodies was resuspended in 6 M guanidine hydrochloride, 100 mM sodium phosphate, 10 mM Tris-HCl, pH 8.0. After centrifugation, the protein was refolded in 100 mM sodium phosphate, 10 mM Tris-HCl, pH 8.0, and purified by elution from a Ni-NTA (His-Select, Sigma) gravity-flow chromatography column with 300 mM imidazole in the same buffer. The protein was digested with TEV-protease (20 μg per mg of protein) over night and purified using reverse phase high-pressure liquid chromatography (RP-HPLC) on a Zorbax 300SB-C3 column employing a gradient of 10-80 % (vol/vol) acetonitrile in water containing 0.1% (vol/vol) TFA for 15 min at a flow rate of 4 ml/min and at 80 °C, followed by lyophilization.

**ITC.** ITC was performed in 20 mM sodium phosphate, 50 mM NaCl, pH 7.4, at 30 °C on a Microcal iTC200 calorimeter (GE Healthcare). Affinities to $\alpha$-syn were determined with $\beta$-wrapins/ZA$\beta_3$ as titrant in the cell at a concentration of ~60 µM, and $\alpha$-syn at approximately 10-fold higher concentration as titrant in the syringe. Affinities to A$\beta$ were obtained with A$\beta$ as titrant in the cell at a concentration of ~10 µM, and $\beta$-wrapins/ZA$\beta_3$ at approximately 10-fold higher concentration as titrant in the syringe. Heats of post-saturation injections were averaged and subtracted from each injection to correct for heats of dilution and mixing. Dissociation constants were obtained from a nonlinear least-squares fit to a 1:1 binding model using MicroCal Origin.

**SPR.** Synthetic IAPP, N-terminally modified with biotin and an aminohexanoyl spacer and amidated at the C-terminus (Bachem), was dissolved in 20 mM sodium acetate, 50 mM NaCl, pH 4.0, and immobilized on a series S sensor chip SA (GE Healthcare) to ~1300 response units (RU) on a BIAcore T200 (GE Healthcare). The running buffer was 10 mM HEPES, pH 7.4, 150 mM NaCl, 3 mM EDTA, and 0.005% (v/v) Tween 20 surfactant. Measurements were performed at a flow rate of 30 µl/min and 25 °C. The data were fitted using a two-state 1:1 binding reaction model, consisting of an initial complex formation step with association rate constant $k_{a1}$ and dissociation rate constant $k_{d1}$ and a subsequent conformational change in the complex with forward and reverse rate constants $k_{a2}$ and $k_{d2}$. The overall equilibrium dissociation constant $K_d$ was calculated using the equation: $K_d=k_{d1}*k_{d2}/(k_{a1}(k_{d2}+k_{a2}))$. The signals of an uncoated reference cell and the signals generated by injection of running buffer were subtracted from the sensorgrams.

**NMR Spectroscopy.** NMR spectra were acquired on a 900 MHz VNMRS spectrometer (Varian) equipped with a cryogenically cooled Z-axis pulse-field-gradient triple resonance probe. The temperature was 25 °C except for the tau K18$\Delta$K280/AA samples which were analyzed at 5 °C. The [*NA*]-component was added in slight excess relative to the [*U*-15N]-component. The buffers were: 20 mM sodium phosphate, 50 mM NaCl, pH 7.4 (A$\beta$, $\alpha$-syn, and IAPP samples); 20 mM sodium phosphate, 50 mM NaCl, pH 7.0 (tau K18$\Delta$K280/AA samples); 15 mM sodium phosphate, 50 mM NaCl, pH 5.8 (huPrP(23-144) samples). NMR data were processed using NMRPipe[5] and analyzed with CcpNmr.[6]

**Amyloid Formation.** Fibrillation was performed in round-bottom 96-well black plate (Nunc) in an Infinite M1000 plate reader (Tecan). $\alpha$-Syn fibrillation was done at 37 °C in 20 mM NaPi buffer, 50 mM NaCl, pH 6.0, under orbital shaking with 1 glass bead per microplate well. A$\beta$ fibrillation was done at 37 °C in 20 mM NaPi buffer, 50 mM NaCl, pH 7.4, under orbital shaking with 1 glass bead per microplate well. IAPP fibrillation was done at 30 °C in 20 mM NaPi buffer, 50 mM NaCl, pH 6.0, under quiescent conditions. Amyloid formation was followed by Thioflavin T fluorescence at 480 nm (excitation 440 nm).

**Toxicity Assay.** The viability of SH-SY5Y neuroblastoma cells was assessed with an MTT assay (Cell Proliferation Kit I, Roche Diagnostics) as described before.[1] Protein samples were aged under amyloid formation conditions as described in the section above for 44 h (Aβ), 24 h (α-syn), or 30 min (IAPP) at a protein concentration of 50 μM (Aβ), 100 μM (α-syn), or 50 μM (IAPP), respectively, and diluted into the cell culture medium to the final concentrations given in Figure 3 D-F.

**Size Exclusion Chromatography.** Size exclusion chromatography was performed at 25°C by injecting 200 μl of 60 μM protein solutions in 20 mM NaPi, 50 mM NaCl, pH 7.4, onto a Superdex 10/300 column connected to an Äkta Purifier System (GE Healthcare).
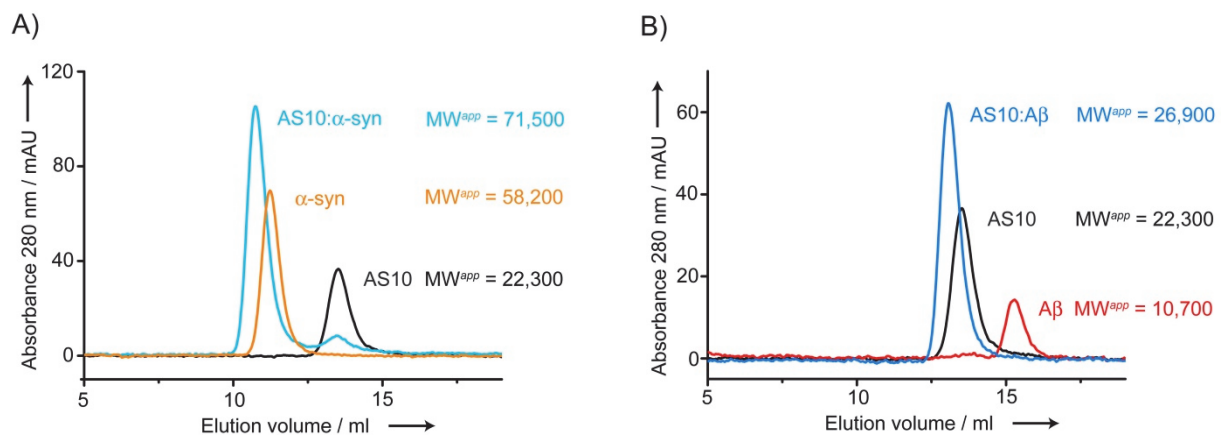
**Supporting Figures**



**Figure S1.** AS10 binds monomers of α-syn and Aβ. Size exclusion chromatography of the AS10:α-syn (A) and AS10:Aβ (B) complexes and their free components on a Superdex 75 10/300 column at a protein concentration of 60 μM. The apparent molecular weight (MW) of all three proteins in their free states is higher than their actual MW (MW(AS10) = 15,100; MW (α-syn) = 14,500; MW (Met-Aβ$_{1-40}$) = 4,500) as a consequence of their (partially) disordered character.[7] The apparent MW of the complexes is lower than the sum of the apparent MWs of the components, demonstrating that (i) AS10 binds monomers of the amyloidogenic proteins and (ii) compaction occurs upon complex formation due to folding coupled to binding. Monomer binding is in agreement with the 1:1 stoichiometry observed by ITC (Figure 2 A and B) and with the similarity of the NMR spectra of bound AS10 to those of ZAβ$_3$ (Figure 2 D and Figure S2) and AS69[1] in their complexes with monomeric Aβ or α-syn, respectively.

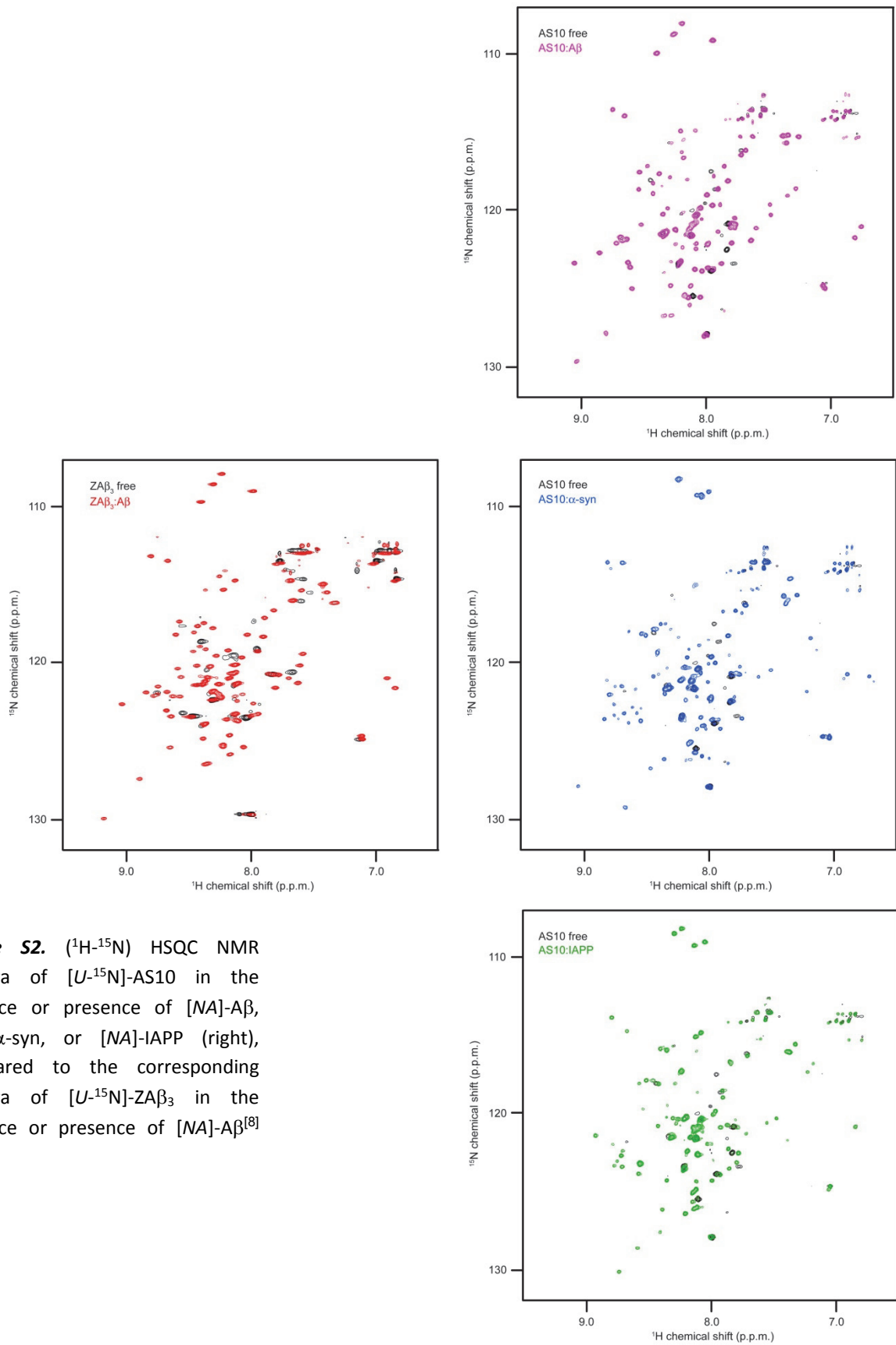***Figure S2.*** ($^1$H-$^{15}$N) HSQC NMR spectra of [$U$-$^{15}$N]-AS10 in the absence or presence of [*NA*]-Aβ, [*NA*]-α-syn, or [*NA*]-IAPP (right), compared to the corresponding spectra of [$U$-$^{15}$N]-ZAβ$_3$ in the absence or presence of [*NA*]-Aβ[8] (left).
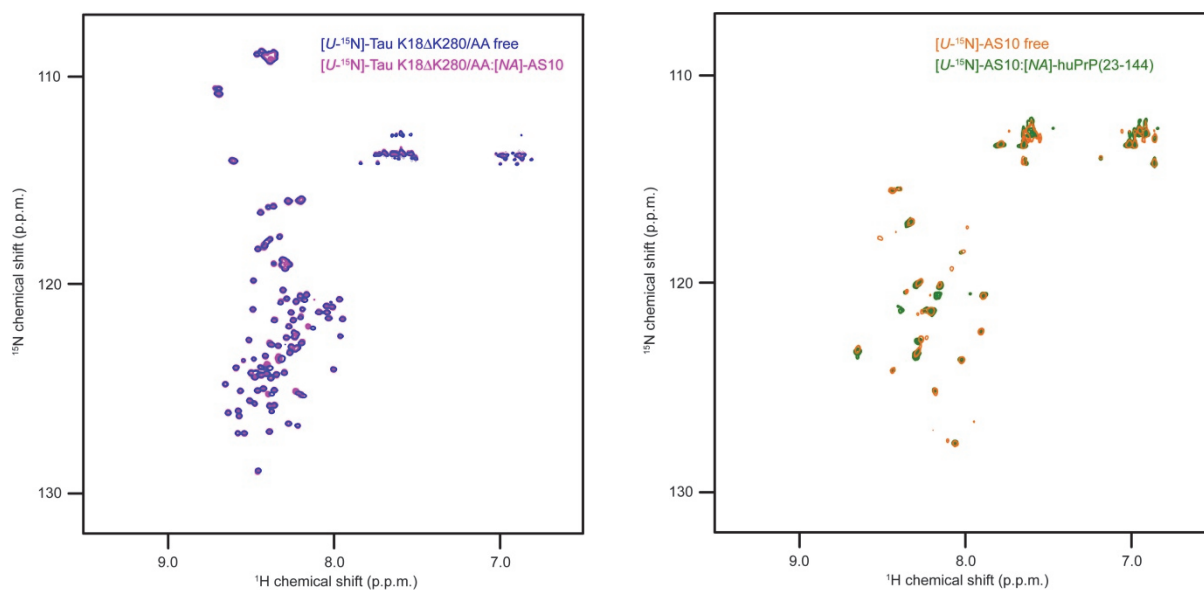
**Figure S3.** Left, ($^1$H-$^{15}$N) HSQC NMR spectra of [$U$-$^{15}$N]-Tau K18ΔK280/AA in the absence or presence of [$NA$]-AS10. Buffer, 20 mM sodium phosphate, 50 mM NaCl, pH 7.0. Right, ($^1$H-$^{15}$N) HSQC NMR spectra of [$U$-$^{15}$N]-AS10 in the absence or presence of [$NA$]-huPrP(23-144). Buffer, 15 mM sodium phosphate, 50 mM NaCl, pH 5.8.

## References

[1]     E. A. Mirecka, H. Shaykhalishahi, A. Gauhar, S. Akgül, J. Lecher, D. Willbold, M. Stoldt, W. Hoyer, *Angew. Chem. Int. Ed. Engl.* **2014**, *53*, 4227-4230.

[2]     B. Macao, W. Hoyer, A. Sandberg, A. C. Brorsson, C. M. Dobson, T. Härd, *BMC Biotechnol.* **2008**, *8*, 82.

[3]     C. S. Grüning, E. A. Mirecka, A. N. Klein, E. Mandelkow, D. Willbold, S. F. Marino, M. Stoldt, W. Hoyer, *J. Biol. Chem.* **2014**, *289*, 23209-23218.

[4]     a) R. A. Moore, C. Herzog, J. Errett, D. A. Kocisko, K. M. Arnold, S. F. Hayes, S. A. Priola, *Protein Sci.* **2006**, *15*, 609-619; b) R. Zahn, C. von Schroetter, K. Wüthrich, *FEBS Lett.* **1997**, *417*, 400-404.

[5]     F. Delaglio, S. Grzesiek, G. W. Vuister, G. Zhu, J. Pfeifer, A. Bax, *J. Biomol. NMR* **1995**, *6*, 277-293.

[6]     W. F. Vranken, W. Boucher, T. J. Stevens, R. H. Fogh, A. Pajon, M. Llinas, E. L. Ulrich, J. L. Markley, J. Ionides, E. D. Laue, *Proteins* **2005**, *59*, 687-696.

[7]     a) B. Fauvet, M. K. Mbefo, M. B. Fares, C. Desobry, S. Michael, M. T. Ardah, E. Tsika, P. Coune, M. Prudent, N. Lion, D. Eliezer, D. J. Moore, B. Schneider, P. Aebischer, O. M. El-Agnaf, E. Masliah, H. A. Lashuel, *J. Biol. Chem.* **2012**, *287*, 15345-15364; b) W. Hoyer, T. Härd, *J. Mol. Biol.* **2008**, *378*, 398-411.

[8]     W. Hoyer, C. Grönwall, A. Jonsson, S. Ståhl, T. Härd, *Proc. Natl Acad. Sci. USA* **2008**, *105*, 5099-5104.

# Discussion

Misfolding of α-synuclein that leads to the generation of self-assembling conformers, forming toxic oligomers and fibril deposits, constitutes a defining step at the outset of familial and idiopathic forms of PD and other LB disorders, collectively known as synucleinopathies. It is to note that synucleinopathies primarily give rise to intracellular aggregates, though recently it has been demonstrated that aggregates also occur outside the cells following their secretion [461, 462]. These in turn might act as seeds and further contribute to the aggravation of the disease progress. However, it also presents the opportunity to target these extracellular aggregates, for instance as evidenced by a recent study employing an α-synuclein mAb (Syn303) directed against exogenously generated preformed fibrils. Results revealed that blocking the uptake of these fibrils limited the amount of seeds and prevented their further cell-to-cell propagation, both contributing to arresting the progression of pathology [463].

As previously indicated an appealing therapeutic strategy to tackle synucleinopathies might involve interfering with the aggregation process by stabilizing the native form of α-synuclein and thus preventing its misfolding and subsequent aggregation. This, however, would require the intracellular expression of drug ligands. Moreover, the prevailing conditions in the cell milieu are not to be overlooked, since these might impose certain limitations and as a result undermine the stability and functioning of liable ligands. For instance, intrabodies were shown to be effective inhibitors of α-synuclein aggregation *in vitro*; however, due to the critical role of the disulfide bond in maintaining their conformation and structural stability they are rendered susceptible to the prevailing conditions within the cells [350].

The β-wrapin AS69 is an engineered binding protein selected against α-synuclein from a combinatorial library based on the $Z_{Aβ3}$ scaffold and occurs as a dimer with two identical subunits. Subunits linkage is achieved through the disulfide bond formed between Cys-28 residues on each subunit. AS69 specifically binds to α-synuclein monomers and can effectively counteract its aggregation *in vitro* at sub-stoichiometric concentrations. However, *in vivo* application of the ligand might be hindered by the reducing conditions in the cytoplasm, since formation of the homodimer is essential for high affinity binding to occur, as shown by structural studies and reinforced with evidence gleaned from experiments performed under reducing conditions. In order to

remediate this obstacle, it was devised to fuse two individual AS69 monomers and create a head-to-tail homodimer for *in vivo* application.

# 1 Role of the disulfide bond in AS69

Disulfide bonds are an inherent component of numerous proteins, especially membrane and secreted proteins, and therefore their efficient formation is deemed to be essential for maintaining the structural integrity and proper functioning of proteins. Disulfide bonds are associated with conformational stability, which connotes that proper folding of proteins is strictly tied to the correct formation of their respective inbuilt disulfide bonds [417, 418]. For instance, the presence of intradomain disulfide bond in antibodies significantly contributes to their stability [356]. Besides, it can confer certain functional capabilities to proteins, such as enzymes that can shuffle between an activated and deactivated state by simply breaking-and-reforming their disulfide bonds. Formation and rearrangement of the disulfide bonds is in principle a thiol-disulfide (SH↔SS) exchange reaction that is kinetically and thermodynamically influenced by the environment [419]. The ratio of SH:SS affects the folding kinetics and stability of proteins. Formation of the disulfide bonds is influenced by various factors including the concentration of thiolate anions, the accessibility, reactivity, and proximity of the SH and SS groups [420]. In the eukaryotic cells the reducing environment of the cytosol hinders the generation of disulfide bonds; on the contrary, the ER lumen has a more favorable redox state that is contributed by the abundant presence of glutathione and various other mechanisms [420]. However, the oxidizing capacity of the ER is likely to be compromised in pathological conditions due to disruption of the cellular respiratory chain leading to drastic increases in the level of ROS. This in turn can have catastrophic implications for various cellular processes, including for the function of numerous proteins that rely on the redox state of the disulfide bond in their structure.

Cys-28 residues are conserved throughout the β-wrapin variants, consistent with the premise that disulfide bonds are generally conserved among related proteins [421]. Likewise, formation of the inter-subunit disulfide bond is essential for AS69 to avidly bind to α-synuclein. This is largely due to the key role of the disulfide bond in bringing the α-1 helices of the binder into contact with each other, thereby facilitating the formation of the hydrophobic tunnel-like cavity that serves as an interaction interface where strong hydrogen bonds are formed with the target. In the absence of the disulfide bond this optimal interface for interaction is no longer maintained and might collapse. Results of this work provide evidence elucidating and confirming the role of the

disulfide bond. Binding thermodynamics measured by ITC before and after the reduction of the disulfide bond showed a 1000-fold difference in the binding affinity of AS69. This observation is in line with the diminished affinity of a mutated $Z_{A\beta3}$ following substitution of Cys-28 with Ser-28, where the decreased affinity observed was associated with the requirement for cooperative association of two $Z_{A\beta3}$C28S molecules with Aβ monomer [399]. Increased affinity following engineering of disulfide bonds, i.e. cysteine residues, into an Affibody affinity ligand (ZSPA-1) was also observed, where the disulfide bridge was indicated to stabilize the binding surface of the ligand [423].

SEC elution profile and thermal melting experiments performed under oxidizing and reducing conditions show that the disulfide bond confers conformational compactness and thereby contribute to increased structural stability of AS69. Increased thermal and chemical stability afforded by the formation of disulfide bonds has been demonstrated previously as well [422-429] and is suggested to be due to the reduced conformational entropy of the unfolded state [430].

As indicated above, the rate of disulfide bond formation is influenced by the proximity of the reactive thiol groups, therefore tethering individual molecules through a linker would entail shrinking the spatial gap and thus contribute to the accelerated formation of disulfide bond.

## 2 Selection of an optimal linker for single chain AS69

An important consideration in construction of fusion proteins is the selection of a suitable linker. The nature and length of the linker are both critical to protein architecture, i.e. conformational dynamics, and function, and therefore to achieving the desired characteristics. Two factors are suggested to be important in preventing disturbance of the interconnected domain functions, linker flexibility and hydrophilicity [431]. An optimal linker, for instance, should confer the appropriate level of flexibility and separation to avoid structural perturbations that could arise due to aberrant interactions between the linked moieties and hamper the stability and activity of the fusion protein [410].

Flexible linkers are generally introduced into fusion proteins to remove steric constraints and allow the attached domains to pivot or move freely [405]. The most widely used flexible linker between domains of fusion proteins is (GGGGS)$_n$. This linker is especially suitable when certain movements or interactions are required. An important application of this linker is in tethering the immunoglobulin domains in the

scFv format where the flexibility of the linker permits the correct orientation of the $V_H$ and $V_L$ domains [432-434]. The glycine-serine linker is also shown to help increase biological activity of the fusion protein [358, 435, 436].

For generation of single chain head-to-tail fusion of AS69 four constructs were created and studied for comparison. (1) Direct fusion of the two subunits without an additional linker sequence. (2) Insertion of a 15 amino acid version of the disordered, flexible linker of the Oct-1 POU domain with an additional TEV protease cleavage site, yielding the AS69-Oct1-TEV construct. (3) Introduction of two repeats of the glycine-serine flexible linker with each repeat flanking the intervening TEV protease cleavage site, which resulted in the construct AS69-GS2-TEV. (4) The AS69-GS3 construct where the two AS69 subunits are spaced by three repeats of the glycine-serine linker.

Direct subunit fusion has been previously reported for $Z_{A\beta3}$ where the head-to-tail dimeric ligand retained its target-binding functionality [398, 400, 422]. However, this observation did not uphold in case of AS69 and led to the complete loss of functional binding as revealed by ITC measurements. It should be noted that the first 13 residues at the N-terminus of $Z_{A\beta3}$ remain disordered when bound to Aβ and are not involved in interaction with the β-hairpin portion of Aβ, hence it could serve as a linker [398]. Similarly the N-terminal part in AS69 is disordered in complex with α-synuclein. Although AS69 and ZAβ3 bear significant sequence resemblance, their respective targets i.e. α-synuclein and Aβ have a vastly diverse sequence composition, in particular with respect to the residues surrounding the respective β-hairpin in each complex. It might be speculated that the loss of α-synuclein binding potential in directly linked AS69 might be due to structural perturbations caused by unusual interactions leading to binding-incompetent conformations. Direct fusion of moieties has been previously evidenced to result in undesirable outcomes including loss of function or impaired activity of the fusion protein [435, 436]. Likewise, the AS69-Oct1-TEV flexible linker appeared to interfere with binding, as shown by ITC measurement where titration with α-synuclein only produced very slow association. Conversely, the glycine-serine rich linkers, i.e. GS2-TEV and GS3, were both able to restore AS69 binding to the disulfide-linked AS69 level. Hence, the AS69-GS3 construct was considered for further analysis.

Results showed that the linker did not cause any interference with the thermodynamic binding of the single chain AS69 to α-synuclein; to the contrary, binding to α-synuclein was promoted due to the accelerated formation of the disulfide bond. Moreover, the

aggregation inhibitory effects of the single chain ligand showed consistency with those of AS69, exhibiting complete inhibition of aggregation at stoichiometric concentrations while delaying the lag-phase of aggregation at sub-stoichiometric concentrations. Furthermore, thermal melting profile showed that the linker promotes stability of the single chain AS69.

Numerous factors are associated with enhanced protein stability, such as reduction of the conformational entropy in the unfolded state, formation of salt bridges i.e. hydrogen bonding and electrostatic interactions, among others [437, 438].

Linker length and composition are suggested to affect folding and refolding rates and consequently the stability of fusion protein [439]. A suitable linker should have a length and residue make up that provide optimum stability equilibrium by maintaining a balance between fast refolding and slow unfolding. Work by Robinson and Sauer under denaturing conditions demonstrated that linkage of fusion proteins involving too long linkers entail slow refolding of the protein due to the larger conformational space available for the connected domains to sample from before folding takes place. Moreover, too short linker sequences were shown to decrease the folding rate, since in such a scenario maintaining the linkage of the subunits in their native conformation would concur with excessive strain introduced into the native structure [439].

With regard to the linker composition, the presence of glycine residues in the linker sequence confers high flexibility. This is due to the absence of a side chain (β-carbon) that allows the backbone chain to access the torsion angles and acquire a specific fold [440]. However, too high a number of glycine residues in the linker is also not favorable, as it is suggested to ensue decreased stability [439]. Small residues such as glycine and serine contribute to the linker stability by forming hydrogen bonds with water [405]. Furthermore, formation of stabilizing interaction through hydrogen bonds is suggested for serine, though it is not clear whether such interactions occur within the linker or with the fused moieties [439].

Overall, flexibility is afforded to the linker sequence by amino acid residues such as threonine, serine, and glycine due to their small size and polar nature [408, 409]. Conversely, proline residues are associated with increased stiffness of the sequence caused by the lack of amide hydrogen, which prevents formation of hydrogen bonds with other amino acids [441]. Though, with respect to Oct-1 POU linker, it is unlikely that the presence of a single proline residue in its sequence would have a significant effect on its flexibility.

Taken together, comparing the results of the stated constructs it could be deduced that binding affinity of AS69 to α-synuclein is highly sensitive not only to the length but also to the composition of the linker sequence.

# 3 *In vivo* application of β-wrapins

Expression of mutant forms of α-synuclein (A53T or A30P) and overexpression of the wild-type protein are associated with formation of aggregates [248, 442, 443]. Moreover, some forms of soluble oligomers are implicated as the primary toxic species contributing to α-synuclein pathogenesis [137, 143, 240, 293-295, 298]. The proposed mechanisms of α-synuclein induced toxicity has been pointed out earlier in this work (*see section 2.5*).

Findings of this work are in agreement with other studies that observed toxicity in the cultured cells following addition of *in vitro* generated α-synuclein aggregates [444]. Addition of exogenous aggregates led to a drastic reduction in the viability of human neuroblastoma SH-SY5Y cells as assessed with MTT assay; whereas equivalent concentrations of the recombinant monomeric α-synuclein did not alter cell viability. Furthermore, this work revealed that the single-chain engineered β-wrapin AS69-GS3 efficiently inhibited formation of α-synuclein aggregates, as determined by Thioflavin T fluorescence, and rescued viability of SH-SY5Y cells. Likewise, the second β-wrapin molecule AS10 displayed equivalent inhibitory activity in blocking aggregation and toxicity of not only α-synuclein but also of Aβ and IAPP.

Although the experimental setup, i.e. addition of exogenously generated α-synuclein to cultured cells, would appear artificial; it does present a model imitating toxicity induced by extracellular species of α-synuclein to adjacent cells, in line with a recent hypothesis suggesting that in the diseased state α-synuclein might be secreted by amyloid afflicted cells or released following cell rupture and thus give rise to extracellular α-synuclein that can directly or indirectly cause damage to neighboring cells [315-317, 463] (*see section 2.6*).

The degree of the β-wrapins mediated rescue of SH-SY5Y cells was primarily dependent on the concentration of the ligand in relation to that of the target. Thermodynamics of β-wrapins binding reveals binding to occur at an equimolar ratio with the target(s), i.e. dimeric β-wrapin binds monomeric target in a 1:1 stoichiometry as previously observed for $Z_{Aβ3}$ and Aβ [398, 400], thus explaining stoichiometric inhibition of aggregation and the resulting cell rescue through monomer sequestration. What underlie the effects of β-wrapins at substoichiometric concentrations, is not

straightforward. At these concentrations the observed lag time of the target protein(s) aggregation is prolonged and cell survival is measurably enhanced.

*In vitro* studies show that fibril growth and disassembly involve accretion and dissociation of monomers, respectively; where fibril growth is posited to be a highly cooperative process extending the fibril ends at a constant rate [445]. This illustrates the importance of the monomeric form of α-synuclein to the disease progress. Furthermore, a recent study documented a conformational change in the initially formed oligomers of α-synuclein that subsequently gave rise to the cell damaging, more stable and compact oligomers and finally to mature fibril [457]. However, it was observed that the structural conversion was remarkably slow, pointing to the presence of a large kinetic barrier.

It might be plausible to conjecture that β-wrapins interfere with the fibril growth process not only by impeding the recruitment of monomeric α-synuclein, but also by binding to the initially formed oligomers which might lead to increasing the kinetic barrier and thus precluding the conformational change. Moreover, dissociation of the preformed oligomers and to a lesser extent fibrils is not to rule out, as evidenced for $Z_{Aβ3}$ [400]. These proposed mechanisms are not necessarily mutually exclusive and might operate concurrently.

β-wrapins exert their effects by entrapping a highly hydrophobic region in the sequence of α-synuclein that undergoes structural change forming a β-hairpin upon binding with the β-wrapin(s). This region corresponds to residues 35-56 and harbors the majority of the reported mutations in α-synuclein sequence, thus underscoring its importance and relevance to aggregation (*see section 2.4.1.2*). The β-hairpin conformation has been proposed to be a component of Aβ intermediate oligomers [399] and globulomer oligomers [460]. This is likely to be the case in oligomeric species of α-synuclein as well. Therefore, sequestration of this region is likely to block not only clustering of the hydrophobic residues and the resulting tendency to self-assemble, but also aberrant interaction between α-synuclein and key mediators of α-synuclein associated toxicity.

In contradistinction to β-wrapins, the majority of molecules developed to inhibit Aβ growth exert their effects by stabilizing high-molecular weight oligomeric intermediates on the amyloid pathway [188]. Similar mechanisms are proposed for molecules developed to target α-synuclein as well [344, 458, 459].

Overall, findings of this work provide added evidence that avoidance of protein aggregation can constitute a viable strategy in tackling amyloidogenesis.

## Concluding remarks and future work

This work successfully constructed a single-chain version of the β-wrapin AS69 by fusing the individual subunits through a suitable flexible linker, $(G_4S)_3$. The resulting construct preserves all features of the disulfide linked AS69 dimer with regard to its binding thermodynamics and potential in inhibiting the aggregation of α-synuclein. In addition, the linker adds further to the stability of the construct and significantly enhances the formation of the functionally essential disulfide bridge between the subunits. Suitability of the covalently linked construct for *in vivo* application was confirmed by testing in SH-SY5Y neuroblastoma cell line. Results revealed that at stoichiometric concentration the exposed cells were thoroughly rescued from α-synuclein toxicity, while at substoichiometric concentrations cell survival was markedly promoted. The single-chain construction concept has also been applied to other β-wrapins, including AS10.

The human neuroblastoma SH-SY5Y cell line possesses the complete dopaminergic system and therefore constitutes a helpful cellular model for preliminary investigation of various pivotal aspects in the pathogenesis of PD and for screening the potential of putative therapeutic ligands [464]. Furthermore, in comparison to other systems cellular models have the added advantage of having a human genetic background. However, since cellular models are rather simplified systems and cannot recapitulate the entire chain of events involved in the pathogenesis of PD, other models have evolved to gain an elaborate understanding of the specific aspects and sequence of events underlying the disease progression. For instance *S. cerevisiae* [465], *Drosophila Melanogaster* [466], *C. elegans* [467], and various *tg* mouse models [141, 260, 468].

The fruit fly (*Drosophila Melanogaster)* has emerged as a suitable model for PD pathogenesis, since both the developing and adult fly possess clusters of dopaminergic neurons that are shown to undergo enhanced degeneration in the presence of soluble α-synuclein oligomers [137]. Since soluble oligomers of α-synuclein are central to PD pathology, this model presents an obvious advantage. Moreover, another appealing feature of this model is the short timeframe required for the disease to develop and to study the effects of potential therapeutic ligands in rescuing the loss of dopaminergic neurons. A head-to-tail construct of Z$_{Aβ3}$ has been previously tested by its co-expression in the brains of the fly that either expressed the Aβ42 variant or the more aggressive familial AD associated E22G mutant variant of Aβ42 [400]. Hence, the drosophila model of PD would be an ideal next model system for evaluating the

therapeutic potential of single chain AS69-GS3 in rescuing the α-synuclein induced neurotoxicity.

The single chain AS69 construct can also be employed for affinity maturation of the β-wrapins, considering that individual subunits can be independently engineered to create diversity either by site-directed or random mutagenesis and thus optimize the affinity and target specificity. Second generation libraries have previously been successfully generated for Affibodies [469, 470], and scFv [471, 472] yielding binders with an affinity in the low picomolar range. In case of the HER2-binding Affibody molecule, affinity maturation led to a 2200 fold increase in affinity towards the target [473].

# Bibliography

[1] Onuchic JS, Wolynes PG: Theory of protein folding. Curr. Opin. Struct. Biol. 2004; 14:70-75

[2] Fersht AR, Daggett V. Protein folding and unfolding at atomic resolution. Cell 2002; 108:573-82.

[3] Lee C, Yu MH. Protein Folding and Diseases. J Biochem Mol Biol. 2005; 38:275-80

[4] Dobson CM. Principles of protein folding, misfolding and aggregation. Semin Cell Dev Biol. 2004; 15:3-16

[5] Lindorff-Larsen K, Piana S, Dror RO, Shaw DE. How fast-folding proteins fold. Science. 2011; 334:517-20

[6] Sosnick TR, Barrick D. The folding of single domain proteins--have we reached a consensus? Curr Opin Struct Biol. 2011; 21:12-24

[7] Kim PS, Baldwin RL: Specific intermediates in the folding reactions of small proteins and the mechanism of protein folding. Annu Rev Biochem 1982; 51:459-489.

[8] Oas TG, Kim PS. A peptide model of a protein folding intermediate. Nature 1988 336: 42-48.

[9] Pande V. S., Grosberg AYu, Tanaka T., Rokhsar D. S: Pathways for protein folding: is a new view needed? Curr. Opin. Struct. Biol. 1998; 8:68-79.

[10] Maity H, Maity M, Krishna MMG, Mayne L, Englander SW. Protein folding: The stepwise assembly of foldon units. Proc. Natl. Acad. Sci. 2005; 102: 4741-46.

[11] Bryngelson JD, Onuchic JN, Socci ND, Wolynes PG. Funnels, pathways, and the energy landscape of protein folding: A synthesis. Proteins 1995; 21:167-195.

[12] Onuchic JN, Luthey-Schulten Z, Wolynes PG. Theory of protein folding: the energy landscape perspective. Annu Rev Phys Chem. 1997; 48:545-600

[13] Dobson CM, Sali A, Karplus M. Protein folding: a perspective from theory and experiment. Angew Chem Int Ed Eng 1998; 37:868-93.

[14] Dill KA. Polymer principles and protein folding. Protein Sci. 1999 Jun; 8(6):1166-80.

[15] Dinner AR, Sali A, Smith LJ, Dobson CM, Karplus M. Understanding protein folding via free-energy surfaces from theory and experiment. Trends Biochem Sci. 2000; 25:331-9.

[16] Gruebele M. Protein folding: the free energy surface. Curr Opin Struct Biol. 2002; 12:161-8

[17] Onuchic JN, Wolynes PG, Luthey- Schulten Z, Socci ND. Toward an outline of the topography of a realistic protein-folding funnel. Proc. Natl. Acad. Sci. USA 1995; 92:3626-30

[18] Dill KA, Chan HS: From Levinthal to pathways to funnels. Nat Struct Biol 1997; 4:10-19.

[19] Jahn TR, Radford SE. Folding versus aggregation: polypeptide conformations on competing pathways. Arch Biochem Biophys. 2008; 469:100-17.

[20] Wolynes PG, Onuchic JN, Thirumalai D. Navigating the folding routes. Science. 1995; 267:1619-20.

[21] Paci E., Lindorff-Larsen K., Dobson C. M., Karplus M., Vendruscolo M. Transition state contact orders correlate with protein folding rates. J. Mol. Biol. 2005; 352, 495-500.

[22] Sosnick T. R. Kinetic barriers and the role of topology in protein and RNA folding. Protein Sci. 2008; 17:1308-18

[23] Krishna MM, Englander SW. A unified mechanism for protein folding: predetermined pathways with optional errors. Protein Sci. 2006; 16:449-64.

[24] Bartlett AI, Radford SE. An expanding arsenal of experimental methods yields an explosion of insights into protein folding mechanisms. Nat Struct Mol Biol. 2009; 16:582-8.

[25] Brockwell DJ, Radford SE. Intermediates: ubiquitous species on folding energy landscapes? Curr Opin Struct Biol. 2007; 17:30-7

[26] Fersht AR. Transition-state structure as a unifying basis in protein-folding mechanisms: contact order, chain topology, stability, and the extended nucleus mechanism. Proc Natl Acad Sci USA 2000; 97:1525-9.

[27] Cheung MS, Garcia AE, Onuchic JN. Protein folding mediated by solvation: water expulsion and formation of the hydrophobic core occur after the structural collapse. Proc Natl Acad Sci USA 2002; 99:685-90.

[28] Vendruscolo M., Paci E., Karplus M., Dobson C.M., Proc. Natl. Acad. Sci. USA 2003; 100:14817-14821

[29] Clark PL. Protein folding in the cell: reshaping the folding funnel. Trends Biochem Sci. 2004; 29:527-34.

[30] Ellis RJ, Minton AP. Protein aggregation in crowded environments. Biol. Chem. 2006; 387:485-497.

[31] Hartl FU, Hayer-Hartl M. Molecular chaperones in the cytosol: from nascent chain to folded protein. Science 2002; 295:1852-8.

[32] Panchenko AR, Luthey-Schulten Z, Wolynes PG. Foldons, protein structural modules, and exons. Proc Natl Acad Sci USA 1996; 93:2008-13.

[33] Dobson CM, Sali A, and Karplus M. Protein Folding: A Perspective from Theory and Experiment. Angew. Chem. Int. Ed. 1998; 37:868-893

[34] Capaldi AP, Kleanthous C, Radford SE. Im7 folding mechanism: Misfolding on a path to the native state. Nature Struct Biol 2002; 9: 209-16.

[35] Gething M-J, Sambrook J. Protein folding in the cell. Nature 1992; 355:33-45.

[36] Frydman J. Folding of newly translated proteins *in vivo*: The role of molecular chaperones. Annu. Rev. Biochem. 2001; 70:603-47

[37] Dobson CM. Protein folding and disease: a view from the first Horizon symposium. Nature Rev Drug Disc 2003; 2:154-60.

[38] Morimoto RI. Proteotoxic stress and inducible chaperone networks in neurodegenerative disease and aging. Genes Dev. 2008; 22:1427-38

[39] Parsall DA, Kowal AS, Singer MA, Lindquist S. Protein disaggregation mediated by heat-shock protein Hsp104. Nature 1994; 372:475.

[40] Fedorov, A.N. and Baldwin, T.O. Process of biosynthetic protein folding determines the rapid formation of native structure. J. Mol. Biol. 1999; 294, 579-586

[41] Seckler, R, Fuchs A, King J, Jaenicke R. Reconstitution of the thermostable trimeric phage P22 tailspike protein from denatured chains *in vitro*. J. Biol. Chem. 1989; 264, 11750-11753

[42] Schubert U, Anton LC, Gibbs J, Orbyry CC, Yewdell JW, Bennink JR. Rapid degradation of a large fraction of newly synthesized proteins by proteasomes. Nature 2000; 404:770-4.

[43] Yewdell, J.W. Serendipity strikes twice: The discovery and rediscovery of defective ribosomal products (DRiPS). Cell. Mol. Biol. 2005; 51:635-641

[44] Travers, K. J. et al. Functional and genomic analyses reveal an essential coordination between the unfolded protein response and ER-associated degradation. Cell 2000; 101:249-258.

[45] Csermely P. Chaperone overload is a possible contributor to 'civilization diseases'. Trends Genet 2001; 17:701-4

[46] Bence NF, Sampat RM, Kopito RR. Impairment of the ubiquitin-proteosome system by protein aggregation. Science 2001; 292: 1552-5

[47] Dobson CM. Getting out of shape: Protein misfolding diseases. Nature 2002; 418:729-30

[48] Fändrich M, Forge V, Buder K, Kittler M, Dobson C M, Diekmann S. Myoglobin forms amyloid fibrils by association of unfolded polypeptide segments. Proc. Natl. Acad. Sci. U.S.A. 2003; 100:15463-15468.

[49] Dobson CM. Protein misfolding, evolution and disease. Trends Biochem Sci 1999; 24:329–32.

[50] Chiti F, Webster P, Taddei N, Clark A, Stefani M, Ramponi G, et al. Designing conditions for *in vitro* formation of amyloid protofilaments and fibrils. Proc Natl Acad Sci USA 1999; 96:3590-4.

[51] Relini A, Marano N, Gliozzi A. Misfolding of amyloidogenic proteins and their interactions with membranes. Biomolecules. 2014; 4:20-55

[52] Chiti F, Dobson CM. Protein misfolding, functional amyloid, and human disease. Annu Rev Biochem. 2006; 75:333-66.

[53] Pepys MB. Amyloidosis. Annu Rev Med. 2006; 57:223-41

[54] Kelly J. Alternative conformation of amyloidogenic proteins and their multi-step assembly pathways. Curr Opin Struct Biol 1998; 8:101-6.

[55] Chiti F, Dobson CM. Amyloid formation by globular proteins under native conditions. Nat Chem Biol. 2009; 5:15-22

[56] Plakoutsi G, Bemporad F, Monti M, Pagnozzi D, Pucci P, Chiti F. Exploring the mechanism of formation of native-like and precursor amyloid oligomers for the native acylphosphatase from sulfolobus solfataricus. Structure 2006; 14, 993-1001

[57] De Simone A, Dhulesia A, Soldi G, Vendruscolo M, Hsu SD, Chiti F, Dobson CM. Experimental free energy surfaces reveal the mechanisms of maintenance of protein solubility. Proc. Natl. Acad. Sci. USA 2011; 108, 21057-21062

[58] Bouchard M, Zurdo J, Nettleton EJ, Dobson CM, Robinson CV. Formation of insulin amyloid fibrils followed by FTIR simultaneously with CD and electron microscopy. Protein Sci. 2000; 9:1960-1967

[59] Dobson CM. The structural basis of protein folding and its links with human disease. Philos Trans R Soc Lond B Biol Sci. 2001; 356:133-45

[60] Koo EH, Lansbury Jr PT, Kelly JW. Amyloid diseases: abnormal protein aggregation in neurodegeneration. Proc Natl Acad Sci USA 1999; 96:9989-90.

[61] Nielsen L, Khurana R, Coats A, Frokjaer S, Brange J, Vyas S, Uversky V, Fink A. Effect of environmental factors on the kinetics of insulin fibril formation: Elucidation of the molecular mechanism. Biochemistry 2001; 40:6036-6046.

[62] Bekard IB, Dunstan DE. Shear-induced deformation of bovine insulin in couette flow. J. Phys. Chem. B 2009; 113:8453-8457.

[63] Diaz-Espinoza R, Mukherjee A, Soto C. Kosmotropic anions promote conversion of recombinant prion protein into a PrPSc-like misfolded form. PLoS One 2012; 7:e31678.

[64] Fändrich M. Oligomeric Intermediates in Amyloid Formation: Structure Determination and Mechanisms of Toxicity. J Mol Biol. 2012; 421:427-40.

[65] Rubin J, Khosravi H, Bruce KL, Lydon ME, Behrens SH, Chernoff YO, Bommarius AS. Ion-specific effects on prion nucleation and strain formation. J. Biol. Chem. 2013; 288:30300-30308.

[66] Ow S, Dunstan DE. The effect of concentration, temperature and stirring on hen egg white lysozyme amyloid formation. Soft Matter 2013; 9:9692-9701.

[67] Mangione PP, Esposito G, Relini A, Raimondi S, Porcari R, Giorgetti S, et al. Structure, folding dynamics, and amyloidogenesis of D76N ß2-microglobulin: Roles of shear flow, hydrophobic surfaces, and a-crystallin. J. Biol. Chem. 2013; 288:30917-30.

[68] Chiti F, Calamai M, Taddei N, Stefani M, Ramponi G, Dobson CM. Studies of the aggregation of mutant proteins *in vitro* provide insights into the genetics of amyloid diseases. Proc. Natl. Acad. Sci. USA 2002; 99:16419-16426.

[69] Chiti F, Stefani M, Taddei N, Ramponi G, Dobson CM. Rationalisation of mutational effects on peptide and protein aggregation rates. Nature 2003; 424:805-8.

[70] Calloni G, Lendel C, Campioni S, Giannini S, Gliozzi A, Relini A, Vendruscolo M, Dobson CM, Salvatella X, Chiti F. Structure and dynamics of a partially folded protein are decoupled from its mechanism of aggregation. J. Am. Chem. Soc. 2008; 130, 13040-13050.

[71] Uversky VN, Yamin G, Souillac PO, Goers J, Glaser CB, Fink AL. Methionine oxidation inhibits fibrillation of human alpha-synuclein *in vitro*. FEBS Lett. 2002; 517:239-244

[72] Morozova-Roche LA, Zurdo J, Spencer A, Noppe W, Receveur V, Archer DB, Joniau M, Dobson CM. Amyloid fibril formation and seeding by wild-type human lysozyme and its disease-related mutational variants. J. Struct. Biol. 2000; 130:339-351.

[73] Booth DR, Sunde M, Bellotti V, Robinson CV, Hutchinson WL, Fraser PE, et al. Instability, unfolding and aggregation of human lysozyme variants underlying amyloid fibrillogenesis. Nature 1997; 385:787-93

[74] Ramirez-Alvarado M, Merkel JS, Regan L. A systematic exploration of the influence of the protein stability on amyloid fibril formation *in vitro*. Proc Natl Acad Sci USA 2000; 97:8979-84

[75] Alonso Vilatela ME, López-López M, Yescas-Gómez P. Genetics of Alzheimer's disease. Arch. Med. Res. 2012; 43:622-631.

[76] Gilead S, Gazit E. Inhibition of amyloid fibril formation by peptide analogues modified with alpha-aminoisobutyric acid. Angew. Chem. Int. Ed. Engl. 2004; 43 (31): 4041-4

[77] Perutz MF, Johnson T, Suzuki M, Finch JT. Glutamine repeats as polar zippers: Their possible role in inherited neurodegenerative diseases. Proc. Natl. Acad. Sci. USA 1994; 91:5355-5358.

[78] Zoghbi .Y, Orr HT. Glutamine repeats and neurodegeneration. Annu. Rev. Neurosci. 2000; 23:217-247.

[79] Shehi E, Fusi P, Secundo F, Pozzuolo S, Bairati A, Tortora P. Temperature-dependent, irreversible formation of amyloid fibrils by a soluble human ataxin-3 carrying a moderately expanded polyglutamine stretch (Q36). Biochemistry 2003; 42:14626-14632.

[80] Zhang T, Faraggi E, Li Z, Zhou Y. Intrinsically semi-disordered state and its role in induced folding and protein aggregation. Cell Biochem. Biophys. 2013; 67:1193-1205

[81] Steward A, Adhya S, Clarke J. Sequence conservation in Ig-like domains: the role of highly conserved proline residues in the fibronectin type III superfamily. J. Mol. Biol. 2002; 318:935–40

[82] Pawar AP, Dubay KF, Zurdo J, Chiti F, Vendruscolo M, Dobson CM. Prediction of "Aggregation-prone" and "Aggregation-susceptible" Regions in Proteins Associated with Neurodegenerative Diseases. J Mol Biol 2005; 350 (2): 379-92.

[83] Parrini C,Taddei N, Ramazzotti M, Degl'Innocenti D, Ramponi G, Dobson CM, Chiti F. Glycine residues appear to be evolutionarily conserved for their ability to inhibit aggregation. Structure 2005; 13:1143–51

[84] Bellotti V, Chiti F. Amyloidogenesis in its biological environment: challenging a fundamental issue in protein misfolding diseases. Curr Opin Struct Biol. 2008; 18:771-9.

[85] Shen L, Adachi T, Vanden Bout D, Zhu X-Y. A mobile precursor determines amyloid-β peptide fibril formation at interfaces. J. Am. Chem. Soc. 2012; 134:14172-14178.

[86] Nault L, Guo P, Jain B, Brechet Y, Brucker F, Weidenhaupt M. Human insulin adsorption kinetics, conformational changes and amyloidal aggregate formation on hydrophobic surfaces. Acta Biomater. 2013; 9:5070-5079.

[87] Relini A, Canale C, de Stefano S, Rolandi R, Giorgetti S, et al. Collagen plays an active role in the aggregation of β2-microglobulin under physiopathological conditions of dialysis-related amyloidosis. J. Biol. Chem. 2006; 281:16521-16529.

[88] Gorbenko GP, Kinnunen PK. The role of lipid-protein interactions in amyloid-type protein fibril formation. Chem. Phys. Lipids 2006; 141:72-82.

[89] Relini, A.; Marano, N.; Gliozzi, A. Probing the interplay between amyloidogenic proteins and membranes using lipid monolayers and bilayers. Adv. Colloid Interface Sci. 2014; 207:81-92

[90] Davidson WS, Jonas A, Clayton DF, George JM. Stabilization of α-synuclein secondary structure upon binding to synthetic membranes. J. Biol. Chem. 1998; 273:9443-9449.

[91] Jo E, McLaurin J, Yip CM, St. George-Hyslop P, Fraser PE. α-Synuclein membrane interactions and lipid specificity. J. Biol. Chem. 2000; 275:34328-34334.

[92] Apostolidou M, Jayasinghe SA, Langen R. Structure of α-helical membrane-bound human islet amyloid polypeptide and its implications for membrane-mediated misfolding. J. Biol. Chem. 2008; 283:17205-17210.

[93] Ferreon ACM, Gambin Y, Lemke EA, Deniz AA. Interplay of a-synuclein binding and conformational switching probed by single-molecule fluorescence. Proc. Natl. Acad. Sci. USA 2009; 106:5645-5650.

[94] Fantini J, Yahi N. The driving force of α-synuclein insertion and amyloid channel formation in the plasma membrane of neural cells: Key role of ganglioside- and cholesterol-binding domains. Adv. Exp. Med. Biol. 2013; 991:15-26.

[95] Fantini J, Yahi N, Garmy N. Cholesterol accelerates the binding of Alzheimer's β-amyloid peptide to ganglioside GM1 through a universal hydrogen-bond-dependent sterol tuning of glycolipid conformation. Front. Physiol. 2013; 4:120.

[96] Zhao H, Tuominen E.KJ, Kinnunen PKJ. Formation of amyloid fibers triggered by phosphatidylserine-containing membranes. Biochemistry 2004; 43:10302-10307.

[97] Butterfield SM, Lashuel HA. Amyloidogenic protein-membrane interactions: mechanistic insight from model systems. Angew Chem Int Ed Engl. 2010; 49:5628-54

[98] Jahn TR, Radford SE. The Yin and Yang of protein folding. FEBS J. 2005 Dec; 272:5962-70.

[99] Sunde M, Blake CCF. From the globular to the fibrous state: protein structure and structural conversion in amyloid formation. Q. Rev. Biophysics 1998; 31:1-39

[100] Wetzel R, Shivaprasad S, Williams AD. Plasticity of amyloid fibrils. Biochemistry 2007; 46:1-10.

[101] Bhak G, Choe YJ, Paik SR. Mechanism of amyloidogenesis: nucleation-dependent fibrillation versus double-concerted fibrillation. BMB Rep. 2009; 42:541-51

[102] Goldsbury C, Frey P, Olivieri V, Aebi U, Müller SA. Multiple assembly pathways underlie amyloid-β fibril polymorphisms. J. Mol. Biol. 2005; 352:282-298.

[103] Naiki H, Gejyo F. Kinetic analysis of amyloid fibril formation. Methods Enzymol. 1999; 309:305-318.

[104] Carulla N, Caddy G L, Hall D R, Zurdo J, Gairi M, Feliz M, Giralt E, Robinson CV, Dobson CM. Molecular recycling within amyloid fibrils. Nature 2005; 436:554-558.

[105] Harper JD, Lansbury Jr PT. Models of amyloid seeding in Alzheimer's disease and scrapie: mechanistic truths and physiological consequences of the time-dependent solubility of amyloid proteins. Annu Rev Biochem 1997; 66:385-407.

[106] Bhak G, Lee J-H, Hahn J-S, Paik SR. Granular assembly of α-synuclein leading to the accelerated amyloid fibril formation with shear stress. PLoS ONE 2009; 4:e4177

[107] Knowles TP, Waudby CA, Devlin GL, Cohen SI, Aguzzi A, Vendruscolo M, Terentjev E.M, Welland ME, Dobson CM. An analytical solution to the kinetics of breakable filament assembly. Science 2009; 326: 1533-1537.

[108] Heldt CL, Zhang S, Belfort G. Asymmetric amyloid fibril elongation: A new perspective on a symmetric world. Proteins: Struct. Funct. Bioinforma. 2011; 79:92-98

[109] Bellotti V, Stoppini M. Protein Misfolding Diseases. The Open Biology Journal, 2009; 2:228-234

[110] Glabe CG. Structural classification of toxic amyloid oligomers. J Biol Chem. 2008; 283(44):29639-43

[111] Lashuel HA, Hartley D, Petre BM, Walz T, Lansbury Jr PT. Neurodegenerative disease: amyloid pores from pathogenic mutations. Nature 2002; 418:291

[112] Armen RS, Alonso DO, Daggett V.Anatomy of an amyloidogenic intermediate: conversion of beta-sheet to alpha-sheet structure in transthyretin at acidic pH. Structure. 2004; 12:1847-63.

[113] Meinhardt J, Sachse C, Hortschansky P, Grigorieff N, Fändrich M. Aβ(1–40) fibril polymorphism implies diverse interaction patterns in amyloid fibrils. J. Mol. Biol. 2009; 386:869-877

[114] Kayed R1, Head E, Sarsoza F, Saing T, Cotman CW, Necula M, Margol L, et al. Fibril specific, conformation dependent antibodies recognize a generic epitope common to amyloid fibrils and fibrillar oligomers that is absent in prefibrillar oligomers. Mol. Neurodegener. 2007; 2:18.

[115] Bolognesi B, Kumita JR, Barros TP, Esbjorner EK, Luheshi LM, Crowther DC, Wilson MR, Dobson CM, Favrin G, Yerbury JJ. ANS binding reveals common features of cytotoxic amyloid species. ACS Chem Biol. 2010; 5:735-40.

[116] Puchtler H, Sweat F, Levine M. On the binding of Congo red by amyloid. J Histochem Cytochem 1961; 10:355-364.

[117] Eanes ED, Glenner GG. X-ray diffraction studies on amyloid filaments. J Histochem Cytochem 1968; 16:673-677.

[118] Cohen AS, Shirahama T, Skinner M. Electron microscopy of amyloid. In Electron Microscopy of Protein 1982 (Harris I, ed.), pp. 165-205. Academic Press, London, UK.

[119] Kirschner DA, Abraham C, Selkoe DJ. X-ray diffraction from intraneuronal paired helical filaments and extraneuronal amyloid fibers in Alzheimer disease indicates cross-beta conformation. Proc. Natl. Acad. Sci. U S A 1986; 198683:503-507

[120] LeVine H III. Thioflavine T interaction with synthetic Alzheimer's disease beta-amyloid peptides: detection of amyloid aggregation in solution. Protein Sci 1993; 2:404-410.

[121] Sunde M, Blake CCF. The structure of amyloid fibrils by electron microscopy and X-ray diffraction. Adv Prot Chem 1997; 50:123-59.

[122] Fändrich M, Dobson CM. The behaviour of polyamino acids reveals an inverse side chain effect in amyloid structure formation. EMBO J 2002; 21(21):5682-90.

[123] Nilsson MR. Techniques to study amyloid fibril formation *in vitro*. Methods 2004; 34 (1):151-60.

[124] Eisenberg D, Jucker M. The amyloid state of proteins in human diseases. Cell 2012; 148:1188-1203.

[125] Liu C, Sawaya MR, Cheng P, Zheng J, Nowick JS, Eisenberg D. Characteristics of amyloid-related oligomers revealed by crystal structures of macrocyclic β-sheet mimics. J. Am. Chem. Soc. 2011; 133: 67366744.

[126] Iwata K, Fujiwara T, Matsuki Y, Akutsu H, Takahashi S, Naiki H, Goto Y. 3D structure of amyloid protofilaments of beta2-microglobulin fragment probed by solid-state NMR. Proc Natl Acad Sci USA 2006; 103(48): 18119-24.

[127] Liu C, Zhao M, Jiang L, Cheng P, Park J, Sawaya MR, Pensalfini A, Gou D, Berk AJ, Glabe CG, Nowick J, Eisenberg D. Out-of-register β-β suggest a pathway to toxic amyloid aggregates. Proc. Natl. Acad. Sci. USA 2012; 109:20913-20918.

[128] Chamberlain A, MacPhee CE, Zurdo J, Morozova-Roche LA, Hill HAO, Dobson CM, et al. Ultrastructural organisation of amyloid fibrils by atomic force microscopy. Biophys. J. 2000; 79:3282-93.

[129] Dobson CM, Karplus M. The fundamentals of protein folding: bringing together theory and experiment. Curr Opin Struct Biol 1999; 9:92-101.

[130] Petkova AT, Yau WM, Tycko R. Experimental constraints on quaternary structure in Alzheimer's beta-amyloid fibrils. Biochemistry. 2006; 45:498-512.

[131] Makin OS, Atkins E, Sikorski P, Johansson J, Serpell LC. Molecular basis for amyloid fibril formation and stability. Proc Natl Acad Sci USA 2005; 102(2): 315-20.

[132] Marshall KE, Serpell LC. Insights into the Structure of Amyloid Fibrils. The Open Biology Journal, 2009; 2:185-192

[133] Bradbury J. Chaperones: keeping a close eye on protein folding. Lancet 2003; 361:1194-5.

[134] Winklhofer KF, Tatzelt J, Haass C. The two faces of protein misfolding: gain- and loss-of-function in neurodegenerative diseases. EMBO J. 2008; 27:336-49.

[135] Kirkitadze MD, Bitan G & Teplow DB. Paradigm shifts in Alzheimer's disease and other neurodegenerative disorders: the emerging role of oligomeric assemblies. J Neurosci Res 2002; 69:567-577.

[136] Stefani M, Dobson CM. Protein aggregation and aggregate toxicity: new insights into protein folding, misfolding diseases and biological evolution. J Mol Med (Berl). 2003; 81:678-99.

[137] Karpinar DP, Balija MGG, Kügler S, et al. Pre-fibrillar α-synuclein variants with impaired β-structure increase neurotoxicity in Parkinson's disease models, EMBO J. 2009; 28:3256-68

[138] Makin OS, Serpell LC. Structures for amyloid fibrils. FEBS J 2005; 272(23): 5950-61

[139] Glabe CG. Common mechanisms of amyloid oligomer pathogenesis in degenerative disease. Neurobiol Aging. 2006; 27:570-5

[140] Haass C, Selkoe DJ. Soluble protein oligomers in neurodegeneration: lessons from the Alzheimer's amyloid beta-peptide. Nat Rev Mol Cell Biol 2007; 8:101-112

[141] Masliah E, Rockenstein E, Veinbergs I, Mallory M, et al. Dopaminergic loss and inclusion body formation in alpha-synuclein mice: Implications for neurodegenerative disorders. Science 2000; 287:1265-69

[142] Nilsberth C, Westlind-Danielsson A, Eckman CB, et al. The 'Arctic' APP mutation (E693G) causes Alzheimer's disease by enhanced Abold beta protofibril formation. Nat Neurosci. 2001; 4:887-93.

[143] Lashuel HA, Petre BM, Wall J, Simon M, Nowak RJ, Walz T, Lansbury PT Jr. α-Synuclein, especially the Parkinson's disease-associated mutants, forms pore-like annular and tubular protofibrils. J. Mol. Biol. 2002; 322:1089-1102

[144] Caughey B, Lansbury PT Jr. Protofibrils, pores, fibrils, and neurodegeneration: separating the responsible protein aggregates from the innocent bystanders. Annu. Rev. Neurosci. 2003; 26:267-298.

[145] Fändrich M. Oligomeric intermediates in amyloid formation: structure determination and mechanisms of toxicity. J Mol Biol. 2012; 421:427-40

[146] Arispe N, Pollard HB, Rojas E. β-Amyloid Ca2+-channel hypothesis for neuronal death in alzheimer disease. Mol Cell Biochem 1994; 140:119-25.

[147] Hashimoto M, Rockenstein E, Crews L, Masliah E. Role of protein aggregation in mitochondrial dysfunction and neurodegeneration in Alzheimer's and Parkinson's diseases. Neuromol Med 2003; 4: 21-36.

[148]

[149] Saitoh T, Horsburgh K, Masliah E. Hyperactivation of signal transduction systems in Alzheimer's disease. Ann NY Acad Sci 1993; 695:34-41.

[150] Schubert D, Behl C, Lesley R, Brack A, Dargusch R, Sagara Y, Kimura H. Amyloid peptides are toxic via a common oxidative mechanism. Proc Natl Acad Sci USA 1995; 92:1989-93.

[151] Shoffner JM. Oxidative phosphorylation defects and Alzheimer's disease. Neurogenetics 1997; 1:13-9.

[152] Walsh DM, Klyubin I, Fadeeva JV, Cullen WK, Anwyl R, Wolfe MS, Rowan MJ, Selkoe DJ. Naturally secreted oligomers of amyloid beta protein potently inhibit hippocampal long-term potentiation *in vivo*. Nature 2002; 416:535-9.

[153] Shintani T, Klionsky DJ. Autophagy in health and disease: a double-edged sword. Science 2004; 306:990-5.

[154] Engel MF, Khemtémourian L, Kleijer CC, et al. Membrane damage by human islet amyloid polypeptide through fibril growth at the membrane. Proc. Natl. Acad. Sci. USA 2008; 105: 6033–6038.

[155] Pieri L, Madiona K, Bousset L, Melki R. Fibrillar alpha-synuclein and huntingtin exon 1 assemblies are toxic to the cells. Biophys. J. 2012; 102:2894–2905.

[156] Milanesi L, Sheynis T, Xue WF, Orlova EV, Hellewell AL, Jelinek R, Hewitt EW, Radford SE, Saibil HR. Direct three-dimensional visualization of membrane disruption by amyloid fibrils. Proc. Natl. Acad. Sci. USA 2012; 109: 20455–20460.

[157] Schauerte JA, Wong PT, Wisser KC, Ding H, Steel DG, Gafni A. Simultaneous single-molecule fluorescence and conductivity studies reveal distinct classes of Aβ species on lipid bilayers. Biochemistry 2010; 49: 3031–3039.

[158] Knowles TP, Vendruscolo M, Dobson CM. The amyloid state and its association with protein misfolding diseases. Nat Rev Mol Cell Biol. 2014; 15:384-96

[159] Lee HG, Zhu X, Takeda A, Perry G, Smith MA. Emerging evidence for the neuroprotective role of alpha-synuclein. Exp Neurol. 2006; 200:1-7.

[161] Alzheimer's Association. Alzheimer's disease facts and figures. Alzheimers Dement. 2010; 6:158-94.

[162] Hardy J, Gwinn-Hardy K.  Genetic classification of primary neurodegenerative disease. Science. 1998; 282:1075-9.

[163] Hashimoto M, Masliah E. Alpha-synuclein in Lewy body disease and Alzheimer's disease. Brain Pathol. 1999; 9:707-20.

[164] Braak H, Braak E. Pathoanatomy of Parkinson's disease. J Neurol. 2000; 247 Suppl 2:II3-10.

[165] McCann H, Stevens CH, Cartwright H, Halliday GM. A-Synucleinopathy phenotypes. Parkinsonism Relat Disord. 2014; 20 Suppl 1:S62-7

[166] Kim WS, Kågedal K, Halliday GM. Alpha-synuclein biology in Lewy body diseases. Alzheimers Res Ther. 2014; 6:73

[167] Spillantini MG, Schmidt ML, Lee VM, Trojanowski JQ, Jakes R, Goedert M. Alpha-synuclein in Lewy bodies. Nature 1997; 388:839-40.

[168] Gai WP, Power JH, Blumbergs PC, Blessing WW. Multiple-system atrophy. A new alpha-synuclein disease? Lancet 1998; 352:547–48.

[169] Wami Marui, Eizo Iskei, Masanori Kato, Hiroyasu Akatsu, Kenji Kosaka. Pathological entity of dementia with Lewy bodies and its differentiation from Alzheimer's disease. Acta Neuropathologica 2004; 108: 121–8

[170] Newell KL, Boyer P, Gomez-Tortosa E, Hobbs W, Hedley-Whyte ET, Vonsattel JP, Hyman BT. Alpha-synuclein immunoreactivity is present in axonal swellings in neuroaxonal dystrophy and acute traumatic brain injury. J Neuropathol Exp Neurol 1999; 58:1263–1268.

[171] Gelb DJ, Oliver E, Gilman S: Diagnostic criteria for Parkinson disease. Arch Neurol 1999; 56:33-39.

[172] Maroteaux L, Campanelli JT, Scheller RH. Synuclein: a neuron-specific protein localized to the nucleus and presynaptic nerve terminal.J Neurosci. 1988; 8:2804-15.

[173] Ueda K, Fukushima H, Masliah E, Xia Y, Iwai A, Yoshimoto M, Otero DA, Kondo J, Ihara Y, Saitoh T. Molecular cloning of cDNA encoding an unrecognized component of amyloid in Alzheimer disease. Proc Natl Acad Sci U S A 1993; 90:11282-11286.

[174] Iwai A, Masliah E, Yoshimoto M, Ge N, Flanagan L, de Silva HA, Kittel A, Saitoh T. The precursor protein of non-A beta component of Alzheimer's disease amyloid is a presynaptic protein of the central nervous system. Neuron 1995; 14:467-475.

[175] Barbour R, Kling K, Anderson JP, Banducci K, Cole T, Diep L, Fox M, et al. Red blood cells are the major source of alpha-synuclein in blood. Neurodegener Dis 2008; 5: 55-9

[176] Bungeroth M, Appenzeller S, Regulin A, Völker W, Lorenzen I, Grötzinger J, Pendziwiat M, Kuhlenbäumer G. Differential aggregation properties of alpha-synuclein isoforms. Neurobiol Aging. 2014; 35:1913-9.

[177] McLean PJ, Kawamata H, Shariff S, Hewett J, Sharma N, Ueda K, Breakefield XO, Hyman BT. Torsin A and heat shock proteins act as molecular chaperones: suppression of alpha-synuclein aggregation. J. Neurochem. 2002; 83:846–854.

[178] Lee HJ, Choi C, Lee SJ. Membrane-bound alpha-synuclein has a high aggregation propensity and the ability to seed the aggregation of the cytosolic form. J. Biol. Chem. 2002; 277: 671–8

[179] Yu S, Li X, Liu G, Han J, Zhang C, Li Y, Xu S, Liu C, Gao Y, Yang H, Uéda K, Chan P . Extensive nuclear localization of alpha-synuclein in normal rat brain neurons revealed by a novel monoclonal antibody. Neuroscience 2007; 145: 539-55

[180] Liu G, Zhang C, Yin J, Li X, Cheng F, Li Y, Yang H, Uéda K, Chan P, Yu S. Alpha-Synuclein is differentially expressed in mitochondria from different rat brain regions and dose-dependently down-regulates complex I activity. Neurosci. Lett. 2009; 454:187-92.

[181] Uversky VN. Alpha-synuclein misfolding and neurodegenerative diseases, Curr. Protein Pept. Sci. 2008; 9:507-540.

[182] Abeliovich A, Schmitz Y, Farinas I, Choi-Lundberg D, Ho WH, Castillo PE, Shinsky N, et al. Mice lacking alpha-synuclein display functional deficits in the nigrostriatal dopamine system. Neuron 2000; 25: 239-52.

[183] Masliah E, Rockenstein E, Veinbergs I, Sagara Y, Mallory M, Hashimoto M, Mucke L. Beta-amyloid peptides enhance alpha-synuclein accumulation and neuronal deficits in a transgenic mouse model linking Alzheimer's disease and Parkinson's disease. Proc Natl Acad Sci U S A. 2001; 98:12245-50.

[184] Murphy DD, Rueter SM, Trojanowski JQ, Lee VM. Synucleins are developmentally expressed, and alpha-synuclein regulates the size of the presynaptic vesicular pool in primary hippocampal neurons. J Neurosci 2000; 20:3214–3220.

[185] Di Rosa G, Puzzo D, Sant'Angelo A, Trinchese F, Arancio O. Alpha-synuclein: between synaptic function and dysfunction. Histol Histopathol. 2003; 18:1257-66.

[186] Bonini NM, Giasson BI. Snaring the function of alpha-synuclein. Cell 2005; 123:359-361.

[187] Burre J, Sharma M, Tsetsenis T, Buchman V, Etherton MR, Sudhof TC. Alpha-synuclein promotes SNARE-complex assembly *in vivo* and *in vitro*. Science 2010; 329:1663-1667.

[188] Lashuel HA, Overk CR, Oueslati A, Masliah E. The many faces of α-synuclein: from structure and toxicity to therapeutic target. Nat Rev Neurosci. 2013; 14:38-48

[189] Zhu M, Qin ZJ, Hu D, Munishkina LA, Fink AL. Alpha-synuclein can function as an antioxidant preventing oxidation of unsaturated lipid in vesicles, Biochemistry 2006; 45:8135-42.

[190] da Costa CA1, Ancolio K, Checler F. Wild-type but not Parkinson's disease-related ala-53→Thr mutant alpha-synuclein protects neuronal cells from apoptotic stimuli. J. Biol. Chem. 2000; 275:24065-24069.

[191] Dev KK, Hofele K, Barbieri S, Buchman VL, van der Putten H. Part II: alpha-synuclein and its molecular pathophysiological role in neurodegenerative disease. Neuropharmacology 2003; 45:14-44.

[192] Quilty MC, King AE, Gai WP, Pountney DL, West AK, Vickers JC, Dickson TC. Alpha-synuclein is upregulated in neurones in response to chronic oxidative stress and is associated with neuroprotection. Exp. Neurol. 2006; 199:249-56

[193] Manning-Bog AB, McCormack AL, Purisai MG, Bolin LM, Di Monte DA. Alpha-synuclein overexpression protects against paraquati nduced neurodegeneration. J. Neurosci. 2003; 23:3095-99

[194] Chandra S, Fornai F, Kwon HB, et al. Double-knockout mice for α- and β-synucleins: effect on synaptic functions. Proc. Natl Acad. Sci. USA 2004; 101:14966–14971.

[195] Chandra S, Gallardo G, Fernandez-Chacon R, Schluter OM, Sudhof TC. α-synuclein cooperates with CSPα in preventing neurodegeneration. Cell 2005; 123:383-96.

[196] Lavedan C. The synuclein family. Genome Res. 1998; 8:871-80.

[197] Beyer K. Alpha-synuclein structure, posttranslational modification and alternative splicing as aggregation enhancers. Acta Neuropathol. 2006; 112: 237–51

[198] Beyer K, Domingo-Sábat M, Lao JI, Carrato C, Ferrer I, Ariza A. Identification and characterization of a new alpha-synuclein isoform and its role in Lewy body diseases. Neurogenetics. 2008; 9:15-23.

[199] Eliezer D, Kutluay E, Bussell Jr. R., Browne G. Conformational properties of alpha-synuclein in its free and lipid-associated states. J. Mol. Biol. 2001; 307:1061-1073.

[200] Breydo L, Wu JW, Uversky VN. A-synuclein misfolding and Parkinson's disease. Biochim Biophys Acta. 2012; 1822:261-85

[201] Giasson BI, Murray IV, Trojanowski JQ, Lee VM. A hydrophobic stretch of 12 amino acid residues in the middle of α-synuclein is essential for filament assembly. J. Biol. Chem. 2001; 276:2380-86.

[202] Drescher M, Huber M, Subramaniam V.Hunting the chameleon: structural conformations of the intrinsically disordered protein alpha-synuclein. Chembiochem. 2012; 13:761-8

[203] Campen A, Williams RM, Brown CJ, Meng J, Uversky VN, unker AK. TOP-IDP-scale: a new amino acid scale measuring propensity for intrinsic disorder. Protein Pept. Lett. 2008; 15:956-963.

[204] Uversky VN. Unusual biophysics of intrinsically disordered proteins. Biochimica et Biophysica Acta 2013; 1834:932-951

[205] Uversky VN. Intrinsically disordered proteins may escape unwanted interactions via functional misfolding, Biochim. Biophys. Acta 2011; 1814:693-712.

[206] Zhao M, CascioD, Sawaya MR, Eisenberg D. Structures of segments of α- synuclein fused to maltose-binding protein suggest intermediate states during amyloid formation. Protein Sci. 2011; 20:996–1004.

[207] Fernández CO, Hoyer W, Zweckstetter M, Jares-Erijman EA, Subramaniam V, Griesinger C, Jovin TM. NMR of alpha-synuclein-polyamine complexes elucidates the mechanism and kinetics of induced aggregation, EMBO J. 2004; 23:2039-2046.

[208] Bertoncini CW, Jung YS, Fernandez CO, Hoyer W, Griesinger C, Jovin TM, Zweckstetter M. Release of long-range tertiary interactions potentiates aggregation of natively unstructured alpha-synuclein, Proc. Natl Acad. Sci. U. S. A. 2005; 102:1430-35.

[209] Uversky VN, Li J, Fink AL. Evidence for a partially folded intermediate in alpha-synuclein fibril formation. J. Biol. Chem. 2001; 276:10737-10744.

[210] Bartels T, Choi JG, Selkoe DJ. Alpha-synuclein occurs physiologically as a helically folded tetramer that resists aggregation. Nature 2011; 477:107-110.

[211] Wang W, Perovic I, Chittuluru J, Kaganovich A, Nguyen LT et al. A soluble α-synuclein construct forms a dynamic tetramer. Proc. Natl Acad. Sci. USA 2011; 108:17797-802.

[212] Fauvet B, Mbefo MK, Fares MB, et al. α-Synuclein in central nervous system and from erythrocytes, mammalian cells, and Escherichia coli exists predominantly as disordered monomer. J. Biol. Chem. 2012; 287:15345-64.

[213] Binolfi A, Theillet FX, Selenko P. Bacterial in-cell NMR of human α-synuclein: a disordered monomer by nature? Soc. Trans. 2012; 40:950-4.

[214] Gurry T, Ullman O, Fisher CK, Perovic I, Pochapsky T, Stultz CM. The dynamic structure of α-synuclein multimers. J Am Chem Soc. 2013; 135:3865-72

[215] Dunker AK, Lawson JD, Brown CJ, Williams RM, et al. Intrinsically disordered protein, J. Mol. Graph. Model. 2001; 19:26-59.

[216] Dunker AK, Bondos SE, Huang F, Oldfield CJ. Intrinsically disordered proteins and multicellular organisms. Semin Cell Dev Biol. 2014. doi: 10.1016/j.semcdb.2014.09.025.

[217] Wood SJ, Wypych J, Steavenson S, Louis JC, Citron M, Biere AL. alpha-Synuclein fibrillogenesis is nucleation-dependent. Implications for the pathogenesis of Parkinson's disease, J. Biol. Chem. 1999; 274:19509-19512.

[218] Miake H, Mizusawa H, Iwatsubo T, Hasegawa M. Biochemical characterization of the core structure of alpha-synuclein filaments, J. Biol. Chem. 2002; 277:19213-19219.

[219] Der-Sarkissian A, Jao CC, Chen J, Langen R. Structural organization of alpha-synuclein fibrils studied by site-directed spin labeling, J. Biol. Chem. 2003; 278:37530-35.

[220] Apetri MM, Maiti NC, Zagorski MG, Carey PR, Anderson VE. Secondary structure of alpha-synuclein oligomers: characterization by Raman and atomic force microscopy, J. Mol. Biol. 2006; 355:63–71.

[221] Nemani VM, Lu W, Berge V, Nakamura K, Onoa B, Lee MK, Chaudhry FA, Nicoll RA, Edwards RH. Increased expression of α-synuclein reduces neurotransmitter release by inhibiting synaptic vesicle reclustering after endocytosis. Neuron 2010; 65:66–79.

[222] Scott DA, Tabarean I, Tang Y, Cartier A, Masliah E, Roy S. A pathologic cascade leading to synaptic dysfunction in α-synuclein-induced neurodegeneration. J. Neurosci. 2010; 30:8083–95.

[223] Cookson MR, van der Brug M. Cell systems and the toxic mechanism(s) of α-synuclein. Exp Neurol. 2007; 209:5-11.

[224] Spinelli KJ, Taylor JK, Osterberg VR, Churchill MJ, Pollock E, Moore C, Meshul CK, Unni VK. Presynaptic Alpha-Synuclein Aggregation in a Mouse Model of Parkinson's Disease. J Neurosci. 2014; 34:2037-50

[225] Uversky VN, Li J, Fink AL. Metal-triggered structural transformations, aggregation, and fibrillation of human alpha-synuclein. A possible molecular NK between Parkinson's disease and heavy metal exposure, J. Biol. Chem. 2001; 276:44284-96.

[226] Uversky VN, Li J, Fink AL. Pesticides directly accelerate the rate of α-synuclein fibril formation: a possible factor in Parkinson's disease. FEBS Lett. 2001; 500:105-108.

[227] Cohlberg JA, Li J, Uversky VN, Fink AL. Heparin and other glycosaminoglycans stimulate the formation of amyloid fibrils from alpha-synuclein *in vitro*. Biochemistry 2002; 41:1502-1511.

[228] Shtilerman MD, Ding TT, Lansbury PT Jr. Molecular crowding accelerates fibrillization of alpha-synuclein: could an increase in the cytoplasmic protein concentration induce Parkinson's disease? Biochemistry 2002; 41:3855-3860.

[229] Lee M, Hyun D, Halliwell B, Jenner P. Effect of the overexpression of wild-type or mutant alpha-synuclein on cell susceptibility to insult. J Neurochem. 2001; 76:998-1009.

[230] Narayanan V, Scarlata S. Membrane binding and self-association of alpha-synucleins. Biochemistry 2001; 40:9927-9934.

[231] Munishkina L, Phelan C, Uversky V, Fink A. Conformational behavior and aggregation of alpha-synuclein in organic solvents: Modeling the effects of membranes. Biochemistry 2003; 42:2720-30.

[232] Uversky VN, Li J, Fink AL. Trimethylamine-N-oxide-induced folding of alpha-synuclein. FEBS Lett. 2001; 509:31-35.

[233] Maraganore DM, de Andrade M, et al. Collaborative analysis of alpha-synuclein gene promoter variability and Parkinson disease. JAMA 2006; 296:661-670.

[234] Rajput A, Vilarino-Guell C, et al. Alpha-synuclein polymorphisms are associated with Parkinson's disease in a Saskatchewan population. Mov Disord 2009; 24:2411-2414.

[235] Pankratz N, Wilk JB, Latourelle JC, DeStefano AL, et al. Genome-wide association study for susceptibility genes contributing to familial Parkinson disease. Hum Genet 2009; 124:593-605.

[236] Polymeropoulos MH, Lavedan C, Leroy E, Ide SE, Dehejia A, Dutra A. Pike B, Root H, Rubenstein J, Boyer R, et al. Mutation in the alpha-synuclein gene identified in families with Parkinson's disease. Science 1997; 276: 2045-7.

[237] Bussell Jr. R, Eliezer D. Residual structure and dynamics in Parkinson's disease associated mutants of alpha-synuclein, J. Biol. Chem. 2001; 276:45996-46003.

[238] Krüger R, Kuhn W, Müller T, Woitalla D, Graeber M, Kösel S et al. Ala30Pro mutation in the gene encoding alpha-synuclein in Parkinson's disease. Nat Genet 1998; 18:106–8

[239] Zarranz JJ, Alegre J, Gómez-Esteban JC, et al. The new mutation, E46K, of alpha-synuclein causes Parkinson and Lewy body dementia. Annals of Neurology 2004; 55:164-73.

[240] Winner B, Jappelli R, Maji SK, Desplats PA, Boyer L, Aigner S. et al. *In vivo* demonstration that α-synuclein oligomers are toxic. Proc. Natl Acad. Sci. USA 2011; 108:4194-99.

[241] Taschenberger G, Garrido M, Tereshchenko Y, Bähr M, Zweckstetter M, Kügler S. Aggregation of α-synuclein promotes progressive *in vivo* neurotoxicity in adult rat dopaminergic neurons. Acta Neuropathol. 2011; 123:671-83

[242] Lesage S, Anheim M, Letournel F, Bousset L, Honore A, Rozas N, Pieri L, Madiona K, Durr A, Melki R, Verny C, Brice A. G51D alpha-synuclein mutation causes a novel Parkinsonian-pyramidal syndrome. Ann Neurol 2013; 73:459–471.

[243] Proukakis C, Dudzik CG, Brier T, MacKay DS, Cooper JM, Millhauser GL, Houlden H, Schapira AH. A novel alpha-synuclein missense mutation in Parkinson disease. Neurology 2013; 80:1062-1064.

[244] Singleton AB, Farrer M, Johnson J, Singleton A, Hague S, Kachergus J, Hulihan M, Peuralinna T, Dutra A, Nussbaum R, et al. alpha-Synuclein locus triplication causes Parkinson's disease. Science 2003; 302:841.

[245] Chartier-Harlin MC, Kachergus J, Roumier C, Mouroux V, Douay X, Lincoln S, Levecque C, Larvor L. Alpha-synuclein locus duplication as a cause of familial Parkinson's disease. Lancet 2004; 364:1167-1169.

[246] Ibanez P, Bonnet AM, Debarges B, Lohmann E, Tison F, Pollak P, Agid Y, Durr A, Brice A. Causal relation between alpha-synuclein gene duplication and familial Parkinson's disease. Lancet 2004; 364:1169-1171.

[247] Fuchs J, Nilsson C, Kachergus J, Munz M, Larsson EM, Schule B, Langston JW, Middleton FA, Ross OA, Hulihan M, Gasser T, Farrer MJ. Phenotypic variation in a large Swedish pedigree due to SNCA duplication and triplication. Neurology 2007; 68:916-22.

[248] Smith WW, Jiang H, Pei Z, Tanaka Y, Morita H, Sawa A, Dawson VL, Dawson TM, Ross CA. Endoplasmic reticulum stress and mitochondrial cell death pathways mediate A53T mutant alphasynuclein-induced toxicity. Hum Mol Genet 2005; 14:3801-3811.

[249] Lee KW, Chen W, Junn E, Im JY, et al. Enhanced phosphatase activity attenuates α-synucleinopathy in a mouse model. J. Neurosci. 2011; 31:6963–6971

[250] Paleologou KE, Oueslati A, Shakked G, Rospigliosi CC, Kim HY, Lamberto GR, et al. Phosphorylation at S87 is enhanced in synucleinopathies, inhibits alpha-synuclein oligomerization, and influences synuclein–membrane interactions. J. Neurosci. 2010; 30: 3184-3198.

[251] Nonaka T, Iwatsubo T, Hasegawa M: Ubiquitination of alpha-synuclein. Biochemistry 2005; 44:361–368.

[252] Giasson BI, Duda JE, Murray IV, Chen Q, Souza JM, Hurtig HI, Ischiropoulos H, Trojanowski JQ, Lee VM. Oxidative damage linked to neurodegeneration by selective alpha-synuclein nitration in synucleinopathy lesions. Science 2000; 290:985-989.

[253] Hodara R, Norris EH, Giasson BI, Mishizen-Eberz AJ, Lynch DR, Lee VM, Ischiropoulos H. Functional consequences of alpha-synuclein tyrosine nitration: diminished binding to lipid vesicles and increased fibril formation, J. Biol. Chem. 2004; 279:47746-53.

[254] Uversky VN. Natively unfolded proteins: a point where biology waits for physics. Protein Sci. 2002; 11(4):739-56.

[255] Li W, West N, Colla E, et al. Aggregation promoting C-terminal truncation of alpha-synuclein is a normal cellular process and is enhanced by the familial Parkinson's disease-linked mutations, Proc. Natl. Acad. Sci. U. S. A. 2005; 102: 2162-67.

[256] McLean PJ, Kawamata H, Ribich S, Hyman BT. Membrane association and protein conformation of alpha-synuclein in intact neurons. Effect of Parkinson's disease-linked mutations. J. Biol. Chem. 2000; 275: 8812–6

[257] Perrin RJ, Woods WS, Clayton DF, George JM. Interaction of human alpha-synuclein and Parkinson's disease variants with phospholipids. Structural analysis using site-directed mutagenesis. J Biol Chem 2000; 275:34393-34398.

[258] Grey M, Linse S, Nilsson H, Brundin P, Sparr E. Membrane interaction of α-synuclein in different aggregation states. J Parkinsons Dis. 2011; 1:359-71.

[259] Jin J, Li GJ, Davis J, Zhu D, Wang Y, Pan C, Zhang J. Identification of novel proteins associated with both alpha-synuclein and DJ-1. Mol Cell Proteomics. 2007; 6:845-59.

[260] van der Putten H, Wiederhold KH, Probst A, et al. Neuropathology in mice expressing human alpha-synuclein. J. Neurosci 2000; 20:6021–29.

[261] Yoshimoto M, Iwai A, Kang D, Otero DA, Xia Y, Saitoh T. NACP, the precursor protein of the non-amyloid beta/A4 protein (A beta) component of Alzheimer disease amyloid, binds A beta and stimulates A beta aggregation, Proc. Natl. Acad. Sci. U. S. A. 1995; 92:9141-45.

[262] Masliah E, Rockenstein E, Veinbergs I, Sagara Y, Mallory M, Hashimoto M, Mucke L. beta-amyloid peptides enhance alpha-synuclein accumulation and neuronal deficits in a transgenic mouse model linking Alzheimer's disease and Parkinson's disease. Proc Natl Acad Sci U S A. 2001; 98:12245-50

[263] Mandal PK, Pettegrew JW, Masliah E, Hamilton RL, Mandal R. Interaction between Abeta peptide and alpha synuclein: molecular mechanisms in overlapping pathology of Alzheimer's and Parkinson's in dementia with Lewy body disease. Neurochem Res. 2006; 31:1153-62.

[264] Tsigelny IF, Crews L, Desplats P, Shaked GM, et al . Mechanisms of hybrid oligomer formation in the pathogenesis of combined Alzheimer's and Parkinson's diseases. PLoS One. 2008; 3:e3135.

[265] Jensen PH, Hager H, Nielsen MS, Hojrup P, Gliemann J, Jakes R. alpha-Synuclein binds to Tau and stimulates the protein kinaseA-catalyzed tau phosphorylation of serine residues 262 and 356, J. Biol. Chem. 1999; 274:25481-89.

[266] Jenco JM, Rawlingson A, Daniels B, Morris AJ. Regulation of phospholipase D2: selective inhibition of mammalian phospholipase D isoenzymes by alpha and beta-synucleins, Biochemistry 1998; 37:4901-4909.

[267] Shimura H, Schlossmacher MG, et al. Ubiquitination of a new form of alpha-synuclein by parkin fromhuman brain: implications for Parkinson's disease. Science 2001; 293:263–269.

[268] Engelender S, Kaminsky Z, Guo X, Sharp AH, Amaravi RK. Synphilin-1 associates with alpha-synuclein and promotes the formation of cytosolic inclusions. Nat. Genet. 1999; 22:110-114.

[269] Lindersson E, Jensen PH. Alpha-synuclein binding proteins, in: Kahle PJ, Haass C. (Eds.), Molecular Mechanisms of Parkinson's Disease, Landes Bioscience, 2004.

[270] Alim MA, Hossain MS, Arima K, Takeda K, Izumiyama Y, Nakamura M, Kaji H, Shinoda T, Hisanaga S, Ueda K. Tubulin seeds alpha-synuclein fibril formation. J. Biol. Chem. 2002; 277:2112-2117.

[271] Ahn BH1, Rhim H, Kim SY, Sung YM, et al. alpha-Synuclein interacts with phospholipase D isozymes and inhibits pervanadate-induced phospholipase D activation in human embryonic kidney-293 cells, J. Biol. Chem. 2002; 277:12334-12342.

[272] Peng X, Tehranian R, Dietrich P, Stefanis L, Perez RG. Alpha-synuclein activation of protein phosphatase 2A reduces tyrosine hydroxylase phosphorylation in dopaminergic cells. J. Cell Sci. 2005; 118:3523–3530.

[273] Meulener MC1, Graves CL, Sampathu DM, Armstrong-Gold CE, Bonini NM, Giasson BI. DJ-1 is present in a large molecular complex in human brain tissue and interacts with alpha-synuclein, J. Neurochem. 2005; 93:1524–1532.

[274] Goers J1, Manning-Bog AB, McCormack AL, Millett IS, Doniach S, Di Monte DA, Uversky VN, Fink AL. Nuclear localization of alpha-synuclein and its interaction with histones. Biochemistry 2003; 42:8465-71.

[275] Martinez J, Moeller I, Erdjument-Bromage H, Tempst P, Lauring B. Parkinson's disease-associated alpha-synuclein is a calmodulin substrate. J. Biol. Chem. 2003; 278:17379-87.

[276] Tetzlaff JE, Putcha P, Outeiro TF, Ivanov A, Berezovska O, Hyman BT, McLean PJ CHIP targets toxic alpha-synuclein oligomers for degradation. J. Biol. Chem. 2008; 283:17962–17968.

[277] Uversky VN, Li J, Souillac P, Millett IS, Doniach S, Jakes R, Goedert M, et al. Biophysical properties of the synucleins and their propensities to fibrillate: inhibition of alpha-synuclein assembly by beta- and gamma-synucleins. J Biol Chem 2002; 277: 11970-8.

[278] Hashimoto M, Rockenstein E, Mante M, Mallory M, and Masliah E. beta-Synuclein inhibits alpha-synuclein aggregation: a possible role as an anti-parkinsonian factor. Neuron 2001; 32: 213-23.

[279] Conway KA, Rochet JC, Bieganski RM, Lansbury PT Jr. Kinetic stabilization of the alpha-synuclein protofibril by a dopamine- alpha-synuclein adduct. Science 2001; 294: 1346-1349.

[280] Li J, Zhu M, Manning-Bog AB, Di Monte DA, Fink AL. Dopamine and L-dopa disaggregate amyloid fibrils: implications for Parkinson's and Alzheimer's disease. FASEB J. 2004; 18:962-964.

[281] Stefanis L, Larsen KE, Rideout HJ, Sulzer D, Greene LA. Expression of A53T mutant but not wild-type alpha-synuclein in PC12 cells induces alterations of the ubiquitin-dependent degradation system, loss of dopamine release, and autophagic cell death. J Neurosci. 2001; 21:9549-60.

[282] Meredith GE, Totterdell S, Petroske E, Santa Cruz K, Callison RC Jr, Lau YS. Lysosomal malfunction accompanies alpha-synuclein aggregation in a progressive mouse model of Parkinson's disease. Brain Res. 2002; 956:156-65.

[283] Cuervo AM, Stefanis L, Fredenburg R, Lansbury PT, Sulzer D. Impaired degradation of mutant alpha-synuclein by chaperone-mediated autophagy. Science. 2004; 305:1292-5.

[284] Rideout HJ, Lang-Rollin I, Stefanis L. Involvement of macroautophagy in the dissolution of neuronal inclusions. Int J Biochem Cell Biol. 2004; 36:2551-62.

[285] Rockenstein E, Schwach G, Ingolic E, Adame A, Crews L, Mante M, Pfragner R, Schreiner E, Windisch M, Masliah E. Lysosomal pathology associated with alpha-synuclein accumulation in transgenic models using an eGFP fusion protein. J Neurosci Res. 2005; 80:247-59.

[286] Kragh CL, Ubhi K, Wyss-Coray T, Masliah E. Autophagy in dementias. Brain Pathol. 2012; 22:99-109.

[287] Iwata A, Maruyama M, Akagi T, Hashikawa T, Kanazawa I, Tsuji S, Nukina N. α-synuclein degradation by serine protease neurosin: implication for pathogenesis of synucleinopathies. Hum. Mol. Genet. 2003; 12:2625–2635.

[288] Klucken J, Shin Y, Masliah E, Hyman BT, McLean PJ. Hsp70 reduces α-synuclein aggregation and toxicity. J. Biol. Chem. 2004; 279:25497–2550.

[289] McNaught KS, Mytilineou C, Jnobaptiste R, Yabut J, Shashidharan P, Jennert P, Olanow CW. Impairment of the ubiquitinproteasome system causes dopaminergic cell death and inclusion body formation in ventral mesencephalic cultures. J. Neurochem. 2002; 81:301-306.

[290] Webb JL, Ravikumar B, Atkins J, Skepper JN, Rubinsztein DC. Alpha-Synuclein is degraded by both autophagy and the proteasome. J Biol Chem. 2003; 278:25009-13.

[291] Martinez-Vicente M, Talloczy Z, Kaushik S, Massey AC, Mazzulli J, et al. Dopamine-modified alpha-synuclein blocks chaperone-mediated autophagy. J Clin Invest. 2008; 118:777-88.

[292] Xilouri M, Vogiatzi T, Vekrellis K, Park D, Stefanis L. Abberant alpha-synuclein confers toxicity to neurons in part through inhibition of chaperone-mediated autophagy. PLoS One. 2009; 4:e5515.

[293] Conway KA, Lee SJ, Rochet JC, Ding TT, Williamson RE, Lansbury PT. Jr. Acceleration of oligomerization, not fibrillization, is a shared property of both alpha-synuclein mutations linked to early-onset Parkinson's disease: implications for pathogenesis and therapy. Proc Natl Acad Sci U S A. 2000; 97(2):571–6

[294] Volles MJ, Lansbury PT Jr. Zeroing in on the pathogenic form of alpha-synuclein and its mechanism of neurotoxicity in Parkinson's disease. Biochemistry. 2003; 42:7871-8.

[295] Danzer KM Haasen D, Karow AR, Moussaud S, Habeck M, Giese A, Kretzschmar H, Hengerer B, Kostka M. Different species of α-synuclein oligomers induce calcium influx and seeding. J. Neurosci. 2007; 27:9220-32.

[296] Mosharov EV, Staal RG, Bove J, Prou D, Hananiya A, et al. Alpha-synuclein overexpression increases cytosolic catecholamine concentration. J Neurosci 2006; 26:9304-11

[297] Larsen KE, Schmitz Y, Troyer MD, Mosharov E, et al. Alpha-synuclein overexpression in PC12 and chromaffin cells impairs catecholamine release by interfering with a late step in exocytosis. J Neurosci 2006; 26:11915-11922.

[298] Gosavi N, Lee HJ, Lee JS, Patel S, Lee SJ. Golgi fragmentation occurs in the cells with prefibrillar alphasynuclein aggregates and precedes the formation of fibrillar inclusion. J Biol Chem 2002; 277:48984–92

[299] Smith WW, Margolis RL, Li X, Troncoso JC, Lee MK, Dawson VL, Dawson TM, Iwatsubo T, Ross CA. Alpha-synuclein phosphorylation enhances eosinophilic cytoplasmic inclusion formation in SH-SY5Y cells, J. Neurosci. 2005; 25:5544-5552.

[300] Alim MA1, Ma QL, Takeda K, Aizawa T, Matsubara M, et al. Demonstration of a role forα-synuclein as a functional microtubule-associated protein. J. Alzheimers Dis. 2004; 6:435–442.

[301] Hsu LJ, Sagara Y, Arroyo A, Rockenstein E. et al. α-synuclein promotes mitochondrial deficit and oxidative stress. Am. J. Pathol. 2000; 157:401-10

[302] Orth M, Tabrizi SJ, Schapira AH, Cooper JM. Alpha-synuclein expression in HEK293 cells enhances the mitochondrial sensitivity to rotenone. Neurosci Lett 2003; 351:29–32.

[303] Ved R, Saha S, Westlund B, Perier C et al. Similar patterns of mitochondrial vulnerability and rescue induced by genetic modification of alpha-synuclein, parkin, and DJ-1 in Caenorhabditis elegans. J Biol Chem 2005; 280:42655-68.

[304] Devi L, Raghavendran V, Prabhu BM, Avadhani NG, and Anandatheerthavarada HK. Mitochondrial import and accumulation of alpha-synuclein impair complex I in human dopaminergic neuronal cultures and Parkinson disease brain. J Biol Chem 2008; 283: 9089-100.

[305] Snyder H, Mensah K, Theisler C, Lee J, Matouschek A, Wolozin B. Aggregated and monomeric alphasynuclein bind to the S6′ proteasomal protein and inhibit proteasomal function. J Biol Chem 2003; 278:11753-59

[306] Hashimoto M, Kawahara K, Bar-On P, Rockenstein E, Crews L, Masliah E. The role of α-synuclein assembly and metabolism in the pathogenesis of Lewy body disease. J. Mol. Neurosci. 2004; 24:343-52.

[307] Ding Q, Dimayuga E, Martin S, Bruce-Keller AJ, Nukala V, Cuervo AM, Keller JN. Characterization of chronic low-level proteasome inhibition on neural homeostasis. J Neurochem 2003; 86:489-97

[308] Baptista MJ, O'Farrell C, Daya S, Ahmad R, Miller DW, Hardy J, Farrer MJ, Cookson MR. Co-ordinate transcriptional regulation of dopamine synthesis genes by alpha-synuclein in human neuroblastoma cell lines. J Neurochem 2003; 85:957–968.

[309] Petrucelli L, O'Farrell C, Lockhart PJ, et al. Parkin protects against the toxicity associated with mutant alpha-synuclein: proteasome dysfunction selectively affects catecholaminergic neurons. Neuron 2002; 36:1007–1019.

[310] Stokes AH, Hastings TG, Vrana KE. Cytotoxic and genotoxic potential of dopamine. J Neurosci Res 1999; 55:659–665.

[311] Xu J, Kao SY, Lee FJ, Song W, Jin LW, Yankner BA. Dopamine-dependent neurotoxicity of alpha-synuclein: a mechanism for selective neurodegeneration in Parkinson disease. Nat. Med. 2002; 8:600–606.

[312] Cookson MR. α-Synuclein and neuronal cell death. Molecular Neurodegeneration 2009; 4:9

[313] Lee HJ, Suk JE, Bae EJ, Lee JH, Paik SR, Lee SJ. Assembly-dependent endocytosis and clearance of extracellular α-synuclein. Int. J. Biochem. Cell. Biol. 2008; 40:1835-49.

[314] Soper JH, Roy S, Stieber A, Lee E, Wilson RB, Trojanowski JQ, Burd CG, Lee VMY. α-Synuclein-induced Aggregation of Cytoplasmic Vesicles in Saccharomyces cerevisiae. Mol. Biol. Cell. 2008; 19:1093–1103.

[315] Danzer KM, Kranich LR, Ruf WP, Cagsal-Getkin O, Winslow AR, Zhu L, et al. Exosomal cell-to-cell transmission of alpha synuclein oligomers. Mol Neurodegener. 2012; 7:42.

[316] Desplats P, Lee HJ, Bae EJ, Patrick C, Rockenstein E, Crews L, et al. Inclusion formation and neuronal cell death through neuron-to-neuron transmission of alpha-synuclein. Proc Natl Acad Sci USA. 2009; 106:13010-15.

[317] Lee HJ, Suk JE, Patrick C, Bae EJ, Cho JH, Rho S, et al. Direct transfer of alpha-synuclein from neuron to astroglia causes inflammatory responses in synucleinopathies. J Biol Chem. 2010; 285:9262-72.

[318] Valera E, Masliah E. Immunotherapy for neurodegenerative diseases: focus on α-synucleinopathies. Pharmacol. Ther. 2013; 138:311-22.

[319] Tokuda T, Salem SA, Allsop D, Mizuno T, Nakagawa M, Qureshi MM, Locascio JJ, et al. Decreased alpha-synuclein in cerebrospinal fluid of aged individuals and subjects with Parkinson's disease. Biochem Biophys Res Commun 2006; 349: 162-6.

[320] Mollenhauer B, Cullen V, Kahn I, Krastins B, Outeiro TF, Pepivani I, Ng J, et al. Direct quantification of CSF alpha-synuclein by ELISA and first cross-sectional study in patients with neurodegeneration. Exp Neurol 2008; 213: 315-25.

[321] van Dijk KD, Bidinosti M, Weiss A, Raijmakers P, Berendse HW, van de Berg WD. Reduced alpha-synuclein levels in cerebrospinal fluid in Parkinson's disease are unrelated to clinical and imaging measures of disease severity. Eur J Neurol. 2014; 21:388-94.

[322] El-Agnaf OM, Salem SA, Paleologou KE, Curran MD, Gibson MJ, Court JA, Schlossmacher MG, et al. Detection of oligomeric forms of alpha-synuclein protein in human plasma as a potential biomarker for Parkinson's disease. FASEB J 2006; 20: 419-25.

[323] Heise H, Hoyer W, Becker S, Andronesi OC, Riedel D, Baldus M. Molecular-level secondary structure, polymorphism, and dynamics of full-length alpha-synuclein fibrils studied by solid-state NMR. Proc Natl Acad Sci U S A. 2005; 102:15871-6

[324] Kim HY, Cho MK, Kumar A, Maier E, Siebenhaar C, Becker S, Fernandez CO, Lashuel HA, Benz R, Lange A, Zweckstetter M. Structural properties of pore-forming oligomers of alpha-synuclein. J Am Chem Soc. 2009; 131:17482-9.

[325] Celej MS, Sarroukh R, Goormaghtigh E, Fidelio GD, Ruysschaert JM, Raussens V. Toxic prefibrillar α-synuclein amyloid oligomers adopt a distinctive antiparallel β-sheet structure. Biochem J. 2012; 443:719-26.

[326] van Rooijen BD, van Leijenhorst-Groener KA, Claessens MM, Subramaniam V. Tryptophan fluorescence reveals structural features of alpha-synuclein oligomers.J Mol Biol. 2009; 394(5):826-33.

[327] Mysling S, Betzer C, Jensen PH, Jorgensen TJ.Characterizing the dynamics of α-synuclein oligomers using hydrogen/deuterium exchange monitored by mass spectrometry. Biochemistry. 2013; 52:9097-103.

[328] Gallea JI, Celej MS. Structural insights into amyloid oligomers of the Parkinson disease-related protein α-synuclein. J Biol Chem. 2014; 289:26733-42.

[329] Waxman EA, Giasson BI. Molecular mechanisms of alpha-synuclein neurodegeneration. Biochim Biophys Acta. 2009; 1792:616-24

[330] Cheng B, Gong H, Xiao H, Petersen RB, Zheng L, Huang K. Inhibiting toxic aggregation of amyloidogenic proteins: a therapeutic strategy for protein misfolding diseases. Biochim Biophys Acta. 2013; 1830:4860-71.

[331] Ahmad E, Ahmad A, Singh S, Arshad M, Khan AH, Khan RH. A mechanistic approach for islet amyloid polypeptide aggregation to develop anti-amyloidogenic agents for type-2 diabetes, Biochimie 2011; 93:793–805.

[332] Liu FF, Dong XY, He L, Middelberg AP, Sun Y. Molecular insight into conformational transition of amyloid beta-peptide 42 inhibited by (−)-epigallocatechin-3-gallate probed by molecular simulations, J. Phys. Chem. B 2011; 115 :11879–87.

[333] Herczenik E, Gebbink MF. Molecular and cellular aspects of protein misfolding and disease, FASEB J. 2008; 22:2115–2133.

[334] Bieschke J, Russ J, Friedrich RP, Ehrnhoefer DE, Wobst H, Neugebauer K, Wanker EE. EGCG remodels mature alpha-synuclein and amyloid-beta fibrils and reduces cellular toxicity, Proc. Natl. Acad. Sci. U. S. A. 2010; 107:7710–15.

[335] Ehrnhoefer DE, Bieschke J, Boeddrich A, Herbst M, Masino L, Lurz R, Engemann S, Pastore A, Wanker EE. EGCG redirects amyloidogenic polypeptides into unstructured, off-pathway oligomers, Nat. Struct. Mol. Biol. 2008; 15:558–66.

[336] Pandey N, Strider J, Nolan WC, Yan SX, Galvin JE. Curcumin inhibits aggregation of alpha-synuclein, Acta Neuropathol. 2008; 115:479–489.

[337] Ahmad B, Lapidus LJ. Curcumin prevents aggregation in α-synuclein by increasing reconfiguration rate. J Biol Chem. 2012; 287:9193-9.

[338] Nakagawa K, Miyazawa T. Absorption and distribution of tea catechin, (−)-epigallocatechin-3-gallate, in the rat, J. Nutr. Sci. Vitaminol. (Tokyo) 1997; 43:679–84.

[339] Yang F, Lim GP, Begum AN, Ubeda OJ, Simmons MR, Ambegaokar SS, Chen PP, Kayed R, Glabe CG, Frautschy SA, Cole GM. Curcumin inhibits formation of amyloid beta oligomers and fibrils, binds plaques, and reduces amyloid *in vivo*, J. Biol. Chem. 2005; 280:5892–5901.

[340] Zhu M, Rajamani S, Kaylor J, Han S, Zhou F, Fink AL. The flavonoid baicalein inhibits fibrillation of alpha-synuclein and disaggregates existing fibrils, J. Biol. Chem. 2004; 279:26846–26857.

[341] Lu JH, Ardah MT, Durairajan SS, Liu LF, Xie LX, Fong WF, Hasan MY, Huang JD, El-Agnaf OM, Li M. Baicalein inhibits formation of alpha-synuclein oligomers within living cells and prevents Abeta peptide fibrillation and oligomerisation, ChemBioChem 2011; 12:615–24.

[342] El-Agnaf OM, Paleologou KE, Greer B, Abogrein AM, King JE, Salem SA, Fullwood NJ, Benson FE, Hewitt R, Ford KJ, Martin FL, Harriott P, Cookson MR, Allsop D. A strategy for designing inhibitors of alpha-synuclein aggregation and toxicity as a novel treatment for Parkinson's disease and related disorders, FASEB J. 2004; 18:1315–1317.

[343] Masliah E, Rockenstein E, Adame A, Alford M, Crews L, Hashimoto M, Seubert P, Lee M, Goldstein J, Chilcote T, Games D, Schenk D. Effects of alpha-synuclein immunization in a mouse model of Parkinson's disease. Neuron. 2005; 46:857-68.

[344] Masliah E, Rockenstein E, Mante M, Crews L, Spencer B, et al. Passive immunization reduces behavioral and neuropathological deficits in an alpha-synuclein transgenic model of Lewy body disease. PLoS ONE. 2011; 6:e19338

[345] Reynolds AD, Banerjee R, Liu J, Gendelman HE, Mosley RL. Neuroprotective activities of CD4+CD25+ regulatory T cells in an animal model of Parkinson's disease.J Leukoc Biol. 2007; 82:1083-94.

[346] Reynolds AD, Stone DK, Hutter JA, Benner EJ, Mosley RL, Gendelman HE. Regulatory T cells attenuate Th17 cell-mediated nigrostriatal dopaminergic neurodegeneration in a model of Parkinson's disease. J Immunol. 2010; 184:2261–2271

[347] Schneeberger A, Mandler M, Mattner F, Schmidt W. Vaccination for Parkinson's disease. Parkinsonism Relat Disord. 2012; 18(Suppl 1):S11–S13.

[348] Wilcock DM, Colton CA. Anti-amyloid-beta immunotherapy in Alzheimer's disease: relevance of transgenic mouse studies to clinical trials. J Alzheimers Dis. 2008; 15:555-69.

[349] Bae EJ, Lee HJ, Rockenstein E, Ho DH, Park EB, Yang NY, Desplats P, Masliah E, Lee SJ. Antibody-aided clearance of extracellular α-synuclein prevents cell-to-cell aggregate transmission. J Neurosci. 2012; 32:13454-69.

[350] Zhou, C; Przedborski, S. Intrabody and Parkinson's disease. Biochimica et Biophysica Acta 2009; 1792: 634-42.

[351] Zhou C, Emadi S, Sierks MR, Messer A. A human single-chain Fv intrabody blocks aberrant cellular effects of overexpressed alpha-synuclein. Mol Ther. 2004; 10:1023-31.

[352] Lynch SM, Zhou C, Messer A. An scFv intrabody against the nonamyloid component of alpha-synuclein reduces intracellular aggregation and toxicity. J Mol Biol. 2008; 377:136-47.

[353] Banta S, Dooley K, Shur O. Replacing antibodies: engineering new binding proteins. Annu Rev Biomed Eng. 2013; 15:93-113

[354] Galzie Z. What is protein engineering? Biochemical Education 1991; 19:74-75

[355] Turanli-Yildiz B, Alkim C, Cakar ZP. Protein Engineering. Rijeka; Intech 2012: 33-40.

[356] Hagihara Y, Saerens D2. Engineering disulfide bonds within an antibody. Biochim Biophys Acta. 2014; 1844:2016-2023.

[357] Feige MJ, Buchner J. Principles and engineering of antibody folding and assembly. Biochim Biophys Acta. 2014; 1844:2024-31.

[358] Silacci M, Baenziger-Tobler N, Lembke W, Zha W, Batey S, Bertschinger J, Grabulovski D. Linker length matters, fynomer-Fc fusion with an optimized linker displaying picomolar IL-17A inhibition potency. J Biol Chem. 2014; 289:14392-8.

[359] Macao B, Hoyer W, Sandberg A, Brorsson AC, Dobson CM, Härd T. Recombinant amyloid beta-peptide production by co-expression with an affibody ligand. BMC Biotechnol. 2008; 8:82.

[360] Grönwall C, Ståhl S. Engineered affinity proteins--generation and applications. J Biotechnol. 2009; 140:254-69.

[361] Baloch AR, Baloch AW, Sutton BJ, Zhang X. Antibody mimetics: promising complementary agents to animal-sourced antibodies. Crit Rev Biotechnol. 2014:1-8.

[362] Murali R, Greene MI. Structure based antibody-like peptidomimetics. Pharmaceuticals (Basel). 2012; 5:209-35.

[363] Niebecker R, Kloft C. Safety of therapeutic monoclonal antibodies. Curr Drug Saf. 2010; 5:275-86.

[364] Bhogal N. Immunotoxicity and immunogenicity of biopharmaceuticals: design concepts and safety assessment. Curr Drug Saf. 2010; 5:293-307.

[365] Renberg B, Nordin J, Merca A, et al. Affibody molecules in protein capture microarrays: evaluation of multidomain ligands and different detection formats. J Prot Res 2007; 6: 171–9.

[366] Chames P, Van Regenmortel M, Weiss E, Baty D. Therapeutic antibodies: successes, limitations and hopes for the future. Br J Pharmacol 2009; 157:220–33.

[367] Hey T, Fiedler E, Rudolph R, Fiedler M. Artificial, non-antibody binding proteins for pharmaceutical and industrial applications. Trends Biotechnol 2005; 23:514–22.

[368] Binz HK, Amstutz P, Plückthun A. Engineering novel binding proteins from nonimmunoglobulin domains. Nat Biotechnol. 2005; 23:1257-68.

[369] Gebauer M, Skerra A. Engineered Protein Scaffolds as Next-Generation Antibody Therapeutics. Curr. Opin. Chem. Biol. 2009; 13: 245–255.

[370] Lehmann A. Ecallantide (DX-88): A Plasma Kallikrein Inhibitor for the Treatment of Hereditary Angioedema and the Prevention of Blood Loss in On-Pump Cardiothoracic Surgery. Expert Opin. Biol. Ther. 2008; 8:1187–99.

[371] Wurch T, Pierre´ A, Depil S. Novel protein scaffolds as emerging therapeutic proteins: from discovery to clinical proof-of-concept. Trends Biotechnol 2012; 30:575–82.

[372] Dennis MS, Lazarus RA. Kunitz domain inhibitors of tissue factor-factor VIIa. II. Potent inhibitors selected from libraries by phage display. J. Biol. Chem. 1994; 269:22129-36.

[373] Binz HK, Amstutz P, Kohl A, Stumpp MT, Briand C, Forrer P, Grutter MG,Plückthun A. High-affinity binders selected fromdesigned ankyrin repeat protein libraries. Nat. Biotechnol. 2004; 22:575–582.

[374] Silverman J, Liu Q, Bakker A, To W, Duguay A, et al. Multivalent avimer proteins evolved by exon shuffling of a family of human receptor domains. Nat. Biotechnol. 2005; 23:1556–61.

[375] Beste G, Schmidt FS, Stibora T, Skerra A. Small antibody-like proteins with prescribed ligand specificities derived from the lipocalin fold. Proc. Natl. Acad. Sci. U.S.A. 1999; 96:1898–1903.

[376] Nord K, Gunneriusson E, Ringdahl J, Ståhl S, Uhlén M, Nygren PÅ. Binding proteins selected from combinatorial libraries of an alpha-helical bacterial receptor domain. Nat. Biotechnol. 1997; 15:772-77.

[377] Ebersbach H, Fiedler E, Scheuermann T, Fiedler M, Stubbs MT, Reimann C, Proetzel G, Rudolph R, Fiedler U. Affilin-novel binding molecules based on human gamma-B-crystallin, an all beta-sheet protein. J Mol Biol. 2007; 372:172-85.

[378] Mouratou B, Schaeffer F, Guilvout I, et al. Remodeling a DNA binding protein as a specific *in vivo* inhibitor of bacterial secretin PulD. Proc Natl Acad Sci, 2007; 104: 17983–8.

[379] Schlatter D, Brack S, Banner DW, et al. Generation, characterization and structural data of chymase binding proteins based on the human Fyn kinase SH3 domain. Landes Biosci, 2012; 4:497–508.

[380] Koide A, Bailey CW, Huang X, Koide S. The fibronectin type III domain as a scaffold for novel binding proteins. J. Mol. Biol. 1998; 284:1141-51.

[381] Xu L, Aha P, Gu K, Kuimelis RG, Kurz M. et al. Directed evolution of high-affinity antibody mimics using mRNA display. Chem. Biol. 2002; 9:933–942.

[382] Barbas III CF, Burton DR, Scott JK, Silverman GJ. Phage Display: A Laboratory Manual. Cold Spring Harbor Laboratory Press, Cold Spring Harbor, 2001 NY.

[383] Löfblom J, Wernérus H, Ståhl S. Fine affinity discrimination by normalized fluorescence activated cell sorting in staphylococcal surface display. FEMS Microbiol. Lett. 2005; 248:189–198.

[384] Daugherty PS, Chen G, Olsen MJ, Iverson BL, Georgiou G. Antibody affinity maturation using bacterial surface display. Protein Eng. 1998; 11:825–32.

[385] Harvey B.R, Georgiou G, Hayhurst A, Jeong KJ, Iverson BL, Rogers GK. Anchored periplasmic expression, a versatile technology for the isolation of high-affinity antibodies from Escherichia coli-expressed libraries. Proc. Natl. Acad. Sci. U.S.A. 2004; 101:9193–98.

[386] Boder ET, Wittrup KD. Yeast surface display for screening combinatorial polypeptide libraries. Nat. Biotechnol. 1997; 15:553–557.

[387] Bertschinger J, Grabulovski, D, Neri D. Selection of single domain binding proteins by covalent DNA display. Protein Eng. Des. Sel. 2007; 20:57–68.

[388] Hanes J, Plückthun A. *In vitro* selection and evolution of functional proteins by using ribosome display. Proc. Natl. Acad. Sci. U.S.A. 1997; 94:4937-42.

[389] Nemoto N, Miyamoto-Sato E, Husimi Y, Yanagawa H. *In vitro* virus: bonding of mRNA bearing puromycin at the 3'-terminal end to the C-terminal end of its encoded protein on the ribosome *in vitro.* FEBS Lett. 1997; 414:405–408.

[390] Odegrip R, Coomber D, Eldridge B, Hederer R, Kuhlman PA, Ullman C, FitzGerald K, McGregor D. CIS display: *in vitro* selection of peptides from libraries of protein–DNA complexes. Proc. Natl. Acad. Sci. U.S.A. 2004; 101:1206-10.

[391] Tabuchi I, Soramoto S, Nemoto N, Husimi Y. An *in vitro* DNA virus for *in vitro* protein evolution. FEBS Lett. 2001; 508:309-12.

[392] Nord O, Uhlén M, Nygren PÅ. Microbead display of proteins by cell-free expression of anchored DNA. J. Biotechnol. 2003; 106:1–13.

[393] Koch H, Grafe N, Schiess R, Plückthun, A. Direct selection of antibodies from complex libraries with the protein fragment complementation assay. J. Mol. Biol. 2006; 357:427-441.

[394] Parrish JR, Gulyas KD, Finley Jr. RL. Yeast two-hybrid contributions to interactome mapping. Curr. Opin. Biotechnol. 2006; 17:387–393.

[395] Nygren PA. Alternative binding proteins: Affibody binding proteins developed from a small three-helix bundle scaffold. FEBS J. 2008; 275:2668-76.

[396] Nord K, Nilsson J, Nilsson B, Uhlén M, Nygren PA. A combinatorial library of an alpha-helical bacterial receptor domain. Protein Eng. 1995; 8:601-8.

[397] Grönwall C, Jonsson A, Lindström S, Gunneriusson E, Ståhl S, Herne N. Selection and characterization of Affibody ligands binding to Alzheimer amyloid beta peptides. J Biotechnol. 2007; 128:162-83.

[398] Hoyer W, Härd T. Interaction of Alzheimer's Aβ peptide with an engineered binding protein—thermodynamics and kinetics of coupled folding–binding. J Mol Biol 2008; 378: 398-411.

[399] Hoyer W, Grönwall C, Jonsson A, Ståhl S, Härd T. Stabilization of a beta-hairpin in monomeric Alzheimer's amyloid-beta peptide inhibits amyloid formation. Proc Natl Acad Sci U S A. 2008; 105(13):5099-104.

[400] Luheshi LM, Hoyer W, de Barros TP, van Dijk Härd I, Brorsson AC, Macao B, Persson C, Crowther DC, Lomas DA, Ståhl S, Dobson CM, Härd T. Sequestration of the Abeta peptide prevents toxicity and promotes degradation *in vivo*. PLoS Biol. 2010; 8:e1000334.

[401] Mirecka EA, Shaykhalishahi H, Gauhar A, Akgül Ş, Lecher J, Willbold D, Stoldt M, Hoyer W. Sequestration of a β-hairpin for control of α-synuclein aggregation. Angew Chem Int Ed Engl. 2014; 53:4227-30.

[402] Shaykhalishahi H, Mirecka EA, Gauhar A, Grüning CSR, Willbold D, Härd T, Stoldt M, Hoyer W. A beta-hairpin-binding protein for three different disease-related amyloidogenic proteins. ChemBioChem. 2015. doi: 10.1002/cbic.201402552

[403] Grüning CS, Mirecka EA, Klein AN, Mandelkow E, Willbold D, Marino SF, Stoldt M, Hoyer W. Alternative conformations of the Tau repeat domain in complex with an engineered binding protein. J Biol Chem. 2014; 289:23209-18.

[404] Mirecka EA, Gremer L, Schiefer S, Oesterhelt F, Stoldt M, Willbold D, Hoyer W. Engineered aggregation inhibitor fusion for production of highly amyloidogenic human islet amyloid polypeptide J. Biotechnol. 2014; 191:221-227

[405] Chen X, Zaro JL, Shen WC. Fusion protein linkers: property, design and functionality. Adv Drug Deliv Rev. 2013; 65:1357-69

[406] Reddy Chichili VP, Kumar V, Sivaraman J. Linkers in the structural biology of protein-protein interactions. Protein Sci. 2013; 22:153-67.

[407] Gokhale RS, Khosla C. Role of linkers in communication between protein modules. Curr Opin Chem Biol. 2000; 4:22–27.

[408] George RA, Heringa J. An analysis of protein domain linkers: their classification and role in protein folding. Protein Eng. 2002; 15:871-9.

[409] Argos P. An investigation of oligopeptides linking domains in protein tertiary structures and possible candidates for general gene fusion. J Mol Biol. 1990; 211:943-58.

[410] W. Wriggers, S. Chakravarty, P.A. Jennings. Control of protein functional dynamics by peptide linkers. Biopolymers 2005; 80:736–46

[411] Chen X, Bai Y, Zaro J, Shen WC. Design of an *in vivo* cleavable disulfide linker in recombinant fusion proteins. Biotechniques. 2010; 49:513–518.

[412] Terpe K. Overview of tag protein fusions: from molecular and biochemical fundamentals to commercial systems. Appl Microbiol Biotechnol. 2003; 60:523–533.

[413] Yuste R. Fluorescence microscopy today. Nat Methods. 2005; 2:902–904.

[414] Patel LN, Zaro JL, Shen WC. Cell penetrating peptides: intracellular pathways and pharmaceutical perspectives. Pharm Res. 2007; 24:1977–1992.

[415] Widera A, Norouziyan F, Shen WC. Mechanisms of TfR-mediated transcytosis and sorting in epithelial cells and applications toward drug delivery. Adv Drug Deliv Rev. 2003; 55:1439-66.

[416] Pardridge WM. Biopharmaceutical drug targeting to the brain. J Drug Target. 2010; 18:157–167.

[417] Sevier CS, Kaiser CA. Formation and transfer of disulfide bonds in living cells. Nat Rev Mol Cell Biol. 2002; 3:836-47.

[418] Mamathambika BS, Bardwell JC. Disulfide-linked protein folding pathways. Annu Rev Cell Dev Biol. 2008; 24:211-35.

[419] Hwang C, Sinskey AJ, Lodish HF. Oxidized redox state of glutathione in the endoplasmic reticulum. Science. 1992; 257:1496-502.

[420] Lyles MM, Gilbert HF. Catalysis of the oxidative folding of ribonuclease A by protein disulfide isomerase: dependence of the rate on the composition of the redox buffer. Biochemistry. 1991; 30:613-9.

[421] Thangudu RR, Manoharan M, Srinivasan N, Cadet F, Sowdhamini R, Offmann B. Analysis on conservation of disulphide bonds and their structural features in homologous protein domain families. BMC Struct Biol. 2008; 8:55.

[422] Lindberg H, Johansson A, Härd T, Ståhl S, Löfblom J. Staphylococcal display for combinatorial protein engineering of a head-to-tail affibody dimer binding the Alzheimer amyloid-β peptide. Biotechnol J. 2013; 8:139-45.

[423] Wahlberg E, Härd T. Conformational stabilization of an engineered binding protein. J Am Chem Soc. 2006; 128:7651-60.

[424] Matsumura M, Signor G, Matthews BW. Substantial increase of protein stability by multiple disulphide bonds. Nature 1989; 342:291–293.

[425] Martensson LG, Karlsson M, Carlsson U. Dramatic stabilization of the native state of human carbonic anhydrase II by an engineered disulfide bond. Biochemistry 2002; 41:15867–75.

[426] Eijsink VGH, Bjork A, Gaseidnes S, Sirevag R, Synstad B, van den Burg B, Vriend G. Rational engineering of enzyme stability. J Biotechnol 2004; 113:105–120.

[427] Starovasnik MA, Braisted AC, Wells JA. Structural mimicry of a native protein by a minimized binding domain. Proc Natl Acad Sci U S A. 1997; 94:10080-5.

[428] Härd T. Protein engineering to stabilize soluble amyloid β-protein aggregates for structural and functional studies. FEBS J. 2011; 278:3884-92.

[429] Walker S, Ullman O, Stultz CM. Using intramolecular disulfide bonds in tau protein to deduce structural features of aggregation-resistant conformations. J Biol Chem. 2012; 287:9591-600.

[430] Abkevich VI, Shakhnovich EI. What can disulfide bonds tell us about protein energetics, function and folding: simulations and bioninformatics analysis. J Mol Biol. 2000; 300:975-85.

[431] Arai R, Wriggers W, Nishikawa Y, Nagamune T, Fujisawa T. Conformations of variably linked chimeric proteins evaluated by synchrotron X-ray small-angle scattering. Proteins. 2004; 57:829-38.

[432] Huston JS1, Levinson D, Mudgett-Hunter M, Tai MS, Novotný J, Margolies MN, et al. Protein engineering of antibody binding sites: recovery of specific activity in an anti-digoxin single-chain Fv analogue produced in Escherichia coli. Proc Natl Acad Sci U S A. 1988; 85:5879-83.

[433] Alfthan K, Takkinen K, Sizmann D, Söderlund H, Teeri TT. Properties of a single-chain antibody containing different linker peptides. Protein Eng. 1995; 8:725–731.

[434] Yan DD, Yang FH, Fang J. Construction and expression of bivalent single-chain a

[435] Zhao HL, Yao XQ, Xue C, Wang Y, Xiong XH, Liu ZM. Increasing the homogeneity, stability and activity of human serum albumin and interferon-alpha2b fusion protein by linker engineering. Protein Expr Purif. 2008; 61:73-7.

[436] Bai Y, Shen WC. Improving the oral efficacy of recombinant granulocyte colony-stimulating factor and transferrin fusion protein by spacer optimization. Pharm Res. 2006; 23:2116-21.

[437] Sorensen BR, Faga LA, Hultman R, Shea MA. An interdomain linker increases the thermostability and decreases the calcium affinity of the calmodulin N-domain. Biochemistry. 2002; 41:15-20.

[438] Pokkuluri PR, Raffen R, Dieckman L, Boogaard C, Stevens FJ, Schiffer M. Increasing protein stability by polar surface residues: domain-wide consequences of interactions within a loop. Biophys J. 2002; 82:391-8.

[439] Robinson CR, Sauer RT. Optimizing the stability of single-chain proteins by linker length and composition mutagenesis. Proc Natl Acad Sci U S A. 1998; 95:5929-34.

[440] Ramachandran GN, Sasisekharan V. Conformation of polypeptides and proteins. Adv Protein Chem. 1968; 23:283-438.

[441] Williamson MP. The structure and function of proline-rich regions in proteins. Biochem J. 1994; 297:249–260.

[442] Zhou ZD, Yap BP, Gung AY, Leong SM, Ang ST, Lim TM. Dopamine-related and caspase independent apoptosis in dopaminergic neurons induced by overexpression of human wild type or mutant alpha-synuclein. Exp. Cell Res 2006; 312:156-170

[443] Zhou W, Schaack J, Zawada WM, Freed CR. Overexpression of human alpha-synuclein causes dopamine neuron death in primary human mesencephalic culture. Brain Res 2002; 926:42–50.

[444] Liu CW, Giasson BI, Lewis KA, Lee VM, DeMartino GN, Thomas PJ. A Precipitating Role for Truncated α-Synuclein and the Proteasome in {alpha}-Synuclein Aggregation: implications for pathogenesis of Parkinson disease. J. Biol. Chem 2005; 280:22670-78.

[445] Ban T, Hoshino M, Takahashi S, Hamada D, Hasegawa K, Naiki H, Goto Y. Direct observation of Abeta amyloid fibril growth and inhibition. J Mol Biol. 2004; 344:757-67.

[446] Lashuel, H. A. Hartley DM, Balakhaneh D, Aggarwal A, Teichberg S, Callaway DJ et al. New class of inhibitors of amyloid-β fibril formation. Implications for the mechanism of pathogenesis in Alzheimer's disease. J. Biol. Chem. 2002; 277:42881-90.

[447] Goedert M, Crowther RA, Garner CC. Molecular characterization of microtubule-associated proteins tau and MAP2. Trends Neurosci. 1991; 14:193–9

[448] Copp DH Cheney B. Calcitonin-a hormone from the parathyroid which lowers the calcium-level of the blood. Nature 1962; 193: 381–2.

[449] Goedert M. Alpha-synuclein and neurodegenerative diseases. Nat. Rev. Neurosci. 2001; 2:492-501.

[450] Hardy JA, Higgins GA. Alzheimer's disease: The amyloid cascade hypothesis. Science 1992; 256:184-185.

[451] Prusiner SB. Prions. Proc. Natl. Acad. Sci. U.S.A. 1998; 95:13363-13383

[452] Koch KM. Dialysis-related amyloidosis. Kidney Int. 1992; 41:1416-1429.

[453] Pepys MB, Hawkins PN, Booth DR, Vigushin DM, Tennent G A, Soutar AK, Totty N, Nguyen O, Blake CCF, Terry CJ, Feest TG, Zalin AM, Hsuan JJ. Human lysozyme gene mutations cause hereditary systemic amyloidosis. Nature1993; 362:553-557.

[454] Jaikaran ETAS Clark A. Islet amyloid and type 2 diabetes: from molecular misfolding to islet pathophysiology. Biochim. Biophys. Acta-Mol. Basis Dis. 2001; 1537: 179-203.

[455] Bates G. Huntingtin aggregation and toxicity in Huntington's disease. Lancet 2003; 361:1642-44.

[456] Longhi S, Gagliardi C, Milandri A, Manuzzi L, Rapezzi C. Transthyretin-related amyloidotic cardiomyopathy: looking for the etiological treatment. G Ital Cardiol (Rome). 2014; 15(5):293-300.

[457] Cremades, N. et al. Direct observation of the interconversion of normal and toxic forms of alpha-synuclein. Cell 2012; 149:1048-59.

[458] Lashuel HA, Hartley DM, Balakhaneh D, Aggarwal A, Teichberg S, Callaway DJ.
New class of inhibitors of amyloid-beta fibril formation. Implications for the mechanism of pathogenesis in Alzheimer's disease. J Biol Chem. 2002; 277:42881-90.

[459] Di Giovanni S, Eleuteri S, Paleologou KE, Yin G, Zweckstetter M, Carrupt PA, Lashuel HA. Entacapone and tolcapone, two catechol O-methyltransferase inhibitors, block fibril formation of alpha-synuclein and beta-amyloid and protect against amyloid-induced toxicity. J Biol Chem. 2010; 285:14941-54.

[460] Yu L, et al. Structural characterization of a soluble amyloid β-peptide oligomer. Biochemistry 2009; 48:1870-77.

[461] Guo, J.L., and Lee, V.M. Cell-to-cell transmission of pathogenic proteins in neurodegenerative diseases. Nat. Med. 2014; 20:130–38.

[462] Costanzo, M., and Zurzolo, C. The cell biology of prion-like spread of protein aggregates: mechanisms and implication in neurodegeneration. Biochem. J. 2013; 452:1-17.

[463] Tran HT, Chung CH, Iba M, Zhang B, Trojanowski JQ, Luk KC, Lee VM. A-synuclein immunotherapy blocks uptake and templated propagation of misfolded α-synuclein and neurodegeneration. Cell Rep. 2014; 7:2054-65.

[464] Alberio T, Lopiano L, Fasano M. Cellular models to investigate biochemical pathways in Parkinson's disease. FEBS J. 2012; 279:1146-55.

[465] Outeiro TF, Lindquist S. Yeast cells provide insight into alpha-synuclein biology and pathobiology. Science 2003; 302:1772-75

[466] Feany MB, Bender WW. A Drosophila model of Parkinson's disease. Nature. 2000; 404:394-8.

[467] Nass R, Blakely RD. The Caenorhabditis elegans dopaminergic system: opportunities for insights into dopamine transport and neurodegeneration. Annu Rev Pharmacol Toxicol. 2003; 43:521-44.

[468] Kahle PJ, Neumann M, Ozmen L, Muller V, Odoy S, Okamoto N, et al. Selective insolubility of α-synuclein in human Lewy body diseases is recapitalated in a transgenic mouse model. Am. J. Pathol 2001; 159: 2215-25.

[469] Wikman M, Steffen AC, Gunneriusson E, et al. Selection and characterization of HER2/neu-binding Affibody ligands. Protein Eng Des Sel 2004; 17: 455–62.

[470] Nord K, Nord O, Uhlén M, Kelley B, Ljungqvist C, Nygren PA. Recombinant human factor VIII-specific affinity ligands selected from phage-displayed combinatorial libraries of protein A. Eur J Biochem. 2001; 268:4269-77.

[471] Schier R, McCall A, Adams GP, Marshall KW, et al. Isolation of picomolar affinity anti-c-erbB-2 single-chain Fv by molecular evolution of the complementarity determining regions in the center of the antibody binding site. J Mol Biol 1996; 263: 551–67.

[472] Renaut L, Monnet C, Dubreuil O, Zaki O, Crozet F, Bouayadi K, Kharrat H, Mondon P. Affinity maturation of antibodies: optimized methods to generate high-quality ScFv libraries and isolate IgG candidates by high-throughput screening. Methods Mol Biol. 2012; 907:451-61.

[473] Orlova A, Magnusson M, Eriksson TL, Nilsson M, Larsson B, et al. Tumor imaging using a picomolar affinity HER2 binding affibody molecule. Cancer Res. 2006; 66:4339-48.